Dynamic Instability of Laminated Composite Curved Panels in Hygrothermal Environment

A thesis submitted to

National Institute of Technology, Rourkela

For the award of degree of

Doctor of Philosophy

in

Engineering

by

Manoj Kumar Rath

Under the supervision of

Prof. Shishir Kumar Sahu

Department of Civil Engineering

National Institute of Technology

Rourkela-769008, India

July 2012

Dedicated

To My Parents

CERTIFICATE

This is to certify that the thesis entitled "**Dynamic Instability of Laminated Composite curved panels in Hygrothermal Environment**", being submitted to the National Institute of Technology, Rourkela, India by Manoj Kumar Rath for the award of the degree of **Doctor of Philosophy in Engineering** is a record of bonafide research work carried out by him under my supervision and guidance. This fulfills the requirements of the regulations of the degree. The results embodied in this thesis have not been submitted in part or full to any other university or institute for the award of any degree or diploma.

NIT, Rourkela

Date:

Dr. Shishir Kumar Sahu
Professor, Department of Civil Engineering
National Institute of Technology
Rourkela-769008
Odisha, India

Acknowledgement

I express my deep sense of gratitude and indebtedness to my thesis supervisor Professor. Shishir Kumar Sahu, Department of Civil Engineering, National Institute of Technology, Rourkela, for his invaluable encouragement, helpful suggestions and supervision throughout the course of this work.

I express my sincere thanks to the Director, Prof. S.K. Sarangi, National Institute of Technology, Rourkela for motivating me in this endeavor and providing me the necessary facilities for this study.

I would like to thank Prof N. Roy, Head of the Civil Engineering Department and, Prof. M. Panda, Professor, Civil Engineering department for their help and cooperation during the progress of this work.

I would also like to thank Professor S.K. Sahoo of Mechanical Engineering Department for their invaluable suggestions and help at various stages of the experimental work.

I acknowledge with thanks the help rendered to me by Prof B. C. Roy, HOD, MM Department. Prof B. B. Vernma and lab staff of MM, my friends and other staff of the Civil Engineering Department for their continuous encouragement during the progress of my work.

Last but not least, I am extremely grateful to my wife and children, Saswati and Ayush, for their support and patience during this period.

The author is also thankful to Department of Science and Technology Govt of India for their financial support through the R & D project No SR/S3/MERC/0009/2008 for the material and facility during testing of Composites.

(Manoj Kumar Rath)

ABSTRACT

Composite materials are increasingly used in aerospace, naval and high performance civil engineering structures such as aerospace, submarines, automobiles. The structural components, subjected to in-plane harmonic loads may undergo parametric resonance or dynamic stability due to certain combinations of the applied in-plane forcing parameters and natural frequency of transverse vibration. The parametric instability itself requires investigation of vibration and buckling of structures. The present study deals with free vibration, buckling and parametric resonance behavior of laminated composite plates under in-plane periodic loading under varying temperature and moisture. In this analysis, the effects of various parameters such as number of layers, aspect ratios, side-to thickness ratios, ply orientations, static load factors, lamination angle and the degree of orthotropic are studied.

A simple laminated plate model based on the first order shear deformation theory (FSDT) is developed for the free vibration, buckling and parametric instability effects of composite plates subjected to hygrothermal loading. The principal instability regions are obtained using Bolotin's approach employing finite element method (FEM). An eight-node isoparametric quadratic element is employed in the present analysis with five degree of freedom per node. The element is modified to accommodate the laminated composite plates under hygrothermal environment, considering the effects of transverse shear deformation and rotary inertia. The element stiffness matrix, geometric stiffness matrix due to residual stresses, element mass matrix, geometric stiffness matrix due to applied in-plane loads and nodal load vector of the element are derived using the principle of minimum potential energy. They are evaluated using the Gauss quadrature numerical integration technique. Reduced integration technique is applied to avoid the possible shear locking. A computer program based on FEM in MATLAB environment is developed to perform all necessary computations.

The basic vibration and buckling experiments are performed on the industry driven woven fiber Glass/Epoxy specimens subjected to hygrothermal environment. The specimens were hygrothermally conditioned in a humidity cabinet where the conditions were maintained at temperatures of 300K-425K and relative humidity (RH) ranging from 0-1.0% for moisture concentrations.

The numerical and experimental results show that there is reduction in natural frequencies and buckling loads with increasing temperature and moisture concentration for laminates both for simply supported and clamped boundary conditions. The dynamic instability study using FEM revealed that, due to the static component of load, the instability regions tend to shift to lower frequencies. The onset of instability occurs earlier and the width of dynamic instability regions increases with rise in temperature and moisture concentration for different parameters. With increase in lamination angle, the width of the instability region becomes smaller. The onset of instability occurs later for square plates than rectangular plates with wider instability region with increase of aspect ratio. The ply orientation significantly affects the onset of instability. It is observed that the excitation frequency increases with introduction of curvatures from flat panel to doubly curved panel in hygrothermal environments.

Thus the instability behaviour of laminated composite panels is influenced by increase in number of layers, aspect ratio, side to thickness ratio, increase in static and dynamic load factor, geometry, material, ply lay-up and its orientation. This can be utilized to tailor the design of laminated composite panels in hygrothermal environment.

Keywords: parametric resonance, dynamic instability, woven fiber laminated composite plates, excitation frequencies, hygrothermal environment.

Contents

List of Tables

List of Figures

List of Publications out of this Research Work

Papers in International Journals

1. M. K. Rath and S. K. Sahu (2011): Vibration of Woven Fiber Laminated Composite Plates in Hygrothermal Environment, *Journal of Vibration and Control,* Vol. **18** (13), pp. 1957-1970.

2. M. K. Rath and S. K. Sahu (2011): Static Behavior of Woven Fiber Laminated Composites in Hygrothermal Environment, *Journal of Reinforced plastics and Composites*, Vol.**30** (1), pp.61-76

3. S. K. Sahu, M. K. Rath and R. Sahoo (2012): Parametric Instability of Laminated Composite Doubly Curved Shell Panels Subjected to Hygrothermal Environment, *Advanced Materials Research Journal*, Vol. **383-390**, pp. 3212-3216.

4. M. K. Rath and S. K. Sahu, Experimental and numerical study on buckling effects of woven fiber laminated composite plates in hygrothermal environment, *Journal of Structural Engineering and Mechanics*, under review

5. S.K.Sahu, M.K.Rath and R.Sahoo,(2012) Parametric Resonance Characteristics of Woven Fiber Composite Curved Panels in Hygrothermal Environment, *International Journal of Aeronautical and Space Sciences,* **13(**3), pp.332-348.

6. M. K. Rath and S. K. Sahu, Parametric Instability of Woven Fiber Laminated Composite Plates in Hygrothermal Environment, *International Journal of Mechanical Sciences*, under review.

7. M. K. Rath and S. K. Sahu, Parametric Instability of Composite Plates in Hygrothermal Environment, *International Jounal of Computational Methods in Engineering Science and Mechanics,* under review.

8. M. K. Rath and S. K. Sahu, Dynamic Instability of Woven Fiber Laminated Composite Plates in Hygrothermal Environment, *International Journal of Theoretical and applied Mechanics,* under review.

Papers Presented in International Conferences

1. S. K. Sahu, M. K. Rath and R. Sahoo (2011): Parametric Instability of Laminated Composite Doubly Curved Shell Panels Subjected to Hygrothermal Environment, *the International Conference on Manufacturing Science and Technology (ICMST 2011),* Sep 16-18, 2011 at Singapore.

2. M. K. Rath and S. K. Sahu: Dynamic Response of Woven Fiber Laminated Composite Plates in Hygrothermal Environment, *5th International Conference on Theoretical, Applied, Computational and Experimental Mechanics (ICTACEM 2010),* Dec 27-29, 2010 at IIT, Kharagpur.

3. M. K. Rath and S. K. Sahu: Buckling effects of composite plates in hygrothermal Environment, *5th International Conference on Advances in Mechanical Engineering (ICAME-2011),* June 4-6, 2011 at SVNIT, Surat.

4. M. K. Rath and S. K. Sahu: Dynamic Stability of Woven Fiber Composite Plates in Hygrothermal Environment, *International Conference on Computational Methods in Manufacturing (ICCMM2011),* Dec 15-16, 2011 at IIT Guwahati.

5. M. K. Rath and S. K. Sahu: Parametric Instability of Square Laminated Plates in Hygrothermal Environment, *Fourth International Conference on Structural Stability and Dynamics (ICSSD2012),* Jan 4-6, 2012 at MNIT, Jaipur.

Nomenclature

The principal symbols used in this thesis are presented for easy reference. A single symbol is used for different meanings depending on the context and defined in the text as they occur.

English

a, b	Plate dimensions along x and y axes, respectively
$A_{ij}, B_{ij}, D_{ij}\ S_{ij}$	Extensional, bending-stretching coupling, bending stiffnesses and transverse shear stiffnesses
C, C0	Elevated and reference moisture concentrations
E_{11}, E_{22}	Young's moduli of lamina in both 1 and 2 directions respectively
G_{12}, G_{13}, G_{23}	Shear moduli of lamina with respect to 1, 2 and 3 axes
h	Thickness of plate
[K]	Elastic stiffness matrix
$[K^r_g]$	Geometric stiffness matrix due to hygrothermal load
$[K_g]$	Geometric stiffness matrix due to in-plane load
[M]	Mass matrix
M_x, M_y, M_{xy}	Internal moment resultants.
$M_x{}^N, M_y{}^N, M_{xy}{}^N$	Non-mechanical moment resultants due to moisture and temperature.
n	Number of layers of laminated composite plates

N_x, N_y, N_{xy}	In-plane internal stress resultants.
$N_x{}^N, N_y{}^N, N_{xy}{}^N$	In-plane non-mechanical stress resultants due to moisture and temperature.
N_i	Shape function at a node i
$N^a{}_x, N^a{}_y, N^a{}_{xy}$	Applied in-plane forces per unit length
$N^n{}_x, N^n{}_y, N^n{}_{xy}$	Applied in-plane forces per unit length
N_s	The static portion of load N (t)
N_t	The amplitude of the dynamic portion of N (t)
Q_x, Q_y	Transverse shear resultants.
R_x, R_y, R_{xy}	Radii of curvature of shell
T, T_O	Elevated and reference moisture concentration
u, *v*, *w*	Displacement components in the x, y, z directions

Greek

α, β	Static and dynamic load factors
α_1, α_2	Thermal coefficients along 1 and 2 axes of a lamina, respectively
β_1, β_2	Moisture coefficients along 1 and 2 axes of a lamina, respectively
$\epsilon_x, \epsilon_y, \gamma_{xy}$	In-plane strains of the mid-plane.
$\varepsilon_{xN}, \varepsilon_{yN}, \varepsilon_{xyN}$	Non-mechanical strains due to moisture and temperature
K_x, K_Y, K_{xy}	Curvature of the plate
θ	Fiber orientation in a lamina

κ	Shear correction factor
θ_x, θ_y	Rotations of the plate about x and y axes
υ_{12}, ν_{21}	Poisson's ratios
ρ	Mass density
$(\rho)_k$	Mass density of k_{th} layer from mid-plane.
ξ, η	Natural co-ordinates of an element
ϕ_x, ϕ_y	Shear rotations in x-z and y-z planes, respectively
λ	Critical loads
ω_n	Natural frequency
Ω	Excitation frequency
ε	Total strain
ε_l	Linear strain
ε_{nl}	Non-linear strain

Mathematical Operators

$[\ ]^{-1}$	Inverse of the matrix
$[\ ]^{T}$	Transpose of the matrix
$\frac{\partial}{\partial x}, \frac{\partial}{\partial y}$	Partial derivatives with respect to x and y

Abbreviations

FSDT	First order shear deformation theory
DIR	Dynamic instability region

CHAPTER 1

INTRODUCTION

1.1: Introduction

Composite materials are being increasingly used in aerospace, civil, naval and other high-performance engineering applications due to their light weight, high specific strength, high specific stiffness and low specific density, which reduce the overall operational cost. Besides military aircraft like the B-2 bomber, Nighthawk F117-A fighter, recent advancements in composites in the commercial aircraft sectors including Boeing 787 and Airbus 350/380, all-composite empennages on the Boeing 7J7 and McDonnell Douglas MD-91X, is to limit sonic fatigue caused by the new fuel efficient propfan or unducted fan (UDF) engines. Structures used in the above fields are more often exposed to high temperature as well as moisture. The varying environmental conditions due to moisture absorption and temperature seem to have an adverse effect on the stiffness and strength of the structural composites. This wide range of practical applications demands a fundamental understanding of their vibrations, static and dynamic stability characteristics under hygrothermal conditions.

1.2: Importance of the present structural stability study

Structural elements under in-plane periodic forces may undergo unstable transverse vibrations, leading to parametric resonance, due to certain combination of the values of in-plane load parameters and natural frequency of transverse vibration. This instability may occur below the critical load of the structure under compressive loads over a range or ranges of excitation frequencies. Several means of combating parametric resonance such as damping and vibration isolation may be inadequate and sometimes dangerous with reverse results. In contrast to the principal resonance, the parametric instability may arise not merely at a single excitation frequency but even for small excitation amplitudes and combination of frequencies. The distinction between good and bad vibration regimes of a structure, subjected to in-plane periodic loading can be distinguished through an analysis of dynamic instability region (DIR) spectra. The calculation of these spectra is often provided in terms of natural

frequencies and the static buckling loads. So, the calculation of these parameters with high precision is an integral part of dynamic instability analysis of composite plates and shells in hygrothermal environment.

A comprehensive analysis of the vibration and buckling effects of plates and shells has been studied exhaustively without considering hygrothermal effects. The vibration and buckling aspects of laminated composite panels in hygrothermal environment, which have increasing applications in recent years. The subject on dynamic instability of laminated curved panels in hygrothermal environment has attracted the attention of researchers since it is hitherto not well studied. It is clear from the above discussion that the process of investigating the different aspects of vibration and stability studies on woven fiber laminated composite plates structures in hygrothermal environment are current problem of interest. All these advancements and design requirements place a premium on an in-depth understanding of the response characteristics of such structural components. A thorough review of earlier works done in this area becomes essential to arrive at the objective and scope of the present investigation. The detailed review of literature along with critical discussions is presented in the next chapter.

CHAPTER 2

REVIEW OF LITERATURE

2.1: Introduction

The vast uses of conventional metals, its alloys and the ever increasing demand of composite materials in plates and shells are the subject of research for many years. Though the investigations is mainly focused on dynamic instability analysis of flat and curved panels in hygrothermal environment, some relevant research works on free vibration, buckling and dynamic instability analysis of flat and curved panels subjected to hygrothermal loadings are also considered for the sake of its relevance with the present investigation. Some of the pertinent studies done recently are reviewed elaborately and critically discussed to identify the lacunae in the existing literature. The literature reviewed in this chapter is grouped into three major aspects of dynamics as follows:

In each section, the various aspects of analysis covered are:

- Vibration of laminated composite panels in hygrothermal environment
- Buckling effects of laminated composite panels in hygrothermal environment
- Dynamic instability of laminated composite panels in hygrothermal environment

In each section, the various structural components covered are:

- Plates
- Curved panels

However, some studies on static/bending analysis of composites in hygrothermal environment are studied before dynamic analysis for relevance and completeness.

2.1.1 Static behavior of composites in hygrothermal environment

High-Performance composite materials have received increasing consideration for structural applications because of their low density, high strength, and high stiffness. Their superior strength and stiffness properties, however, are often compromised by

the environment to which they are exposed. A general discussion of the affect of environment on the structural behavior of composite materials was presented by many researchers. Among the environmental factors, those which induce expansional strains (volume change in the absence of surface tractions) are of particular concern. In the case of advanced composite structures, such phenomena are primarily caused by an increase in temperature, absorption by a polymeric matrix material of a swelling agent such as water vapor, and by sudden expansion of absorbed gases in the matrix. In addition to inducing residual stresses, expansional strains can affect the gross response characteristics of a composite structure. In particular, bending deflections, buckling loads and vibration frequencies can be considerably modified by the presence of environmentally induced strains. Thus, if composite materials are to reach their full potential, it will be necessary to consider such environmental factors as temperature and humidity in structural analysis and design. Hence the changes in static characteristics due to the hygrothermal effects seem to be an important consideration in composite analysis and design, which are of practical interest.

An extensive review of earlier works on composite mechanics and its sophistication is presented by Chamis [1989]. Shen and Springer [1976] performed tests on moisture absorption and desorption of composite materials. A series of test using unidirectional composites were performed in the temperature 300-425 K with the material submerged both in moist air and in water. Ishai and Arnon [1977] studied the effects of hygrothermal history on residual strength of glass fiber reinforced plastic laminates. Structural glass fiber/epoxy laminates were exposed to various periods of immersion in water at room and elevated temperatures and tested after oven drying. Aditya and Sinha [1992] investigated on determination of diffusion coefficients for the continuous hygrothermal exposure of laminates of different material combination. Harding and Li [1992] predicted the interlaminar shear strength for glass/epoxy and carbon/epoxy laminates at impact rate of strain by employing a new technique with the help of a double-lap shear specimen, where failure occurs on predetermined interfaces. Govindarajan *et al*. [1993] examined the reason of low interlaminar strength and the consequent possibility of interlaminar failure in composite laminates. Melvin *et al.* [1993] investigated the thermoplastics response to deformation of carbon fiber/epoxy-resin composite laminates has been considered theoretically, and compared with experimental results. It was found that the surface temperature is

strongly dependent on the near-surface lay-up. Harding and Dong [1994] studied the effect of strain rate on the interlaminar shear strength of carbon-fiber-reinforced laminates. Experimental results were obtained at quasi-static and an impact rate of loading for the interlaminar shear strength parallel to the fibers in a unidirectional laminates in which the fiber orientation is 0/90 and ±45. Selzer and Friedrich [1997] examined the mechanical properties and failure behavior of carbon fibre-reinforced polymer composites under the influence of moisture.

Shibasaki and Somiya [1999] investigated the time dependence of degradation phenomena of plain woven AFRP (Aramid fiber reinforced plastic) in hot, wet environmental exposure. Naik *et al.* [2002] presented interlaminar fracture characterization for plain weave fabric E-glass/epoxy laminates. The double cantilever beam test and the end notch flexure test has been used for loading the specimen. Patel and Case [2002] examined the effects of hygrothermal ageing on the durability of a graphite/epoxy woven composite material system. Experimental testing showed that the initial and residual tensile properties of the aged material were virtually unaffected by the imposed environmental aging. Baley *et al*. [2004] investigated the relationship between Glass fiber/Polymer interfaces and interlaminar properties of marine composites. Karbhari [2004] studied e-glass/vinyl ester composites in aqueous environments. In this experiment aqueous immersion of e-glass composites, fabricated by the resin infusion process (unidirectional and bidirectional) were tested to assess the effect of temperature on the short beam shear strength. Ray [2006] conducted mechanical tests on unidirectional carbon composite laminates and woven fiber composite beam specimens at room temperature to assess the environmentally induced damage in composites.

Botelho *et al.* [2006] studied the hygrothermal effects on the interlaminar shear properties of carbon fiber/epoxy composites. The interlaminar shear strength was measured by using short beam shear test and Iosiepescu shear strength. Lua *et al*. [2006] investigated multi-scale dynamic failure prediction tool for marine composite structures. A multi-scale computational framework was established to bridge the response and failure prediction at constituent, ply, and laminated composite level. Zenasni and Bachir [2006] examined the effect of hygro-thermo-mechanical aging on the interlaminar fracture behavior of woven fabric fiber composite materials. Hygro-thermo-mechanical ageing characterization was carried out on double cantilever beam

and notched flexural interlaminar fracture tests in order to determine the loss in crack propagation resistance. Chan *et al.* [2007] proposed an inverse parameter identification technique to determine the elastic interlaminar shear modulus of composite laminates. The technique involved minimizing the difference between an experimentally measured and a numerically determined material response by varying the interlaminar shear modulus in the numerical model. Gigliotti *et al.* [2007] presented the aspects of modeling and the simulation of hygrothermal deformation of composite laminates. The investigation showed the ability of the model to handle complex environmental loading, close to service condition. Sereir and Boualem [2007] investigated the damage of hybrid composites under long term hygrothermal loading and stacking sequence. Fu *et al*. [2008] studied analysis of inter-laminar stresses for composite laminated plate with interfacial damage with a constitutive model. Bergeret *et al.* [1989] examined the influence of the fiber/matrix interface on ageing mechanism of glass fiber reinforced thermoplastic composites in a hygrothermal environment. A study of the properties of short glass fiber reinforced thermoplastic composites based on poly (ethylene terephthalate), poly (butylenes terephthalate) and polyamide-6, 6 in an aggressive environment was reported. Pilli *et al*. [2009] presented the influence of moisture on mechanical behavior and long- term durability of composites. An accelerated humidity test technique was developed where moisture ingression was obtained by increasing the pressure in the test chamber. Tsai *et al.* [2009] investigated the absorption and diffusion of water in carbon fiber/glass fiber hybrid composites. Water absorption experiments, mechanical property test and dynamic mechanical analysis were performed after immersion in water at different temperatures for up to 32 weeks. The behavior of structures subjected to in-plane loads with hygrothermal load is less understood in comparison with structures under ambient temperature. The above studies deal with static analysis of composite plates subjected to hygrothermal loadings. The subsequent literature on composite panels subjected to hygrothermal loadings are classified as vibration, buckling and dynamic stability of composite panels in hygrothermal environment.

2.1.2 Vibration of panels in hygrothermal environment

Due to its significance in structural mechanics, large number of references in the published literature deal with vibration behavior of panels subjected to in-plane

stresses. Exact solutions for panels are available only for free vibration under certain uniform loading conditions under classical boundary conditions. An attempt to have an numerical and experimental solution of the of the free vibration in hygrothermal environment is an important task.

2.1.2.1 Plates

The previous studies on the bending, vibration and buckling of moderately thick plates of different support conditions associated with elevated temperature is reviewed by Tauchert [1991] through 1991. Whitney and Ashton [1971] studied the effect of expansional strains on the elastic response of layered composite plates using a generalized Duhamel-Newmann form of Hooke's law. Numerical results indicate that the expansional strains can substantially affect the gross response characteristics of a composite material. Dhotarad and Ganesan [1978] examined the influence of thermal gradient on natural frequency of rectangular plate vibration using finite difference method and finite element method. Gandhi *et al*. [1988] investigated the nonlinear vibration of moderately thick laminated composite plates in hygrothermal environments. The shear deformable plate theory is modified to account for midplane stretching due to large deflections and dimensional changes in hygrothermal environment. Chen and Lee [1988] presented the thermally induced vibrations of a simply supported orthotropic rectangular plate using differential equation. Chen and Chen [1989] studied the free vibration of the laminated rectangular composite plate exposed to steady state hygrothermal environment using finite element method. Constantinos and Dimitri [1990] examined the effect of elevated temperatures, absorbed moisture, and random external excitation on the dynamic response and structure-borne noise transmission of discretely stiffened flat plates from laminated composite material using analytical approach.

Sai Ram and Sinha [1992] investigated the effects of moisture and temperature on the free vibration of laminated composite plates using finite element method. Noor and Burton [1992] presented analytically the three –dimensional solutions for the free vibrations and buckling of thermally stressed multilayered angle-ply composite plates. Adams and Singh [1995] investigated on the dynamic properties of fiber-reinforced epoxy composites by immersion in sea water. Liu and Huang [1995] studied the free vibration analysis of laminated composite plates subjected to temperature changes

using finite element method to calculate the frequencies of vibration of symmetric cross-ply plates. Eslami and Maerz [1995] investigated the vibration of a symmetric cross-ply plate under unsteady temperature and moisture environment using finite element method. Chen and Chou [1999] presented the free vibration analysis of orthogonal-woven fabric composites analytically using one-dimensional elasto-dynamic analysis. Patel *et al*. [2003] studied static and dynamic characteristics of thick composite laminates exposed to hygrothermal environment using a higher-order finite element method. Rao and Sinha [2003] investigated the effects of temperature and moisture on the free vibration and transient response of multidirectional composites using three dimensional finite element analysis. Shen *et al*. [2004] discussed in detail the effects of hygrothermal conditions on the dynamic response of shear deformable laminated plates resting on elastic foundations using a micro-to-micromechanical analytical model. Huang *et al.* [2004] investigated the nonlinear vibration and dynamic response of shear deformable laminated plates in hygrothermal environments based on higher-order shear deformation plate theory and general Von Karman-type equation of motion.

Young-Wann [2005] examined the vibration characteristics of initially stressed functionally graded rectangular metal and ceramic plates in thermal environment using Rayleigh Ritz method to obtain the frequency equation. Matsunaga [2007] studied the free vibration and stability problems of angle-ply laminated composite and sandwich plates subjected to thermal loading using the method of power series expansion. Atas and Samna [2008] presented an overall view on impact response of woven fabric composite plates. A number of tests were performed to examine the damage process step by step from initiation of damage to final perforation.

Jeyaraj *et al.* [2009] described the vibration and acoustic response characteristics of a fiber-reinforced composite plate in a thermal environment by considering the inherent material damping property of the composite material using finite element method. Lal and Singh [2010] investigated the stochastic free vibration of laminated composite plates subjected to thermal loading with general boundary conditions, taking into account the random material properties and thermal expansion coefficients using finite element method. Gupta *et al*. [2010] studied the thermal gradient effect on vibration of non-homogeneous rectangular plate having bi-direction thickness variation using Rayleigh Ritz method to evaluate the fundamental frequencies.

Fakhari and Ohadi (2011) examined the large amplitude vibration of functional graded material (FGM) plates under thermal gradient and transverse mechanical loads using finite element method. Gupta and Sharma (2011) investigated the effect of linear thermal gradient on vibrations of trapezoidal plates whose thickness varies parabolically using the Raleigh Ritz Technique.

Most of the above studies deal with numerical analysis of vibration behavior of unidirectional composite laminates subjected to hygrothermal conditions. But the experimental studies on the subject are scarce in literature. Anderson and Nayfeh (1996) determined the natural frequencies and mode shapes of laminated composite plates using experimental modal analysis and finite element method. Strait *et al.* [1992] reported experimentally the effect of seawater immersion on the impact resistance of glass fiber reinforced composite materials. The results indicate that moisture induced degradation can significantly reduce the impact resistance of glass fiber reinforced epoxy composites. Naik *et al.* [2000] investigated the static behavior of industry driven woven fabric laminated composite plates under transverse central low-velocity point impact by using a modified Hertz law and a 3D transient finite-element analysis. Chakraborty et *al.* [2000] presented a combined experimental and numerical study of the free vibration of composite FRP plates to determine the respective frequency response functions from which the modal parameters are extracted using finite element method. Chaudhuri *et al.* [2005] presented a combined theoretical and experimental investigation on free vibration of thin anisotropic fiber reinforced plastic rectangular plates. Numerical results presented here pertain to the resonant frequencies of five layer symmetric cross-ply plates with all edges clamped and simply supported, which are, in turn compared with the corresponding experimental results. Botelho *et al*. [2005] obtained experimentally the viscoelastic properties, such as storage modulus and loss modulus of glass/epoxy composites during hygrothermal conditioning. Zai *et al.* [2009] measured experimentally the damping and dynamic stiffness of carbon/epoxy composite beam specimens with a focus on the effect of moisture absorption.

2.1.2.2 Shells

The widespread use of shell structures in aerospace and hydrospace applications has stimulated many researchers to study various aspects of their structural behavior. In

the present study an attempt is made to the reviews on shells in the context of the present work and discussions are limited to vibration and stability.

Huang and Tauchert [1991] investigated the large deformation behavior of anti-symmetric angle-ply laminates under non-uniform temperature loading. A finite element procedure for the geometrically nonlinear analysis of linear viscoelastic laminated composite systems subjected to mechanical and hygrothermal load was presented by Marques and Creus [1994]. The formulation was implemented by considering three-dimensional degenerated shell element. The vibration response of flat and curved panels subjected to thermal and mechanical loads are presented by Librescu and Lin [1996]. Gandhi *et al.* [1998] studied nonlinear vibration of laminated composite plates in hygrothermal environments. In their analysis the formulations were based on the first-order shear deformable plate theory (FSDPT) and the numerical results were only for free vibration of a cantilevered laminated composite beam. Parhi *et al.* [2001] investigated the effect of moisture and temperature on the dynamic behavior of composite laminated plates and shells with or without delaminations. The dynamic analysis of laminated cross-ply composite non-circular thick cylindrical shells subjected to thermal/mechanical load are carried out based on higher-order theory was studied by Ganapathi *et al.* [2002]. The nonlinear free vibration behavior of laminated composite shells subjected to hygrothermal environment was investigated by Naidu and Sinha [2006]. The geometrically non-linear vibrations of linear elastic composite laminated shallow shells under the simultaneous action of thermal fields and mechanical excitations are analysed by Ribeiro and Jansen [2008]. The vibration characteristics of pre- and post-buckled hygro-thermo-elastic laminated composite doubly curved shells were investigated by Kundu and Han [2009]. Panda and Singh [2011] studied the nonlinear free vibration behaviour of single/doubly curved shell panel is addressed within the post-buckled state where thermal post-buckling of shell panel is accounted for a uniform temperature field.

2.1.3: Buckling effects of composite panels in hygrothermal environment

The buckling of mechanical, civil engineering structures under compressive loading has always been a important field of research with the introduction of steel a century

ago. More recently, there is a renewed interest with development of aviation and an aerospace program during the 1960's which is still expanding to offshore and nuclear engineering.

2.1.3.1 Plates

Plenty of studies are available on buckling behavior of composite plates under ambient temperature and moisture conditions and reviewed by Leissa [1987]. Tauchert [1991] reviewed the previous works on buckling and post buckling characteristics associated with elevated temperatures of thin and moderately thick plates having various plan forms and support conditions through 1991. Flags and Vinson [1978] proposed the hygrothermal effects on the buckling of laminated composite plates based on the Theorem of Minimum potential Energy. Chen and Chen [1987] observed the thermal buckling of laminated composite plate subjected to a temperature change using Galerkin's method.

Thagaratnam *et al.* [1989] studied the buckling analysis of composite laminates for critical temperature, based on linear theory and the finite element method using semiloof elements. Chen *et al*. [1991] analysed the thermal buckling of anti-symmetric cross-ply laminates having central circular holes subjected to uniform or non-uniform temperature distribution using finite element method. Sai Ram and Sinha [1992] investigated the effects of moisture and temperature on the buckling of laminated composite plates using finite element method. Sai Ram and Sinha [1992] studied the vibration and buckling of laminated plates with a cutout in hygrothermal environment using the superposition method. Noor and Burton [1992] presented analytically the three-dimensional solutions for the free vibrations and buckling of thermally stressed multilayered angle-ply composite plates. Prabhu and Dhanraj [1993] observed the thermal buckling analysis of symmetric cross-ply and symmetric angle-ply laminates using the finite element method. Chao and Shyu [1996] investigated the nonlinear buckling behavior of fiber-reinforced laminated composite plates under hygrothermal environment using finite element method. Loughlan [1999] studied the influence of bend-twist coupling on the shear buckling response of thin laminated composite plates using finite strip method.

Thompson and Loughlan [2000] examined the control of the post buckling response in thin composite plates using smart technology. Babu and Kant [2000] proposed with

a refined higher order finite element models for thermal buckling of laminated composite and sandwich plates. Spallino and Thierauf [2000] presented the thermal buckling optimization of laminated composite plates subjected to rise in temperature using evolution strategies and a guided random-search method. Shen [2000] examined the influence of hygrothermal effects on the postbuckling of shear deformable laminated plates subjected to uniaxial compression using a micro-to-macro-mechanical analytical model of a laminate. Zenkour and EL-Sheikh [2001] presented the buckling of anisotropic elastic plates analytically using simple and mixed shear deformation theories for various boundary conditions.

Patel *et al*. [2003] studied the static and dynamic characteristics of thick composite laminates exposed to hygrothermal environment using a higher-order finite element method. Xiao and Chen [2005] investigated the dynamic and buckling analysis of a thin elastic-plastic square plate in uniform temperature field using Hamilton's variational principle. Jones [2005] examined the thermal buckling of uniformly heated unidirectional and symmetric cross-ply laminated fiber-reinforced composites uniaxial in-plane restrained simply supported rectangular plates. Shariyat [2007] examined the thermal buckling analysis of rectangular composite multilayered plates under uniform temperature rise using a layerwise plate theory and von Karman strain-displacement equations. Matsunaga [2007] studied the free vibration and stability problems of angle-ply laminated composite and sandwich plates subjected to thermal loading using the method of power series expansion. Singh and Verma [2008] investigated the hygrothermal effects on the buckling of laminated composite plates with random geometric and material properties using finite element method. Kumar and Singh [2008] presented the thermal buckling analysis of laminated composite plates subjected to uniform temperature distribution using finite element method. Lal *et al.* [2009] examined the effects of random system properties on thermal buckling load of laminated composite plates under uniform temperature rise using finite element method. Lal and Singh [2010] presented the effect uncertain system properties thermo-elastic stability of laminated composite plates under nonuniform temperature distribution using a C^0 finite element method. Pandey *et al.* [2010] observed the effects of moisture and temperature on the post buckling response of a laminated composite plate subjected to hygro-thermo-mechanical loadings using finite double Chebyshev series. Dash *et al.* [2011] presented an experimental study on the

effects of corrosion on elastic buckling and post buckling response of unidirectional E-glass/epoxy composite rectangular plates subjected to compressive load and liquid environment exposure.

2.1.3.2 Shells

The studies involving stability of composite shell under hygrothermal loads are much less in literature. The finite element method was applied to study the problem of moisture and temperature effects on the stability of a general orthotropic cylindrical composite shell panels subjected to axial or in-plane shear loading by Lee and Yen [1989]. Shen [1990] investigated the influence of hygrothermal effects on the buckling and postbuckling of composite laminated cylindrical shells subjected to axial compression using a micro-to-macro mechanical analytical model. The effect of hygrothermal conditions on the post buckling of shear deformable laminated cylindrical shells subjected to combined loading of axial compression and external pressure was investigated using micro-to-macro mechanical analytical model by Shen [2001]. The hygrothermoelastic buckling behaviour of laminated composite shells were numerically simulated using geometrically nonlinear finite element method was studiedby Kundu and Han [2009]. The effect of random system properties on the post buckling load of geometrically nonlinear laminated composite cylindrical shell panel subjected to hygro-thermo-mechanical loading is investigated by Lal *et al.* [2011].

2.1.4: Dynamic stability of composite panels in hygrothermal Environment

The study of dynamic stability is an important class of problem in structural mechanics and the first observation of parametric resonance or dynamic instability is attributed to Faraday in 1831.

2.1.4.1 Plates

The behavior of composite panels subjected to in-plane periodic loads is much less understood. Few literatures are available on dynamic instability of unidirectional composite plates under ambient temperature and moisture subjected to periodic in-plane loads. Bert and Birman [1987] studied the dynamic instability of shear deformable anti-symmetric angle-ply plates by using finite element method. Srinivasan and Chelapandi [1986] studied the dynamic stability of rectangular plates

due to periodic in-plane load by using finite strip method. Moorty *et al*. [1990] presented the parametric instability of laminated composite shear deformable flat panels subjected to in-plane edge loads using finite element method. Chen and Yang [1990] investigated on the dynamic stability of laminated composite plates by Galerkin finite element method. Zhou [1991] observed the theory of nonlinear dynamic stability of composite laminated plates using Hamilton principle. Kwon [1991] examined the dynamic instability of layered composite plates by finite element method by using higher-order bending theory. Mond and Cederbaum [1992] presented the dynamic stability of anti-symmetric laminated plates by using the method of multiple scales. Liao and Cheng [1994] observed the dynamic instability of stiffened laminated composite plates subjected to pulsating forces using finite element equation of motion. Balmurugan *et al.* [1996] studied nonlinear dynamic instability of laminated composite plates using finite element model.

Ganapathi [1998] proposed the dynamic instability of laminated composite plates subjected to thermal loads using first order shear deformation theory and Lagrange's equation. Patel *et al.* [1999] investigated on the dynamic instability of laminated composite plates supported on elastic foundations, subjected to periodic in-plane loads, using C^1 eight-nodded shear-flexible plate element. Chatopadhaya and Radu [2000] studied the dynamic instability of composite laminates using a higher order theory. The procedure implemented by using the finite element approach. Sahu and Dutta [2000] investigated the dynamic instability of laminated composite rectangular plates subjected to non-uniform harmonic in-plane edge loading using finite element methods. Wang and Dawe [2002] proposed the dynamic instability of composite laminated rectangular plates by using Lagrange's formulation. Ravi Kumar *et al.* [2003] examined the vibration and dynamic instability behavior of laminated composite plates subjected to partially distribute non conservative follower forces. Liew *et al*. [18] presented the dynamic analysis of laminated composite plates with piezoelectric sensor/actuator patches using mesh free method.

Wu and Shih [2005] presented the dynamic stability of rectangular plates with an edge crack by applying Galerkin's method. Wu and Shih [2006] studied the dynamic instability of arbitrarily laminated skew plates based on Von Karmans plate theory, the large amplitude dynamic equation of thin laminated plates are derived by applying double Fourier series. Chakrabarti and Sheikh [2006] studied the dynamic instability

of laminated sandwich plates subjected to in-plane partial edge loading by using finite element method. Dey and Singh [2006] examined the dynamic stability characteristics of simply supported laminated composite skew plates subjected to a periodic in-plane load by using finite element approach. Saburcu and Evran [2006] observed the dynamic stability of a rotating pre-twisted asymmetric cross-section Timoshenko beam subjected to an axial periodic force. Patel *et al*. [2007] proposed the dynamic instability analysis of stiffened shell panels subjected to partial edge loading along the edges using Hill's infinite determinant. Liew *et al*. [2007] investigated the dynamic stability analysis of thin laminated cylindrical panels under static and periodic axial forces by using the mesh-free Ritz method. Lanhe *et al*. [2007] studied the dynamic stability analysis of FGM plates by the moving least squares differential quadrature method. Udar and Datta [2007] investigated the combination of resonances in parametrically excited simply supported laminated composite doubly curved panels under uniform edge loading using finite element technique. Asha and Sahu [2008] examined the dynamic stability of laminated composite pre-twisted cantilever panels by using finite element method. Chen *et al*. [2009] studied the dynamic stability of laminated hybrid composite plates subjected to periodic uniaxial and bending stress and the instability region is marked by Bolotin's method. Fazilati and Ovesy [2010] presented the dynamic instability analysis of thin walled composite structures using finite strip method. The effects of various parameters on the instability regions were located using Bolotin's approach. Biswas *et al*. [2011] studied the static and dynamic instability characteristics of curved laminates with internal damage subjected to follower loading using finite element approach

2.1.4.2 Shells

The parametric resonance characteristics of composite shells are studied by few investigators without considering the hygrothermal effects. The dynamic stability or phenomenon of parametric resonance in cylindrical shells under periodic loads has attracted much attention due to its detrimental and de-stabilizing effects in many engineering applications. This phenomenon in elastic systems was first studied by Bolotin [1964], where the dynamic instability regions were determined. Yao [1965] examined the non-linear elastic buckling and parametric excitation of a cylinder under axial loads. The parametric instability of circular cylindrical shells was also discussed by Vijayaraghavan and Evan-Iwanowskj [1967].

Based on the donnell's shell equations, the dynamic stability of circular cylindrical shells under both static and periodic compressive forces was examined by Nagai and Yamaki [1988] using Hsu's method. Bert and Birman [1990] extended Yao's [1965] approach to the parametric instability of thick orthotropic shells using higher-order theory. Liao and Cheng [1994] proposed a finite element model with a 3-D degenerated shell element and a 3-D degenerated curved beam element to investigate the dynamic stability of stiffened isotropic and laminated composites plates and shells subjected to in-plane periodic forces. Argento and Scott [1993] employed a perturbation technique to study the dynamic stability of layered anisotropic circular cylindrical shells under axial loading. Using the same method, Argento [1993] later analyzed the dynamic stability of a composite circular cylindrical shell subjected to combined axial and torsional loading. The study of the parametric instability behavior of curved panels, the effects of curvature and aspect ratio on dynamic instability for a uniformly loaded laminated composite thick cylindrical panel is studied by Ganapathi *et al.* [1994] using finite element method.

The dynamic instability of laminated composite circular cylindrical shells is studied by Ganapathi and Balamurugan [1998] using a C^0 shear flexible two nodded axisymmetric shell element. The effects of various parameters such as ply angle, thickness, aspect ratio, axial and circumferential wave numbers on dynamic stability are studied. The dynamic stability of thin cross-ply laminated composite cylindrical shells under combined static and periodic axial force is investigated by NG *et al*. [1998] using Love's classical theory of thin shells. The effects of different lamination scheme and the magnitude of the axial load on the instability regions are examined using Bolotin's method. Most of the above mentioned investigators studied the dynamic stability of uniformly loaded closed cylindrical shells with a simply supported boundary condition. The parametric instability of laminated composite conical shells under periodic loads is studied of Ganapathi *et al.* [1999]. The parametric resonance characteristics of laminated composite doubly curved panels subjected to non-uniform loading was investigated by Sahu and Datta [2001]. The dynamic stability behavior of laminated composite curved panels with cutouts subjected to in-plane static and periodic compressive loads was studied by Sahu and Dutta [2003]. A numerical technique is developed for the dynamic stability analysis of composite laminated cylindrical shell under static and periodic axial forces by

mesh-free kp-Ritz method by Liew *et al.* [2006]. Quantitative results are presented to show the effects of curvature, ply orientation, and degree of orthotropy, geometry and number of layers of laminate on dynamic stability of composite plates for different temperature and moisture concentrations.

The study of the dynamic instability of laminated composite plates and shells in hygrothermal environment are relatively new and there were no references found in this area.

2.1.5: Critical Discussion

On the whole, the focus of the research is changing from vibration to buckling effects and then to dynamic stability. Recently more studies are conducted on woven fiber composites than unidirectional composite materials. The structural configuration has shifted from one dimensional beams to plates and shells. As regards to the methodology, the focus is shifted from numerical method to experimental method for free vibration and buckling effects in hygrothermal environment. More studies are made for dynamic stability of composite plates and shells using finite element methods in hygrothermal environment.

The study reveals that investigators are now concentrating on analysis of complicated aspects of different parameters including hygrothermal conditions of plates and shells. From the above review of literature, the inherent lacunae of earlier investigations which need further attention of future researchers are summarized below.

2.1.5.1: Vibration of composite panels in hygrothermal environment

The literature on free vibration of laminated composite plates under ambient temperature and moisture conditions is vast. However, the studies involving vibration of woven fiber laminated plates subjected to hygrothermal conditions are less in literature.

The previous studies on the bending, vibration and buckling of moderately thick plates of different support conditions associated with elevated temperature is reviewed by Tauchert [1991]. The free vibration of laminated composite plates in hygrothermal environment by using finite element method has also been studied by (Chen and Chen [1989], Sai Ram and Sinha [1992]) analysis lead to analytical method. Most of the

above studies deal with numerical analysis of vibration behavior of unidirectional composite laminates subjected to hygrothermal conditions. However, experimental studies on the free vibration are scarce in literature. Anderson and Nayfeh [1996] determined the natural frequencies and mode shapes of laminated composite plates by experimental modal analysis using finite element method. A combined experimental and numerical study on the free vibration of composite plates to determine the respective frequency response functions from which the modal parameters are extracted using finite element method by (Chakraborty *et al*. [2000], Chaudhury *et. al*. [2005]) without hygrothermal conditions.

The analysis of shell structures has a long history starting with the membrane theory and then the bending theories. The nonlinear free vibration of composite shells in hygrothermal environment has been studied by (Marques and Creus [1994], Librescu and Lin [1996], Parhi *et al.* [2001], Naidu and Sinha [2006], Ribeiro and Jansen [2008]). Nonlinear free vibration behaviour of single/doubly curved shell panel in post-buckled state was investigated by (Kundu and Han [2009], Panda and Singh [2011]). Most of the above studies deal with numerical analysis of free vibration behaviour of unidirectional composite shells under ambient temperature and moisture conditions. However, studies on the free vibration behavior of composite shells subjected to hygrothermal conditions are scarce in literature for which this subject research is for practical interest.

2.1.5.2: Buckling effects of composite panels in hygrothermal environment

Plenty of studies are available on buckling behavior of composite plates under ambient temperature and moisture conditions reviewed the previous works on buckling and post buckling characteristics associated with elevated temperatures of thin and moderately thick plates having various plan forms and support conditions by (Leissa [1987], Tauchert [1991]). Many investigators worked on buckling analysis of laminated composite plates in thermal environment using different methods by (Chen and Chen [1987], Chen *et al.* [1991], Spallino and Thierauf [2000], Xiao and Chen [2005], Jones [2005], Shariyat [2007]). Sai Ram and Sinha [1992] investigated the effects of moisture and temperature on the buckling of laminated composite plates using finite element method analytically. Studies were also conducted for composite

plates in thermal environment using finite element method by (Prabhu and Dhanraj [1993], Singh and Verma [2008], Lal and Singh [2010]). Hygrothermal effects on the buckling of laminated composite plates based on different methods have been proposed by (Flags and Vinson [1978], Shen [2000], Pandey *et al.* [2010]). Most of the above studies deal with numerical analysis of buckling effects of unidirectional composite plates subjected to hygrothermal conditions. However, experimental studies on the buckling effects are scarce in literature. So, the buckling behavior of woven fiber laminated composite plates subjected to hygrothermal environments are of tremendous technical importance for understanding the behavior of laminated composite plates subjected in-plane loads.

Most of the above studies deal with numerical analysis of buckling effects of unidirectional composite shells subjected to hygrothermal conditions. The recent investigations are based on shear deformable cylindrical and doubly curved shells or panels. The study on buckling effects of doubly curved shells subjected to in-plane stresses in hygrothermal environment is new. Hygrothermal buckling and post buckling of composite was investigated by (Shen [1990], Shen [2001]) using micro-to-macro mechanical analytical model. The hygrothermoelastic buckling behaviour of laminated composite shells were numerically simulated using geometrically nonlinear finite element method was studied by Kundu and Han [2009]. The effect of random system properties on the post buckling load of geometrically nonlinear laminated composite cylindrical shell panel subjected to hygro-thermo-mechanical loading is investigated by Lal *et al.* [2011]. However, studies on the buckling effects of woven fiber composite shells in hygrothermal environment are scarce in literature for which this subject needs scope for peer attention.

2.1.5.3: Dynamic stability of composite panels in hygrothermal Environment

The studies on dynamic stability of structures are much less in comparison to static stability and got a boost after Bolotin's [1964] contribution to the literature. The dynamic stability of shear deformable plates was studied by Moorty *et al*. [1990] using finite element method. Mond and Cederbaum [1992] presented the dynamic stability of anti-symmetric laminated plates by using the method of multiple scales. The instability results of thin simply supported plates (Dey and Singh [2006]) plates

are sparsely treated in literature. The dynamic stability of composite plates has been studied using FEM by (Liao and Cheng [1994], Chen and Yang [1990], Chakrabarti and Sheikh [2006]). Bert and Birman [1987] studied the dynamic instability of shear deformable anti-symmetric angle-ply plates by using FEM. Nonlinear dynamic stability of composite plates using different principle wsa proposed by (Cheng-ti [1991], Balmurugan *et al.* [1996]). (Kwon [1991], Chatopadhaya and Radu [2000]) examined the dynamic instability of composite plates by finite element method using higher-order theory. Studies were also conducted for the dynamic stability of rectangular plates due to periodic in-plane load by using finite strip method by (Srinivasan and Chelapandi [1986], Fazilati and Ovesy [2010]). Ganapathi [1998] proposed the dynamic instability of composite plates subjected to thermal loads using first order shear deformation theory and Lagrange's equation. Few literatures are available on dynamic instability of unidirectional composite plates under ambient temperature and moisture subjected to periodic in-plane loads Sahu and Dutta [2000] using finite element methods. No studies are available on parametric instability of industry driven woven fiber laminated composite plates in hygrothermal environment and thus it becomes the subject of this investigation.

The parametric resonance characteristics of composite shells are studied by few investigators without considering the hygrothermal effects. The parametric instability of circular cylindrical shells was studied by (Yao [1965], Vijayaraghavan and Evan-Iwanowskj [1967]. Based on the donnell's shell equations, the dynamic stability of circular cylindrical shells under both static and periodic compressive forces was examined by Nagai and Yamaki [1988]. The dynamic stability of layered anisotropic circular cylindrical shells under axial loading using perturbation technique was investigated by (Argento and Scott [1993], Argento [1993]).

The dynamic instability of a uniformly loaded laminated composite thick cylindrical panel is studied by Ganapathi *et al.* [1994] using finite element method. The dynamic stability of thin cross-ply laminated composite cylindrical shells under combined static and periodic axial force was investigated by NG *et al*. [1998] using Love's classical theory of thin shells. However, studies on the dynamic stability of woven fiber composite shells in hygrothermal environment are scarce in literature for which this subject interest is necessary for investigation.

2.1.6: Aim and scope of the present study

A review of the literature shows that a lot of work has been done on the vibration and buckling of laminated composite plates in hygrothermal environment, but no experimental work is reported in literature on vibration and buckling of industry driven woven fiber composite plates subjected to hygrothermal conditions. Besides this, the dynamic instability of composite plates in ambient environment is only reported. No work is reported in literature on parametric instability of laminated composite plates subjected to hygrothermal environment. The present study is mainly aimed at filling some of the lacunae that exist in the proper understanding of the dynamic stability of laminated composite plates in hygrothermal environment and in-plane periodic loads. Based on the review of literature, the different problems identified for the present investigation are presented as follows

- Experimental and numerical study on vibration of woven fiber laminated composite plates in hygrothermal environment
- Experimental and numerical study on buckling effects of woven fiber laminated composite plates in hygrothermal environment
- Parametric instability of laminated composite plates in hygrothermal environment
- Parametric resonance characteristics of laminated composite shells in hygrothermal environment

Due to its practical importance and uniqueness in the above fields, the influences of various parameters such as aspect ratio, side to thickness ratio, static and dynamic load factors, ply orientations, lamination angle, orthotropic on the parametric resonance characteristics of laminated composite plates under higher temperature and moisture environments are examined in detail. However, a complete parametric study on the static behavior especially the variation of interlaminar shear strength on the loading speed, different proportion of fiber to matrices, type of matrices, exposure time of composite specimens subjected to hygrothermal loading is also is studied for completeness.

CHAPTER 3

MATHEMATICAL FORMULATION

3.1: The Basic Problems

The basic configuration of the problem considered here is a doubly curved panel with in-plane harmonic loadings under hygrothermal environment as shown in figure 3.1.The choice of the doubly curved panel geometry as a basic configuration has been made so that depending on the value of curvature parameter, plate, cylindrical panel and different doubly curved panels such as spherical configurations can be considered as special cases.

The mathematical formulation for vibration, buckling and dynamic stability behavior of laminated composite plates and shells subjected to moisture and temperature are presented. Consider a laminated plate of uniform thickness 't' consisting of a number of thin lamiae, each of which may be arbitrarily oriented at an angle 'θ' with reference to the X-axis of the co-ordinate system as shown in Figures 3.2 and 3.3.

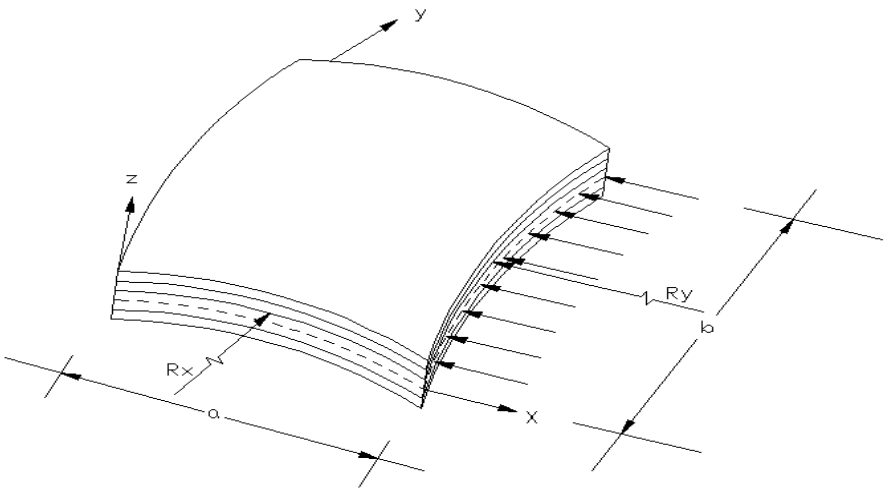

Figure 3.1: Laminated composite curved panels under in-plane harmonic loading under hygrothermal environment

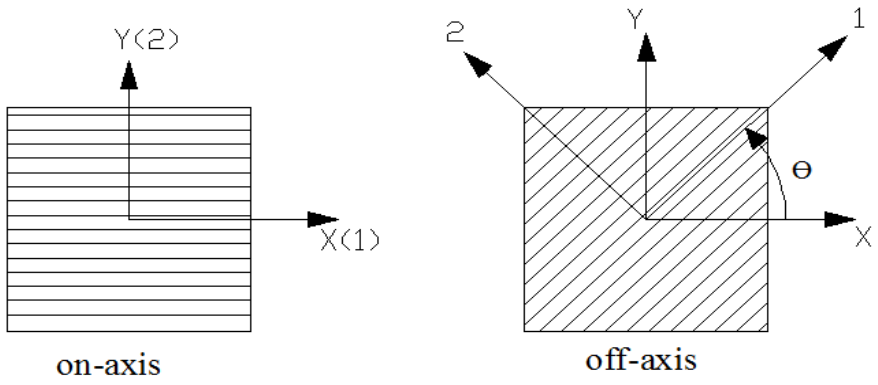

Figure 3.2: Arbitrarily oriented laminated plate

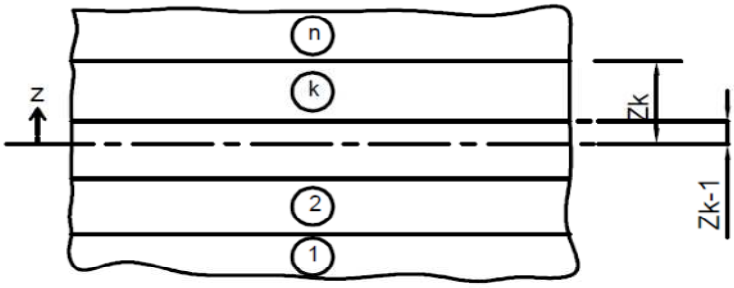

Figure 3.3: Geometry of an n-layered laminate

3.2: Proposed Analysis

The governing equations for the dynamic stability of laminated composite doubly curved panels subjected to hygrothermal loading are developed. The presence of hygrothermal loading in the panel induces a in-plane stress field in the structures. This necessitates the determination of stress field as a prerequisite to the solution of the problem like vibration, buckling and dynamic stability behavior of plates and shells with different temperature and moisture. As the thickness of the structure is relatively smaller, the determination of stress field reduces to the solution of a plane stress problem. Due to the in-plane harmonic load the equation of motion represents second order Mathieu-Hill type. The development of the regions of instability arises from Floquet's theory and the solution is obtaining using Bolotin's approach using finite element method (FEM). The governing differential equations have been developed using first order shear deformation theory (FSDT). The assumptions made in this analysis are summarized as follows:

3.2.1: Assumptions of the Analysis

1. The analysis is linear with a few exceptions. This implies both linear constitutive relations (generalized Hooke's law for the material and linear kinematics) and small displacement to accommodate small deformation theory.

2. The curved panels are of various shapes with no initial imperfections. The considerations of imperfections are less important for dynamic loading.

3. This theory can be considered to be an extension of Sander's theory to doubly curved panels, considering transverse shear and rotary inertia. The straight line that is perpendicular to the neutral surface before deformation remains straight but not normal after deformation (FSDT). The thickness of the shell is small compared with the principal radii of curvature. Normal stress in z direction is neglected.

4. The loading considered is axial with a simple harmonic fluctuation with respect to time.

5. All damping effects are neglected.

3.3: Governing Equations

The governing differential equations for vibration of a shear deformable laminated composite plates and shells in general are specified here. The behavior of laminated composite plates in hygrothermal environment derived on the basis of first order shear deformation theory subjected to in-plane loads are;

$$\frac{\partial N_x}{\partial x}+\frac{\partial N_{xy}}{\partial y}+\frac{Q_x}{R_x}+\frac{Q_y}{R_{xy}}=P_1\frac{\partial^2 u}{\partial t^2}+P_2\frac{\partial^2 \theta_x}{\partial t^2} \tag{3.3.1}$$

$$\frac{\partial N_{xy}}{\partial x}+\frac{\partial N_y}{\partial y}+\frac{Q_y}{R_y}+\frac{Q_x}{R_{xy}}=P_1\frac{\partial^2 v}{\partial t^2}+P_2\frac{\partial^2 \theta_y}{\partial t^2} \tag{3.3.2}$$

$$\begin{aligned}&\frac{\partial Q_x}{\partial x}+\frac{\partial Q_y}{\partial y}-\frac{N_x}{R_x}-\frac{N_y}{R_y}-2\frac{N_{xy}}{R_{xy}}+N_x^a\frac{\partial^2 w}{\partial x^2}+N_y^a\frac{\partial^2 w}{\partial y^2}+N^a{}_{xy}\frac{\partial^2 w}{\partial x\partial y}\\&+N_x^n\frac{\partial^2 w}{\partial x^2}+N_y^n\frac{\partial^2 w}{\partial y^2}+N^n{}_{xy}\frac{\partial^2 w}{\partial x\partial y}=P_1\frac{\partial^2 w}{\partial t^2}\end{aligned} \tag{3.3.3}$$

$$\frac{\partial M_x}{\partial x}+\frac{\partial M_{xy}}{\partial y}-Q_x=P_3\frac{\partial^2 \theta_x}{\partial t^2}+P_2\frac{\partial^2 u}{\partial t^2} \tag{3.3.4}$$

$$\frac{\partial M_{xy}}{\partial x}+\frac{\partial M_{y}}{\partial y}-Q_{y}=P_{3}\frac{\partial^{2}\theta_{y}}{\partial t^{2}}+P_{2}\frac{\partial^{2}v}{\partial t^{2}} \tag{3.3.5}$$

$$(P_{1},P_{2},P_{3})=\sum_{k=1}^{n}\int_{z_{k-1}}^{z_{k}}(\rho)_{k}(1,z,z^{2})dz \tag{3.3.6}$$

3.4: Dynamic stability studies

The equation of motion for vibration of a laminated composite panel in hygrothermal environment, subjected to generalized in-plane load, may be expressed in the matrix form as:

$$[M]\{\ddot{q}\}+[[K]+\left[K^{r}{}_{g}\right]-N(t)[K_{g}]]\{q\}=0 \tag{3.4.1}$$

'q' is the vector of degrees of freedoms (u, v, w, θ_x, θ_y). The in-plane load 'N (t)' may be harmonic and can be expressed in the form:

$$N\ (t)\ =\ N_{s}\ +\ N_{t}Cos\ \ \Omega\ t \tag{3.4.2}$$

Where N_s the static portion of load N (t), N_t the amplitude of the dynamic portion of N (t) and Ω is the frequency of the excitation. The stress distribution in the panel may be periodic. Considering the static and dynamic component of load as a function of the critical load,

$$N_{s}=\alpha N_{cr}\ ,\ \ N_{t}=\beta N_{cr} \tag{3.4.3}$$

Where α and β are the static and dynamic load factors respectively. Using Eq. (5), the equation of motion for panel in hygrothermal environment under periodic loads in matrix form may be obtained as:

$$[M]\{\ddot{q}\}+[[K\ ]+\left[K^{r}{}_{g}\right]-\alpha N_{cr}[K_{g}]-\beta N_{cr}[K_{g}]Cos\Omega t]\{q\}=0 \tag{3.4.4}$$

The above Eq. (3.4.4) represents a system of differential equations with periodic coefficients of the Mathieu-Hill type. The development of regions of instability arises from Floquet's theory which establishes the existence of periodic solutions of periods T and 2T. The boundaries of the primary instability regions with period 2T, where

T=2 π/Ω are of practical importance and the solution can be achieved in the form of the trigonometric series:

$$q(t) = \sum_{k=1,3,5,..}^{\infty} [\{a_k\} Sin(k\Omega t/2) + \{b_k\} Cos(k\Omega t/2)] \qquad (3.4.5)$$

Putting this in Eq. (3.4.4) and if only first term of the series is considered, equating coefficients of Sin Ωt/2 and Cos Ωt/2, the equation (3.4.4) reduces to

$$[M] \sum_{K=1,3,5}^{\infty} -\left(\frac{K\Omega}{2}\right)^2 \left(\{a_K\} Sin(\frac{K\Omega t}{2}) + \{b_K\} Cos\left(\frac{K\Omega t}{2}\right)\right) + [[K] + [K^r{}_g]$$
$$-\alpha P_{cr}[K_g] - \beta P_{cr}[K_g] Cos\Omega t \;] \left(\{a_K\} Sin\left(\frac{k\Omega t}{2}\right) + \{b_K\} + Cos\left(\frac{K\Omega t}{2}\right)\right) = 0 \qquad (3.4.6)$$

Equating the coefficients of the sine and cosine terms leads to a series of algebraic equations for the vectors $\{a\}_K$ and $\{b\}_K$ for determination of instability regions. For non-trival solution, the infinite determinants of the coefficients of the groups of homogeneous equation are equal to zero. Approximate solution can be obtained by truncating the determinants. Principal instability regions, which is of practical interest corresponds to K=1 and for this instability conditions leads to in line with the Bolotin.

$$[\,[K] + [K^r{}_g\,] - \alpha P_{cr}[K_g] \pm \frac{1}{2}\beta P_{cr}[K_g] - \frac{\Omega^2}{4}[M]\,]\{q\} = 0 \qquad (3.4.7)$$

Eq. (3.4.7) represents an eigenvalue problem for known values of α, β and P_{cr}. The two conditions under the plus and minus sign correspond to two boundaries (upper and lower) of the dynamic instability region. The above eigenvalue solution give of Ω, which give the boundary frequencies of the instability regions for the given values of α and β. In this analysis, the computed static buckling load of the panel is considered as the reference load. Before solving the above equations, the stiffness matrix [K] is modified through imposition of boundary conditions. The equation reduces to other problems as follows:

Free Vibration: α=0, β=0 and Ω=2ω

$$[\,[K] + [K^r{}_g]\,] - \omega_n{}^2 \;\; [M\,]\{q\} = 0 \qquad (3.4.8)$$

Buckling: α=1, β=0 and Ω=0

$$[\,[K]+[K^{r}{}_{g}]\,]-\lambda[K_{g}]\{q\}=0 \qquad (3.4.9)$$

3.5: Constitutive Relations

The constitutive relations for the Composite plate and shell subjected to moisture and temperature is given by:

$$\{F\}=[D]\{\varepsilon\}-\{F^{N}\} \qquad (3.5.1)$$

Where $\{F\}=\{N_x,N_y,N_{xy},M_x,M_y,M_{xy},Q_x,Q_y\}^T$

$\{F^N\}=\{N_x{}^N,N_y{}^N,N_{xy},M_x{}^N,M_y{}^N,M_{xy}{}^N,0,0\}^T$

$\{\varepsilon\}=\{\varepsilon_x,\varepsilon_y,\gamma_{xy},K_x,K_y,K_{xy},\varphi_x,\varphi_y\}^T$

$$[D]=\begin{bmatrix} A_{11} & A_{12} & A_{16} & B_{11} & B_{12} & B_{16} & 0 & 0 \\ A_{12} & A_{22} & A_{26} & B_{12} & B_{22} & B_{26} & 0 & 0 \\ A_{16} & A_{26} & A_{66} & B_{16} & B_{26} & B_{66} & 0 & 0 \\ B_{11} & B_{12} & B_{16} & D_{11} & D_{12} & D_{16} & 0 & 0 \\ B_{12} & B_{22} & B_{26} & D_{12} & D_{22} & D_{26} & 0 & 0 \\ B_{16} & B_{26} & B_{66} & D_{16} & D_{26} & D_{66} & 0 & 0 \\ 0 & 0 & 0 & 0 & 0 & 0 & S_{44} & S_{45} \\ 0 & 0 & 0 & 0 & 0 & 0 & S_{45} & S_{55} \end{bmatrix}$$

The non-mechanical force and moment resultants due to moisture and temperature are expressed as follows.

$$\{N_x{}^N,N_y{}^N,N_{xy}{}^N\}^T=\sum_{K=1}^{n}(\overline{Q_{ij}})\{\varepsilon\}_k(z_k-z_{k-1}) \qquad \text{For } i,\ j\ =1,2,6 \qquad (3.5.2)$$

$$\{M_x{}^N,M_y{}^N,M_{xy}{}^N\}^T=\frac{1}{2}\sum_{K=1}^{n}(\overline{Q_{ij}})_k\{\varepsilon\}_k(z_k{}^2-z_{k-1}{}^2) \qquad \text{For } i,\ j\ =1,2,6 \qquad (3.5.3)$$

Where

$$\{\varepsilon\}_N=\{\varepsilon_{xN},\varepsilon_{yN},\varepsilon_{xyN}\}^T=[T]\{\beta_1\beta_2\}_k{}^T(C-C_O)+[T]\{\alpha_1\alpha_2\}_k{}^T(T-T_O) \qquad (3.5.4)$$

in which

$[T]$= Transformation matrix due to moisture and temperature and is given as

$$[T]=\begin{bmatrix}\cos^2\theta & \sin^2\theta \\ \sin^2\theta & \cos^2\theta \\ \sin 2\theta & \cos 2\theta\end{bmatrix} \qquad (3.5.5)$$

The stiffness coefficient is defined as

$$\left(A_{ij},B_{ij},D_{ij}\right)=\sum_{k=1}^{n}\int_{z_{k-1}}^{k}\left[Q_{ij}\right]_k\left(1,z,z^2\right)\mathrm{dz} \qquad \text{(i, j =1.2.6)} \qquad (3.5.6)$$

$$S_{ij}=\kappa\sum_{k=1}^{n}\int_{z_{k-1}}^{k}\left[Q_{ij}\right]_k\,dz \qquad \text{(i, j =4,5)} \qquad (3.5.7)$$

A shear correction factor of 5/6 is included in S_{ij} for all numerical computations in line with previous studies [Wang and Dawe 2002]

$\left(\overline{Q_{ij}}\right)_{\mathrm{k}}$ in equations 11 and 12 is defined as:

$$[\overline{\mathrm{Q_{ij}}}]_k=[T_1]^{-1}\left[Q_{ij}\right]_k[T_1]^{-T} \qquad (i,\ j\ =1,\ 2,\ 6) \qquad (3.5.8)$$

$$\left[\overline{Q}_{ij}\right]_k=[T_2]^{-1}\left[Q_{ij}\right]_k[T_2] \qquad (i,\ j\ =4,\ 5) \qquad (3.5.9)$$

Where $$[T_1]=\begin{bmatrix}\cos^2\theta & \sin^2\theta & \sin\theta\cos\theta \\ \sin^2\theta & \cos^2\theta & -\sin\theta\cos\theta \\ -2\sin\theta\cos\theta & 2\sin\theta\cos\theta & \cos^2\theta-\sin^2\theta\end{bmatrix} \qquad (3.5.10)$$

$$[T_2]=\begin{bmatrix}\cos\theta & \sin\theta \\ -\sin\theta & \cos\theta\end{bmatrix}$$

$$\left[Q_{ij}\right]_k=\begin{bmatrix}Q_{11} & Q_{12} & 0 \\ Q_{12} & Q_{22} & 0 \\ 0 & 0 & Q_{66}\end{bmatrix} \qquad \text{For} \quad i,\ j\ =1,\ 2,\ 6 \qquad (3.5.11)$$

$$\left[Q_{ij}\right]_k=\begin{bmatrix}Q_{44} & 0 \\ 0 & Q_{55}\end{bmatrix} \qquad \text{For} \quad i,\ j\ =4,\ 5 \qquad (3.5.12)$$

In which the on axis stiffnesses are:

$$Q_{11}=\frac{E_{11}}{(1-\nu_{12}\nu_{21})},Q_{12}=\frac{E_{11}\nu_{21}}{(1-\nu_{12}\nu_{21})},Q_{21}=\frac{E_{22}\nu_{12}}{(1-\nu_{12}\nu_{21})},Q_{22}=\frac{E_{22}}{(1-\nu_{12}\nu_{21})},Q_{66}=G_{12} \tag{3.5.13}$$

The off-axis stiffness values are:

$$\begin{aligned}
\overline{Q}_{11} &= Q_{11}m^4+2(Q_{12}+2Q_{66})m^2n^2+Q_{22}n^4\\
\overline{Q}_{12} &= (Q_{11}+Q_{22}-4Q_{66})m^2n^2+Q_{12}(m^4+n^4)\\
\overline{Q}_{22} &= Q_{11}n^4+2(Q_{12}+2Q_{66})m^2n^2+Q_{22}m^4\\
\overline{Q}_{16} &= (Q_{11}-Q_{12}-2Q_{66})m^3n+(Q_{12}-Q_{22}+2Q_{66})n^3m\\
\overline{Q}_{26} &= (Q_{11}-Q_{12}-2Q_{66})mn^3+(Q_{12}-Q_{22}+2Q_{66})m^3n\\
\overline{Q}_{66} &= (Q_{11}+Q_{22}-2Q_{12}-2Q_{66})m^2n^2+Q_{66}(m^4+n^4)
\end{aligned} \tag{3.5.14}$$

The stiffness corresponding to transverse deformations are:

$$\begin{aligned}
\overline{Q}_{44} &= G_{13}m^2+G_{23}n^2\\
\overline{Q}_{45} &= (G_{13}-G_{23})mn\\
\overline{Q}_{55} &= G_{13}n^2+G_{23}m^2
\end{aligned} \tag{3.5.15}$$

Where m=cosθ and n=sinθ; and θ=angle between the arbitrary principal axis with the material axis in a layer.

3.6: Strain Displacement Relations

Green-Lagrange's strain displacement relations are presented in general throughout the analysis. The linear part of the strain is used to derive the elastic stiffness matrix and the non-linear part of the strain is used to derive the geometric stiffness matrix. The total strain is given by

$$\{\varepsilon\}=\{\varepsilon_{l}\}+\{\varepsilon_{nl}\} \tag{3.6.1}$$

The linear generalized shear deformable strain displacement relations are

$$\varepsilon_{xl}=\frac{\partial u}{\partial x}+\frac{w}{R_x}+zk_x \tag{3.6.2}$$

$$\varepsilon_{yl} = \frac{\partial v}{\partial y} + \frac{w}{R_y} + z k_y \tag{3.6.3}$$

$$\gamma_{xyl} = \frac{\partial u}{\partial y} + \frac{\partial v}{\partial x} + \frac{2w}{R_{xy}} + z k_{xy} \tag{3.6.4}$$

$$\gamma_{xzl} = \frac{\partial w}{\partial x} + \theta_x - \frac{u}{R_x} - \frac{v}{R_{xy}} \tag{3.6.5}$$

$$\gamma_{yzl} = \frac{\partial w}{\partial y} + \theta_y - \frac{v}{R_y} - \frac{u}{R_{xy}} \tag{3.6.6}$$

The bending strains k_j are expressed as,

$$k_x = \frac{\partial \theta_x}{\partial x}, \quad k_y = \frac{\partial \theta_y}{\partial y} \tag{3.6.7}$$

$$k_{xy} = \frac{\partial \theta_x}{\partial y} + \frac{\partial \theta_y}{\partial x} + \frac{1}{2}\left(\frac{1}{R_y} - \frac{1}{R_x}\right)\left(\frac{\partial v}{\partial x} - \frac{\partial u}{\partial y}\right) \tag{3.6.8}$$

The non-linear strain components are as follows:

$$\varepsilon_{xnl} = \frac{1}{2}\left(\frac{\partial u}{\partial x}\right)^2 + \frac{1}{2}\left(\frac{\partial v}{\partial x}\right)^2 + \frac{1}{2}\left(\frac{\partial w}{\partial x} - \frac{u}{R_x}\right)^2 + \frac{1}{2} z^2 \left[\left(\frac{\partial \theta_x}{\partial x}\right)^2 + \left(\frac{\partial \theta_y}{\partial x}\right)^2\right] \tag{3.6.9}$$

$$\varepsilon_{ynl} = \frac{1}{2}\left(\frac{\partial u}{\partial y}\right)^2 + \frac{1}{2}\left(\frac{\partial v}{\partial y}\right)^2 + \frac{1}{2}\left(\frac{\partial w}{\partial y} - \frac{v}{R_y}\right)^2 + \frac{1}{2} z^2 \left[\left(\frac{\partial \theta_x}{\partial y}\right)^2 + \left(\frac{\partial \theta_y}{\partial y}\right)^2\right] \tag{3.6.10}$$

$$\gamma_{xynl} = \frac{\partial u}{\partial x}\left(\frac{\partial u}{\partial y}\right) + \frac{\partial v}{\partial x}\left(\frac{\partial v}{\partial y}\right) + \left(\frac{\partial w}{\partial x} - \frac{u}{R_x}\right)\left(\frac{\partial w}{\partial y} - \frac{v}{R_y}\right) + z.$$

$$2\left[\left(\frac{\partial \theta_x}{\partial x}\right)\left(\frac{\partial \theta_x}{\partial y}\right) + \left(\frac{\partial \theta_y}{\partial x}\right)\left(\frac{\partial \theta_y}{\partial y}\right)\right] \tag{3.6.11}$$

3.7: Finite element formulation

An eight nodded isoparametric element is used for static stability analysis of woven fiber composite plates subjected to hygrothermal environment. Five degrees of freedom *u*, *v*, *w*, θ_x and θ_y are considered at each node. The element is modified to accommodate laminated materials and hygrothermal conditions of the panel, based on

first order shear deformation theory where u, *v* and *w* are the displacement components in the x, y, z directions and θ_x and θ_y are the rotations. The stiffness matrix, geometric stiffness matrix due to residual stresses, geometric stiffness matrix due to applied in-plane loads and nodal load vector of the element are derived using the principle of minimum potential energy. The shape function of the element is derived using the interpolation polynomial given below based on Pascal's triangle for convergence criteria.

The displacements are expressed in terms of their nodal values by using the element shape functions and are given by.

$$u(\xi,\eta) = a_1 + a_2\xi + a_3\eta + a_4\xi^2 + a_5\xi\eta + a_6\eta^2 + a_7\xi^2\eta + a_8\xi\eta^2 \qquad (3.7.1)$$

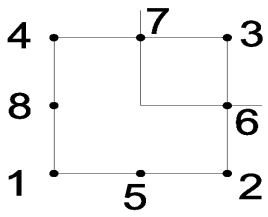

Figure 3.4: Eight nodded isoparametric element

The displacements are expressed in terms of their nodal values by using the element shape functions and are given by.

$$u = \sum_{i=1}^{8} N_i u_i, v = \sum_{i=1}^{8} N_i v_i, w = \sum_{i=1}^{8} N_i w_i \qquad (3.7.2)$$

$$\theta_x = \sum_{i=1}^{8} N_i \theta_{xi}, \theta_y = \sum_{i=1}^{8} N_i \theta_{yi} \qquad (3.7.3)$$

The shape function N_i are defined as

$$N_i = \frac{1}{4}(1+\xi\xi_i)(1+\eta\eta_1)(\xi\xi_1+\eta\eta_1-1) \quad \text{For } i=1, 2, 3 \text{ \& } 4 \qquad (3.7.4)$$

$$N_i = \frac{1}{2}(1-\xi^2)(1+\eta\eta_i) \qquad \text{For } i=5, 7 \qquad (3.7.5)$$

$$N_i = \frac{1}{2}(1-\xi\xi_i)(1-\eta^2) \qquad \text{For } i=6, 8 \qquad (3.7.6)$$

3.7.1: Element elastic stiffness matrix

The linear strain matrix $\{\varepsilon\}$ is expressed as

$$\{\varepsilon\}=[B]\{\delta_e\} \tag{3.7.7}$$

Where $$\{\delta_e\}=\{u_1,v_1,w,\theta_{x1},\theta_{y1}.....,u_8,v_8,w_8\theta_{x8},\theta_{y8}\}^T \tag{3.7.8}$$

$$[B]=\sum_{i=1}^{8}\begin{bmatrix} N_{i,x} & 0 & \frac{N_i}{R_X} & 0 & 0 \\ 0 & N_{i,y} & \frac{N_I}{R_y} & 0 & 0 \\ N_{i,y} & N_{i,x} & \frac{2N_i}{R_{xy}} & 0 & 0 \\ 0 & 0 & 0 & N_{i,x} & 0 \\ 0 & 0 & 0 & 0 & N_{i,y} \\ 0 & 0 & 0 & N_{i,y} & N_{i,x} \\ -\frac{N_i}{R_x} & -\frac{N_i}{R_{XY}} & N_{i,x} & N_i & 0 \\ -\frac{N_i}{R_{xy}} & -\frac{N_i}{R_y} & N_{i,y} & 0 & N_i \end{bmatrix} \tag{3.7.9}$$

$C_0=1/2\left(\frac{1}{R_x}-\frac{1}{R_Y}\right)$ is a term of Sander's theory which accounts for conditions of zero strain for rigid body motion [Chandra sekhar 1989]

Element elastic stiffness matrix is given by

$$[K_e]=\int_{-1}^{+1}\int_{-1}^{+1}[B]^T[D][B]J|d\xi d\eta \tag{3.7.10}$$

3.7.2: Geometric stiffness matrix due to residual stresses $\left[K^r{}_{ge}\right]$

The non-linear strain equations are represented in matrix form:

$$\varepsilon_{nl}=\{\varepsilon_{xnl},\varepsilon_{ynl},\gamma_{xynl}\}^T=[R]\{d\}/2 \tag{3.7.11}$$

Where $$\{d\}=\{u_x,u_y,v_x,v_y,w_x,w_y,\theta_{x,x},\theta_{x,y},\theta_{y,x},\theta_{y,y},\theta_x,\theta_y\}^T \tag{3.7.12}$$

Equations $\{d\}$ may be expressed as:

$$\{d\} = [G]\{\partial_e\} \tag{3.7.13}$$

Where $$[G] = \sum_{i=1}^{8} \begin{bmatrix} N_{i,x} & 0 & 0 & 0 & 0 \\ N_{i,y} & 0 & 0 & 0 & 0 \\ 0 & N_{i,x} & 0 & 0 & 0 \\ 0 & N_{i,y} & 0 & 0 & 0 \\ 0 & 0 & N_{i,x} & 0 & 0 \\ 0 & 0 & N_{i,y} & 0 & 0 \\ 0 & 0 & 0 & N_{i,x} & 0 \\ 0 & 0 & 0 & N_{i,y} & 0 \\ 0 & 0 & 0 & 0 & N_{i,x} \\ 0 & 0 & 0 & 0 & N_{i,y} \\ 0 & 0 & 0 & 1 & 0 \\ 0 & 0 & 0 & 0 & 1 \end{bmatrix} \tag{3.7.14}$$

The geometric stiffness matrix due to residual stresses (hygrothermal loads) is given by

$$[K^r{}_{ge}] = \int_{-1}^{+1}\int_{-1}^{+1} [G]^T [S][G] J\, d\xi d\eta \tag{3.7.15}$$

Where

$$[S] = \begin{bmatrix} S_{11} & & & & & & & & & & & \\ S_{21} & S_{22} & & & & & & & & & & \\ 0 & 0 & S_{33} & & & & & & & & & \\ 0 & 0 & S_{43} & S_{44} & & & & & & & & \\ 0 & 0 & 0 & 0 & S_{55} & & & & & & & \\ 0 & 0 & 0 & 0 & S_{65} & S_{66} & & & & & & \\ 0 & 0 & S_{73} & S_{74} & 0 & 0 & S_{77} & & & & & \\ 0 & 0 & S_{83} & S_{84} & 0 & 0 & S_{87} & S_{88} & & & & \\ S_{91} & S_{92} & 0 & 0 & 0 & 0 & 0 & 0 & S_{99} & & & \\ S_{101} & S_{102} & 0 & 0 & 0 & 0 & 0 & & S_{109} & S_{110} & & \\ 0 & 0 & S_{113} & S_{114} & 0 & 0 & 0 & 0 & 0 & 0 & 0 & \\ S_{121} & S_{122} & 0 & 0 & 0 & 0 & 0 & 0 & 0 & 0 & 0 & 0 \end{bmatrix} \tag{3.7.16}$$

In which

$$S_{11} = S_{33} = S_{55} = N^r{}_x \qquad S_{22} = S_{44} = S_{66} = N^r{}_y$$

$$S_{21} = S_{43} = S_{65} = N^r{}_{xy}, \qquad S_{77} = S_{99} = N_x{}^r\ t^2/12, \qquad S_{88} = S_{1010} = N_y{}^r\ t^2/12$$

$$S_{87} = S_{109} = N^r{}_{xy} t^2/12, \qquad -S_{73} = S_{91} = M^r{}_x, \qquad -S_{84} = S_{102} = M^r{}_y$$

$$-S_{74} = -S_{83} = S_{92} = S_{101} = M^r{}_{xy},\ -S_{113} = S_{121} = Q^r{}_x,\ -S_{114} = S_{122} = Q^r{}_y \quad (3.7.17)$$

3.7.3: Geometric stiffness matrix due to applied loads $\left[K_{ge}\right]$

The first three non-linear strain equations are represented in a matrix form:

$$\left\{\varepsilon_{xnl}, \varepsilon_{ynl}, \gamma_{xynl}\right\}^T = [U]\{f\}/2 \qquad (3.7.18)$$

$$\{f\} = \left\{u_x, u_y, v_x, v_y, w_x, w_y, \theta_{x,x}, \theta_{x,y}, \theta_{y,x}, \theta_{y,y}\right\}^T \qquad (3.7.19)$$

$\{f\}$ is expressed as:

$$\{f\} = [H]\{\delta_e\} \qquad (3.7.20)$$

Where

$$[H] = \sum_{i=1}^{8} \begin{bmatrix} N_{i,x} & 0 & 0 & 0 & 0 \\ N_{i,y} & 0 & 0 & 0 & 0 \\ 0 & N_{i,x} & 0 & 0 & 0 \\ 0 & N_{i,y} & 0 & 0 & 0 \\ 0 & 0 & N_{i,x} & 0 & 0 \\ 0 & 0 & N_{i,y} & 0 & 0 \\ 0 & 0 & 0 & N_{i,x} & 0 \\ 0 & 0 & 0 & N_{i,y} & 0 \\ 0 & 0 & 0 & 0 & N_{i,x} \\ 0 & 0 & 0 & 0 & N_{i,y} \end{bmatrix} \qquad (3.7.21)$$

The geometric stiffness matrix due to applied in-plane loads is given by

$$\left[K_{ge}\right] = \int_{-1}^{+1}\int_{-1}^{+1} [H]^T [P][H] J\, d\xi d\eta \qquad (3.7.22)$$

Where $[P]=\begin{bmatrix} P_{11} & & & & & & & & & \\ P_{21} & P_{22} & & & & & & & & \\ 0 & 0 & P_{33} & & & & & & & \\ 0 & 0 & 0 & P_{44} & & & & & & \\ 0 & 0 & 0 & 0 & P_{55} & & & & & \\ 0 & 0 & 0 & 0 & P_{65} & P_{66} & & & & \\ 0 & 0 & 0 & 0 & 0 & 0 & P_{77} & & & \\ 0 & 0 & 0 & 0 & 0 & 0 & P_{87} & P_{88} & & \\ 0 & 0 & 0 & 0 & 0 & 0 & 0 & 0 & P_{99} & \\ 0 & 0 & 0 & 0 & 0 & 0 & 0 & 0 & P_{109} & P_{1010} \end{bmatrix}$ (3.7.23)

In which

$$P_{11}=P_{33}=P_{55}=N^a{}_x,\ P_{22}=P_{44}=P_{66}=N^a{}_y,\ P_{21}=P_{43}=P_{65}=N^a{}_{xy},$$

$$P_{77}=P_{99}=N^a{}_x t^2/12,\ \ P_{88}=P_{1010}=N^a{}_y t^2/12,\ \ P_{87}=P_{109}=N^a{}_{xy} t^2/12$$

(3.7.24)

3.7.4: The element mass matrix

$$[M_e]=\int_{-1}^{+1}\int_{-1}^{+1}[N]^T[P][N]J|d\xi d\eta \qquad (3.7.25)$$

Where the shape function matrix

$$[N]=\sum_{i=1}^{8}\begin{bmatrix} N_i & 0 & 0 & 0 & 0 \\ 0 & N_i & 0 & 0 & 0 \\ 0 & 0 & N_i & 0 & 0 \\ 0 & 0 & 0 & N_i & 0 \\ 0 & 0 & 0 & 0 & N_i \end{bmatrix} \qquad (3.7.26)$$

$$[P_1]=\begin{bmatrix} P_1 & 0 & 0 & 0 & 0 \\ 0 & P_1 & 0 & 0 & 0 \\ 0 & 0 & P_1 & 0 & 0 \\ 0 & 0 & 0 & I & 0 \\ 0 & 0 & 0 & 0 & I \end{bmatrix} \qquad (3.7.27)$$

In which, $P_1=\sum_{k=1}^{n}\int_{ek-1}^{ek}\rho dz$ And $I=\sum_{K=1}^{n}\int_{ek-1}^{ek}z^2\rho dz$ (3.7.28)

The element load vector due to external transverse static load p per unit area is given

$$\{P_e\} = \iint N_i \begin{bmatrix} p \\ 0 \\ 0 \end{bmatrix} dxdy \,. \qquad (3.7.29)$$

3.7.5: Load vector

The element load vector due to the hygrothermal forces and moments is given by

$$\left\{P^{a}\right\}_e = \int_{-1}^{+1}\int_{-1}^{+1} \left[N_j\right]^T \left\{q^{a}\right\} |J| d\xi d\eta \qquad (3.7.30)$$

3.8: Solution process

The element stiffness matrix, the initial stress stiffness matrix due to hygrothermal load, the mass matrix, geometric stiffness matrix due to applied loads and the load vectors of the element are evaluated by first expressing the integrals in local Natural co-ordinates, ξ and η of the element and then performing numerical integration by using Gaussian quadrature. Then the initial stress resultants $N^i{}_x, N_y{}^i, N^i{}_{xy}, M^i{}_x, M^i{}_y, M^i{}_{xy}, Q^i{}_x$ and $Q^i{}_y$ are obtained Then the element matrices are assembled to obtain the respective global matrices $[K]$, $[M]$, $\left[K^r{}_g\right]$, $\left[K_g\right]$. The next part of the solution involves determination of natural frequencies, buckling load and excitation frequencies from the eigenvalue solution of the equations Eq 3.4.7 through Eq 3.4.9.

3.9: Computer program

A computer program based on MATLAB environment developed to perform all necessary computations. The composite panel is divided into a two-dimensional array of rectangular elements. The element elastic stiffness and mass matrices are obtained with 2x2 gauss points. The geometric stiffness matrix is essentially a function of the in-plane stress distribution in the element due to applied load and residual stress distribution due to hygrothermal load. The overall element stiffness and mass matrices are obtained by assembling the corresponding element matrices using skyline technique. Reduced integration technique is adopted in order to avoid possible shear locking.

A flow chart shown in figure 3.5 is developed for the computational procedures for dynamic instability of laminated composite panels under hygrothermal conditions and in-plane harmonic loading.

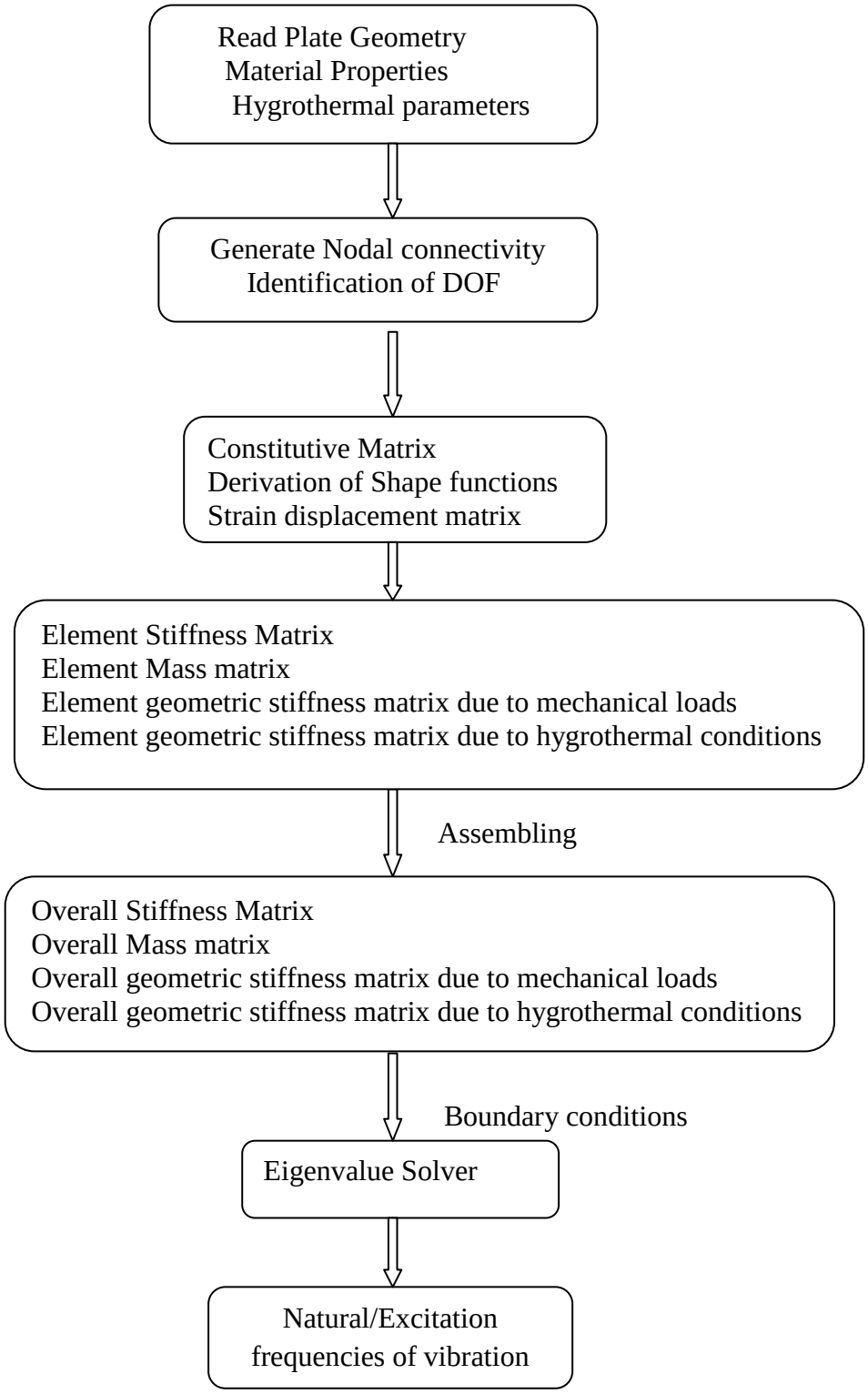

Figure 3.5: Flow chart of Program in MATLAB for instability of Composite panels subjected to hygrothermal loads

CHAPTER 4

EXPERIMENTAL PROGRAMME

4.1: Introduction

The experimental works carried out for the present free vibration and buckling test under hygrothermal conditions are presented in this chapter. Some woven roving Glass/Epoxy composite plates are fabricated for the present experimental work. The percentage of fiber and matrix has taken as 55:45 in weight for fabrication of flat panels.

4.2: Materials Required for Fabrication of Plates

The following constituent materials are used for fabricating the glass/epoxy fiber plate:

- Glass woven roving as reinforcement (FGP, RP-10)
- Epoxy as resin
- Hardener as catalyst (Ciba-Geigy, araldite LY556 and Hardener HY951)
- Polyester resin (MEKP-Methyl Ethyl Ketone Peroxide)
- Polyvinyl alcohol as a releasing agent

4.3: Fabrication procedure for static test specimen

In the present investigation for static behavior (ILSS), two different types of fiber: matrix composite specimens were fabricated. These were (i) Glass: Epoxy (ii) Glass: polyester, (E-glass fibers). Each type preparation of laminates was manufactured by using three different types of weight fractions i.e. 55:45, 60:40 and 65:35. Woven roving E-Glass fibers (FGP, RP-10) were cut into required shape and size according to number of specimens required for testing. Each composite laminates consists of 16 plies of fiber in balanced form as per ASTM specification. For preparation of Epoxy resin matrix, Hardener 8% (Ciba-Geigy, araldite LY556 and Hardener HY951) of the weight of Epoxy were used and for polyester matrix 1% accelerator (cobalt octane 2%) was added first to the polyester resin then 1.5% of catalyst (MEKP-Methyl Ethyl

Ketone Peroxide) added to mixture and stirred thoroughly to get polyester matrix as per ASTM D5687/D5687M-07 [2007]. Subsequent plies were placed one upon another with matrix in each layer to obtain sixteen stacking plies as shown in figure 4.1. A hand roller was used to distribute resin uniformly, compact plies, and to remove entrapped air to minimize void contents in the samples as shown in figure 4.2. The mould and lay up were covered with a release film to prevent the lay up from bonding to the mould surface. Then the resin impregnated fibers were placed in the mould for curing. The laminates were cured at normal temperature (25^0C and 55 % Relative Humidity) under a pressure of 0.2 mpa for 3 days as shown in figure 4.3. After proper curing of laminates the release film were detached the specimens were cut for inter laminar shear strength (ILSS) for three point bend test.

In addition to above the tensile test was conducted for four material constants i.e. E_1, E_2, G_{12}, and υ_{12} where the suffixes 1 and 2 indicate principal material directions. For material characterization of composites, laminate having sixteen layers was fabricated to evaluate the material constants. The constants are determined experimentally by performing unidirectional tensile tests on specimens cut in longitudinal and transverse directions, and at 45_0 to the longitudinal direction, as described in ASTM standard: D 3039/D 3039M-2008.The tensile tests specimens are having a constant rectangular cross section in all cases. The dimension of the specimen was taken as below. The specimens were cut from the plates themselves by diamond cutter or by hex. At least four replicate sample specimens were kept in the hygrothermal chamber at different temperature and moisture concentration for six hours and then tested and mean values adopted. The tests specimens are shown in fig 4.5 and fig 4.6.

For measuring the Young's modulus, the specimen was loaded in INSTRON 1195 universal testing machine (as shown in figure 4.9 monotonically to failure with a recommended rate of extension (rate of loading) of 0.2mm/minute. Specimens were fixed in the upper jaw first and then gripped in the movable jaw (lower jaw).Gripping of the specimen should be as much as possible to prevent the slippage. Here, it was taken as 50mm in each side for gripping. Initially strain was kept at zero. The load, as well as the extension, was recorded digitally with the help of a load cell and an extensometer respectively. From these data, engineering stress vs. strain curve was plotted; the initial slope of which gives the Young's modulus. The ratio of transverse

to longitudinal strain directly gives the Poisson's ratio by using two strain gauges in longitudinal and transverse direction. The shear modulus was determined using the following formula from Jones

$$G_{12} = \frac{1}{\frac{4}{E_{45}} - \frac{1}{E_1} - \frac{1}{E_2} + \frac{2\vartheta_{12}}{E_1}}$$

The values of material constants finally obtained experimentally for different temperature and moisture concentrations are presented in Table 5.16 and 5.17.

4.4: Fabrication procedure for vibration and buckling

Contact moulding in an open mould by hand lay-up was used to combine plies of woven roving in the prescribed sequence. The percentage of fiber and matrix has taken as 55:45 in weight for fabrication of plates. A flat plywood rigid platform was selected. A plastic sheet i.e. a mould releasing sheet was kept on the plywood platform and a thin film of polyvinyl alcohol is applied as a releasing agent by use of spray gun. Laminating starts with the application of a gel coat (epoxy and hardener) deposited on the mould by brush, whose main purpose was to provide a smooth external surface and to protect the fibers from direct exposure to the environment. Ply was cut from roll of woven roving. Layers of reinforcement were placed on the mould at top of the gel coat and gel coat was applied again by brush. Each composite laminates consists of 16 plies of fiber in balanced form as per ASTM specification. Any air which may be entrapped was removed using serrated steel rollers. The process of hand lay-up was the continuation of the above process before the gel coat had fully hardened. After completion of all layer, again a plastic sheet was covered the top of last ply by applying polyvinyl alcohol inside the sheet as releasing agent. Again one flat ply board and a heavy flat metal rigid platform were kept top of the plate for compressing purpose. The plates were left for a minimum of 48 hours before being transported and cut to exact shape for vibration and buckling testing. Figure 4.1 to 4.3 shows the fabrication process of laminated composite plates.

4.4.1: Details of test specimen

The size of specimen was taken as 235 mm×235 mm x 6mm size for plate, 200 mmx25 mm x 6mm size for tensile test and for 45 mm × 6 mm size for three point bend test.

Figure 4.1: placing of woven glass fiber using on gel coat

Figure 4.2: Removal of air entrapment using steel roller

Figure 4.3: Composite plates

Figure 4.4: Instron 1195 UTM machine

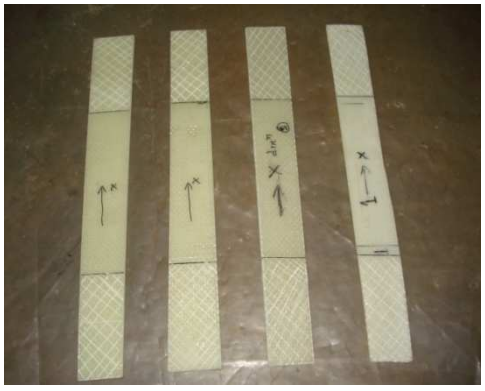

Figure 4.5: Specimen in X direction for tensile testing

Figure 4.6: Specimen in 45^0 directions for tensile testing

4.5: Hygrothermal treatment

The specimens were hygrothermally conditioned in a humidity cabinet as shown in figure 4.5, where the conditions were maintained at a temperature of 323K and relative humidity (RH) ranging from 0-1% for moisture concentration as per ASTM

D5229/D5229M-04[2004]. The humidity cabinet had an inbuilt thermometer for temperature and hygrometer for relative humidity measurements. The temperature variation was maintained between 300K-425K whereas the RH was 0 in temperature bath as shown in figure 4.6. The composite laminates were placed on perforated trays. The hygrothermal conditioning was carried out for every six hours in a total period of thirty six hours.

Figure 4.7 Humidity chamber

Figure 4.8 Temperature bath

4.6: Static Behaviour Experiment Test

Most commonly used test for inter laminar shear strength is the short beam under three point bending. The specimen were tested for three point bend test on the INSTON-1195 material testing machine as shown in figure 4.4 and 4.7 with different cross head velocities to obtain inter laminar shear strength (ILSS) and to study the effects of loading speed for different types of laminates. The test was conducted with speed of 1mm / min, 10mm / min, 100mm / min, 200mm / min and 500mm / min with constant span of 34mm. Then, yield load (max load) were obtained for each type of laminates in which minimum five specimens were tested. Before testing the thickness and width of the specimens were measured accurately at the midpoint. The test specimen was placed in the test fixture and aligned so that its mid point was centered and it's long axis was perpendicular to the loading nose. The same procedure was repeated for all the specimens. The specimens were tested at regular interval of time at a constant cross head speed of 200mm / min. In all the above three cases there five sample specimens were tested at each point of an experiment and then average value was reported. The ILSS value was determined in accordance with ASTM

D2344/D2344M -06 [2006]. The interlaminar shear strength is calculated as $\frac{0.75\times Pb}{b\times t}$, Where P_b is the breaking load in N, b is the width of specimen in mm and d is the thickness of specimen in mm.

Figure 4.9: Complete set up of Instron 1195 machine

4.7: Apparatus required for free vibration test

- Modal hammer. (2302-5)
- Accelerometer. (B&K 4507)
- FFT Analyzer. (Model B&K 3560-C)
- Notebook with PULSE lab shop software.
- Specimens to be tested (Composite plate size 0.235mX 0.235mx0.006m)

4.7.1: Free Vibration Experiment Test

The composite test specimens were fitted properly to the prefabricated iron frame as shown in figure 4.11. The connections of FFT analyzer (Model B&K3560-C) as shown in figure 4.9, laptop shown in figure 10, B&K4507 transducers, B&K2302-5 modal hammer as shown in figure 4.8, and cables to the system were done. The PULSE Lab shop was used during the vibration measurement. The plate was excited in selected points by means of impact hammer (Model 2302-5) and this resulting vibration of the specimens was picked up by the accelerometer. The accelerometer (B&K 4507) was mounted on the specimen as shown in figure 4.12 by means of bees wax. The signal was then subsequently led to the analyzer, where its frequency spectrum was also obtained using the pulse software. Various forms of Frequency

Response Functions (FRF) are directly measured. The coherence is observed for each set of measurement.

Figure 4.10: Modal Impact Hammer

Figures 4.11: The FFT 3560-C analyzer

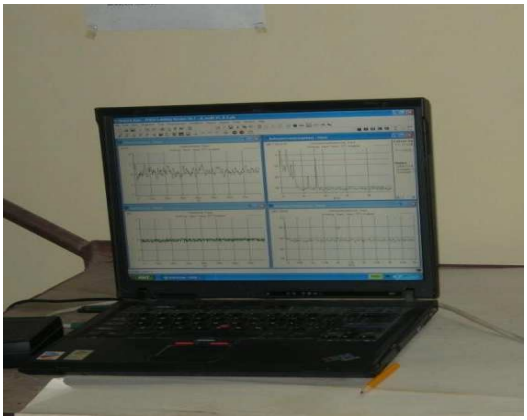

Figure 4.12: Display unit

Figure 4.13: Iron Frame for different B.C. Setup

Figure 4.14: The test frame with specimen (Simply supported boundary condition)

Figure 4.15: The test frame with specimen (Clamped boundary condition)

The output from the analyzer was displayed on the Lab shop screen. The modal parameters obtained from experiments are natural frequencies and modal damping factors as determined from the accelerance, by the “peak picking” method. The

four sides simply supported boundary conditions and four sides clamped position of the composite plate specimens for testing is as shown in 4.12 and 4.13 respectively.

4.8: Buckling Experiment Test

In view of actual real time behavior of laminated composite plates, experimental methods have become important in solving the buckling problem of laminated composite plates. The specimen was clamped at two sides and kept free at two other sides in an iron frame as shown in figure 4.15. The specimen was loaded in axial compression by using an INSTRON 1195 Machine of 600 KN load capacity as shown in figure 4.14. All specimens were loaded slowly unless buckling takes place as shown in figure 4.16. Clamped boundary conditions were simulated along top and bottom edges, restraining 2.5cm length. For axial loading, the test specimens were placed between the two extremely stiff machine heads, of which the lower one was fixed during the test; whereas the upper head was moved downwards by servo hydraulic cylinder. All plates were loaded at constant cross-head speed of 0.5mm/min. The shape of the specimen after buckling is as shown in figure 4.17. The load verses end shortening curve was plotted. The displacement is plotted along x-axis and the load was plotted on the y-axis. The load, which is the initial part of the curve deviated linearity, is taken as the buckling load in KN in line with previous investigators.

Figure 4.16: Instron UTM machine with specimen

Figure 4.17: composite test frame with specimen

Figure 4.18: Specimen before buckling

Figure 4.19: Specimen after buckling

CHAPTER 5

RESULTS AND DISCUSSIONS

5.1: Introduction

The present chapter deals with the results of the analyses of vibration, buckling and parametric resonance characteristics of woven fiber laminated composite plates in hygrothermal environment using the formulation given in the previous chapter. Some results on static behavior especially the variation of inerlaminar shear strength with loading speed and exposure hours proportion of fiber to different matrices are presented for completeness. The statistical integration of the test results is also presented. As explained, the eight-node isoparametric quadratic shell element is used to develop the finite element procedure. The first order shear deformation theory is used to model the plate considering the effects of transverse shear deformation and rotary inertia. The static behavior, vibration and stability characteristics of woven fiber laminated composite plates and shells in hygrothermal environment are studied. The parametric instability studies are carried out for woven fiber laminated composite plates and shells subjected to in-plane periodic loads with static component of load to consider the effect of various parameters in hygrothermal environment. The studies in this chapter are presented separately for plates and shells as follows:

- Convergence Study
- Comparison with previous studies
- New results

5.1.1: Static behaviour of woven fiber composites in hygrothermal environment

The present study involves extensive experimental works to investigate the hygrothermal effects on the mechanical behavior of Glass: Epoxy and Glass: Polyester composites. Static tests involving three points bend tests and subsequent interpolation of statistical parameters including interlaminar shear strength (ILSS)

appears to be of significant important for evaluation of static capacity of composite structures in hygrothermal environment. The present investigation deals with the failure behavior of woven fiber composites under different loading speeds and change in material percentage constituents under hygrothermal conditions. The further investigations were carried out on different types of composites with different constituents of their weight fractions 55:45, 60:40, and 65:35 at a constant speed of 200mm/min in hygrothermal environment and different exposure time.

The statistical analysis of interlaminar shear strength (ILSS) with varying loading speeds of 1,10,100,200 and 500 for different proportion of Glass fiber: Epoxy and Glass fiber: Polyester such as 55:45, 60:40 and 65:35 of a glass/epoxy and a glass/polyster are presented below in Table 5.1-5.2 respectively. The analysis is carried out as per ASTM D-2344, section 12.2. The standard deviation and coefficient of variation of ILSS is less in all higher loading speeds beyond 200mm/min in comparison to lower loading speeds from 1 to100mm/min in glass fiber/epoxy specimens in all three proportions. In glass fiber/polyster composites, the S.D and C.V of ILSS is more for loading speeds beyond 200mm/ min but less from 1 to 100mm/ min in all three proportion. This shows the good degree of quality control of test specimens preparation.

Table 5.1: Statistical variation of ILSS with loading speeds of Glass/Epoxy composites for varying proportion

Loadingspeed(mm/min)	ILSS for different proportion								
	(55:45)			(60:40)			(65:35)		
	Mean	S.D	C.V	Mean	S.D	C.V	Mean	S.D	C.V
1	31	3.1	10	36.7	1.93	5.25	39.4	1.46	9.4
10	34.7	0.0395	0.98	31.6	0.98	3.123	28.4	2.74	9.64
100	22.9	1.5	6.5	21.5	0.92	4.279	19.1	0.181	0.94
200	28.4	0.0053	1.86	29	2.25	7.71	25.2	1.558	6.1
500	27.1	0.0659	0.25	27.1	0.31	1.107	27	2.46	9.11
Average	28.8	0.944	3.918	29.16	1.33	4.298	27.82	1.679	7.03

Table 5.2: Statistical variation of ILSS with loading speeds of Glass/Polyester composites for varying proportion.

Loadingspeed (mm/min)	ILSS for different proportion								
	(55:45)			(60:40)			(65:35)		
	Mean	S.D	C.V	Mean	S.D	C.V	Mean	S.D	C.V
1	18.7	0.11	0.588	18.9	0.374	0.104	21.5	1.97	9.1
10	18.9	0.027	0.0075	18.7	1.363	0.387	18.4	1.11	0.328
100	14.3	1.113	0.544	14.7	0.194	8.97	13.7	0.49	3.6
200	22	2.97	13.50	21.7	0.867	0.184	21.8	1.13	0.239
500	19.7	2.2	11.16	17.2	1.07	0.361	18	5.76	1.77
Average	18.72	1.242	5.159	18.296	0.773	2.00	18.68	2.15	3.00

The variations of inter laminar shear strength (ILSS) with different cross head velocity for glass:epoxy specimens are shown in fig.5.1. As shown, the ILSS of woven roving glass fiber reinforced polymers showed a significant rate sensitivity. In the three weight fraction of fiber-matrix of glass: epoxy, higher ILSS was obtained in low loading speed. As the loading speed increased, the inter laminar shear strength decreased upto 100mm / min for all the three weight fractions. The inter laminar shear strength for glass: epoxy specimens increased with increase in loading speed upto 200mm/min, beyond that the inter laminar shear strength decrease marginlly or remains constant for glass/epoxy with further increase in loading speed. The glass/epoxy specimens with weight fraction 55:45 shows higher ILSS in lower crosshead velocity and the specimens with weight fraction 65:35 shows lowest ILSS among three fractions. However, glass/epoxy specimens with weight fractions 60:40 shows similar ILSS to that of 55:45 after crosshead velocity more than 200mm/minute. In general, the variation of inter laminar shear strengths of glass/epoxy specimens are found significant with increasing loading speed.

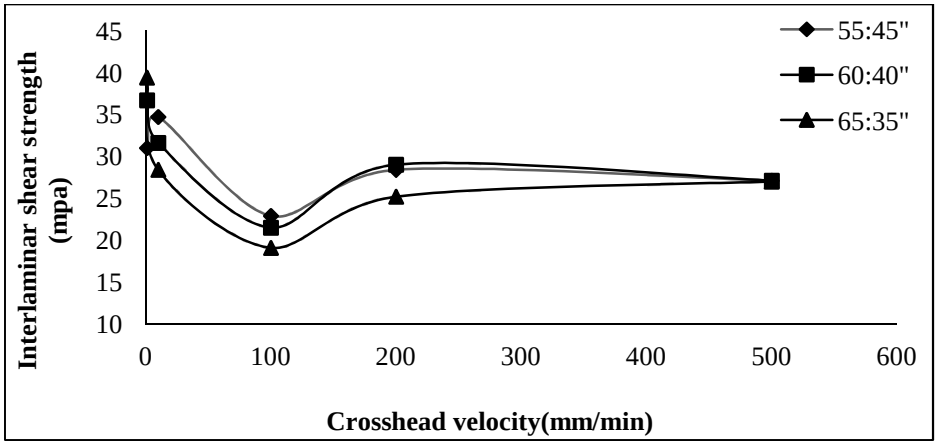

Figure 5.1: Variation of ILSS with different loading speeds of glass/epoxy composites for varying proportion

In case of glass: polyster fibre matrix of three weight fractions, lower ILSS is observed as shown in fig. 5.2 in comparison to glass/epoxy speciens at low loading speed and then decreased in loading speed upto 100 mm/min. The ILSS then increased with increase in loading speed upto 200mm/ min. However, beyond that, the ILSS decreased for all weight fraction of glass: polyester matrix resin. Woven roving Glass Fiber Reinforced Polymer(GFRP) shows a significant rate sensitivity. The variation of inter laminar shear strengths are found with increasing loading speed. It is important note that a change in loading speed can result in a variation of failure loads. When subjected to an increasingly higher impact velocity , a laminate behaves like a more rigid beam or plate, which is less suceptible to bending. This shifts its behavior from that of a flexible rigid beam with very low impact velocity and the failure initiated from the rear surface to that occurs near the point of conact in the case of much higher impact velocity. At intermediate velocities the complex behavior of mixed fracture modes are seen.

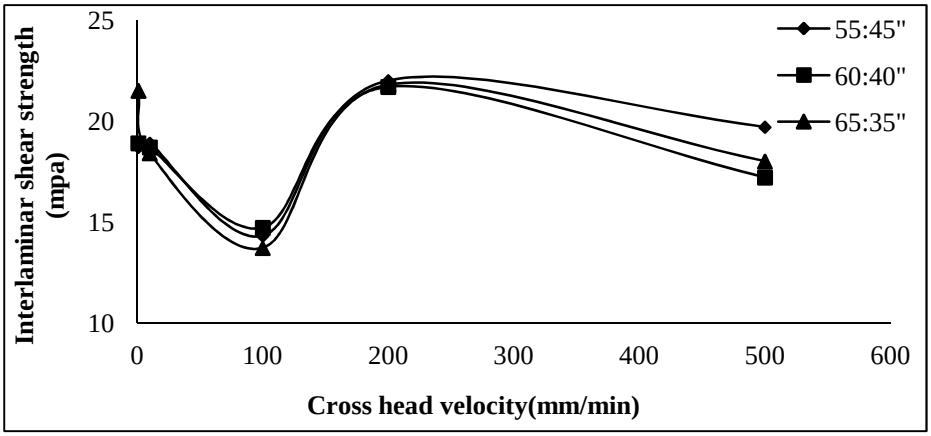

Figure 5.2: Variation of ILSS with different loading speeds of glass/polyester composites for varying proportion

It is observed from figure 5.1 and 5.2 that for woven roving glass fiber laminates with Epoxy matrix shows higher inter laminar shear strengths than Polyster matrix for all weight fractions, since epoxy resin is relatively low molecular weight than polymers and capable of being processed under a variety of conditions. The major advantages of epoxy resins is higher viscosity and exhibit low shrinkage during cure over polyster resins.

The statistical analysis of ILSS with rise in temperature for different proportion of Glass fiber: Epoxy and Glass:Polyester are given in Table 5.3 and Table 5.4 respectively. The glass/epoxy specimens shows higher value of mean ILSS of 32.86 for 60: 40 proportions. However, the glass/epoxy speimens with 55:45 proportion shows least value of S.D. of 2.929 and CV of 8.336 respectively. In both the proportions, the mean, S.D. and C.V. of ILSS decrease with increase of temperature up to 52^0 C and then decrease with increase of temperature. The standard deviation and coefficient of variation of ILSS is less with respect to rise in temperature from 27^0C to 202^0C for glass/epoxy specimens for all proportion.

Table 5.3: Statistical variation of ILSS with temperature of Glass/Epoxy composites for varying proportion.

Temperature ^{0}C	ILSS for different proportion								
	(55:45)			(60:40)			(65:35)		
	Mean	S.D	C.V	Mean	S.D	C.V	Mean	S.D	C.V
27	18.6	3.15	1.693	18.5	4.46	2.41	23	1.276	5.54
52	30.4	3.236	10.64	29.8	3.363	11.28	34.4	3.9	11.33
77	20.5	1.862	9.0	30.2	3.837	12.7	30.2	3.563	11.70
102	32.8	2.86	8.70	39.9	4.20	10.50	31.50	3.60	11.42
127	30.7	3.46	11.27	35	4.1	11.7	31.5	3.60	11.42
152	31.2	4.20	13.46	36.2	4.6	12.7	35.1	3.76	10.59
177	41	3.07	7.48	28.3	2.78	9.82	31.8	3.12	9.811
202	35.9	1.60	4.45	45	2.95	6.55	27.2	2.15	7.90
Average	30.13	2.929	8.336	32.86	3.822	9.732	30.587	2.975	9.44

However, the glass/ polyester specimens shows much less mean value of ILSS in comparison to glass/epoxy specimens. Within the glass/epoxy samples, the specimens with proprtion 55:45 shows highest value of mean of 18.72. The specimens with proprtion 60:40 shows least value of S.D. of 0.773 and C.V. of 2.00 showing better quality control of specimens. The S.D. and C.V. of glass/polyster specimens are also

less in comparison to glass/epoxy specimens for increase in temperature from 27^0C to 202^0C for all weight fractions.

Table 5.4: Statistical variation of ILSS with temperature of Glass/Polyester composites for varying proportion.

Temperature ^{0}C	ILSS for different proportion								
	(55:45)			(60:40)			(65:35)		
	Mean	S.D	C.V	Mean	S.D	C.V	Mean	S.D	C.V
27	5.1	0.62	12.15	12	1.26	10.5	8.5	1.09	12.8
52	24.1	2.41	9.95	20	1.96	9.8	23.7	1.85	7.8
77	19.7	1.69	8.57	20.9	2.18	9.19	23.5	1.13	4.80
102	27	3.13	11.59	21.1	1.56	7.35	23.7	1.96	8.27
127	21.3	2.46	1.54	23.4	2.12	9.05	27.4	2.64	9.63
152	19.3	1.28	6.66	19.4	1.43	7.37	20.5	1.83	8.92
177	25.1	3.32	13.22	20.6	0.86	4.17	21.4	0.65	3.03
202	13	1.26	9.69	20.2	1.28	6.33	20.5	2.16	10.53
Average	19.32	2.02	10.42	19.71	1.58	7.97	21.15	1.66	8.22

The variations of ILSS of glass/epoxy specimens with temperature is shown in shown in fig 5.3. As shown, the values of ILSS for glass: epoxy specimen increase gradually when the temperature is increased from 27^0C to 52^0C and then decrease upto 77^0C. The ILSS for glass: epoxy specimen increased further with the increase of temperature upto 152^0C and there after decreased with increase of temperature for glass: epoxy composite in 55:45 and 60:40 proportions.

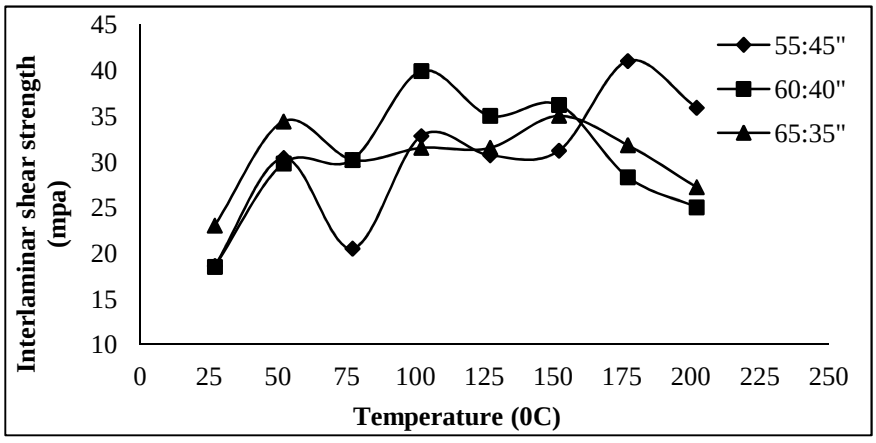

Figure 5.3: Variation of ILSS with different temperature of glass/epoxy composites for varying proportion

However, the values of ILSS for glass: polyester specimen of 65:35 proportion increase when the temperature is upto 52^0C then remains constant upto 152^0C. The

values of ILSS then decrease with increase of temperature. For fiber: polyester composites of 60:40 and 65:35 proportions, the values of ILSS increased gradually when the temperature is increased upto 52^0C and remain constant upto 102^0C.The ILSS for glass: polyester specimens decreased when the temperature is increased upto 152^0C and remains constant with increase in temperature except 55:45 proportion.

As shown in fig 5.4, the ILSS for glass: polyester specimen increase and then decrease with temperature in every 25^0C upto 177^0C and decreased thereafter at the same constant speed of 200mm/ min. The exposure to elevated temperature can result in degradation of mechanical properties, cracking and flaking of polymers. The first form of damage in laminated composite is usually matrix microcracks. Matrix microcracks cause degradation properties in composite laminates and also act as precursors to other forms of damage leading to laminate failure. The moisture absorption is more for sample specimen which is exposed at higher temperature. At higher temperature, the thermal stresses are more which leads to higher mismatch in the thermal strain.

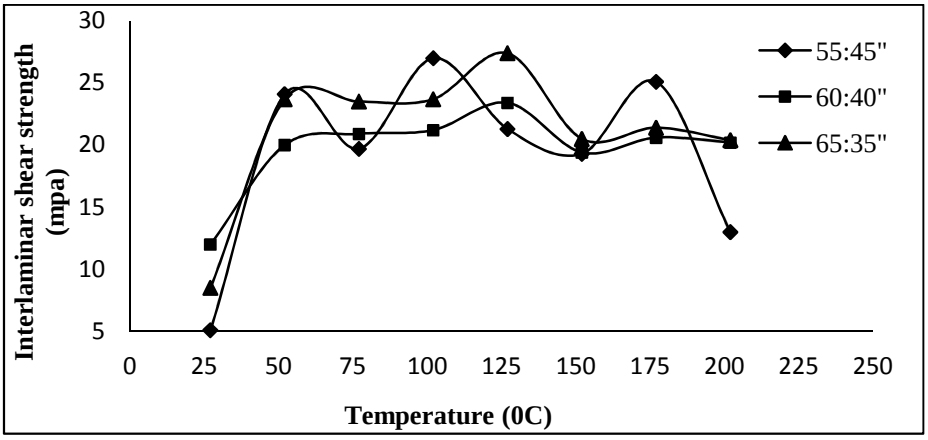

Figure 5.4. Variation of ILSS with different temperature of glass/polyester composites for varying proportion

The statistical analysis of ILSS with rise in moisture concentration from 0.0% to 1.0% at an interval of 0.25% for different proportion of Glass fiber: Epoxy and Glass fiber: Polyester are given in Table 5.5 and Table 5.6 respectively. The mix 55:45 shows mean value of ILSS of 23.8Mpa averaged over the different moisture concentrations considered from 0% to 1.0%.

Table 5.5: Statistical variation of ILSS with moisture concetration of Glass/Epoxy composites for varying proportion.

Moisture concentration,C (%)	ILSS for different proportion								
	(55:45)			(60:40)			(65:35)		
	Mean	S.D	C.V	Mean	S.D	C.V	Mean	S.D	C.V
0	12.7	1.36	10.70	14.5	0.96	6.53	12	1.14	9.5
0.25	27.2	3.12	11.47	23	2.28	9.91	27.3	3.08	11.28
0.50	18.4	1.74	9.45	13.9	1.2	8.70	11.5	1.12	9.74
0.75	32.6	3.11	9.53	35.7	3.69	10.33	33.2	2.56	7.71
1	28.1	2.58	9.18	25.6	2.86	11.17	22.5	1.89	8.40
Average	23.8	2.38	10.06	22.56	2.19	9.328	21.3	1.95	9.32

Table 5.6: Statistical variation of ILSS with moisture concetration of Glass/Polyester composites for varying proportion.

Moisture concentration, C (%)	ILSS for different proportion								
	(55:45)			(60:40)			(65:35)		
	Mean	S.D	C.V	Mean	S.D	C.V	Mean	S.D	C.V
0	9.4	1.07	11.38	15.41	1.79	11.62	18.7	2.21	11.81
0.25	26.6	2.13	8.0	16	1.56	9.75	25	2.69	10.76
0.5	8.9	1.12	12.58	10.6	1.20	11.32	10.4	1.27	12.21
0.75	24	2.27	9.45	24	2.56	10.66	26	1.78	6.84
1	18.9	1.67	8.83	19.3	1.45	7.51	21.9	1.58	7.21
Average	17.56	1.65	10.04	17.06	1.71	10.17	20.4	1.90	9.76

The standard deviation and coefficient of variation of ILSS is less in all proportions with rise in moisture concentration from 0 to 1 for all proportion in glass/epoxy and glass/polyster specimens. Since moisture affects all components of the composite, principally the matrix and the fibre matrix interface but also the fiber itself.

The plasticization process involves the interuption of the van der Waal's bonds between ethers, secondary amines and hydroxyl groups. Polymers with ketones and imides are more resistant to hydrolysis, they have fewer polar groups and this reduces their moisture sensitivity. Plasticization reduces residual stresses and increases viscoelasticity. So the effect of increase in moisture concentration is very similar to an increase in temperature as shown in fig. 5.3 through fig. 5.6. Mechanical damage from moisture induced swelling, surface crazing and matrix microcracking. In general, the glass/polyster shows less value of average ILSS in comparison to glass/epoxy

specimens.However, the value of SD is less in comparison to glass/epoxy specimens showing better quality control.

The variation of ILSS with moisture concentrations of glass/epoxy specimens are presented in fig.5.5. As shown in fig 5.5, the ILSS for glass:epoxy specimen increased and decreased in every 0.25% moisture concentration gradually upto 1 for all proportion of composites. In the glass:polyester composites, as shown in fig.5.6, all the proportion behaves all most same as glaas :epoxy composites at the same constant speed of 200mm/ min.When exposed to humid environment, the positive concentration gradient between the environment and the specimen, the higher pressure outside the specimen favours moisture absorption. When the same specimen is exposed to a relatively dry environment, the conditions get reversed resulting in moisture desorption. The relative rates of absorption and desorption controls the net moisture pickup by the specimen. The ILSS values are seen to going downwards. Amount of moisture absorbed by epoxy matrix is significantly greater than fibers which absorb little or no moisture. This results in significant mismatch in moisture induced volumetric expansion between matrix and ibers leading to evolution of localized stress and strain fields in the composite at the interfacial region.

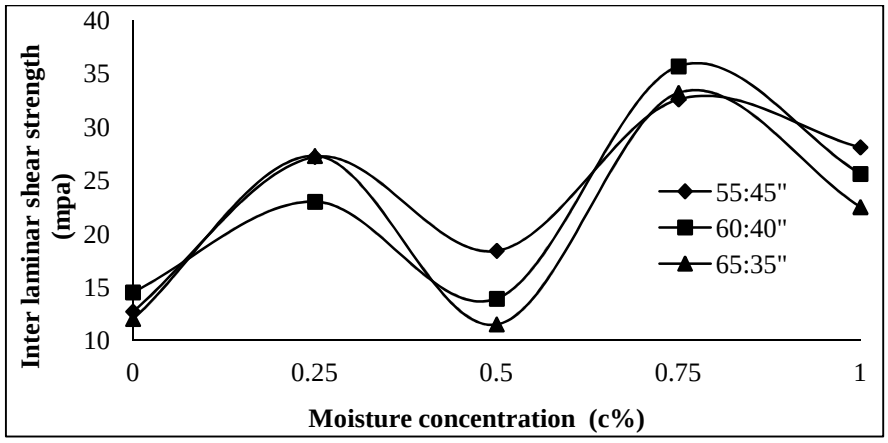

Figure 5.5: Variation of ILSS with different moisture concetration of glass/epoxy composites for varying proportion.

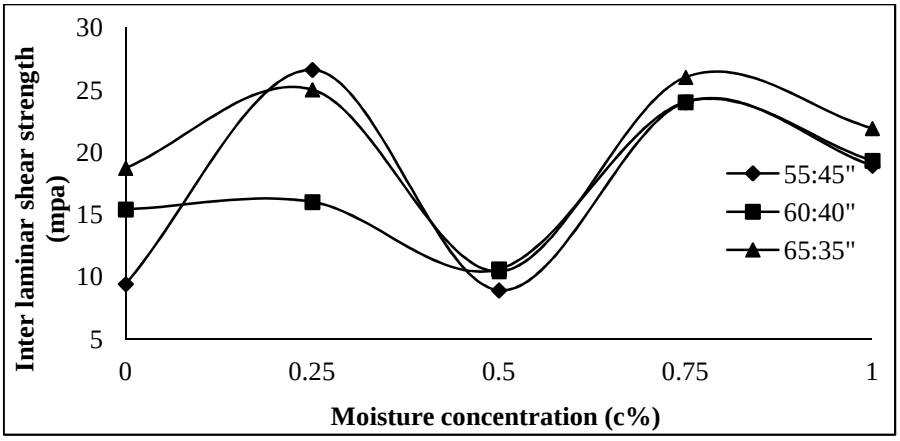

Figure 5.6: Variation of ILSS with different moisture concetration of glass/ Polyester composites for varying proportion.

The statistical analysis of ILSS with rise in exposure time in hours for different proportions of Glass fiber: Epoxy and Glass fiber: Polyester are given in Table 5.7 and Table 5.8 respectively. Unlike the previous cases, the glass/epoxy specimens at proportion 65:35 shows highest value of mean value of ILSS out of all three mixes. The standard deviation and coefficient of variation of ILSS decrease with increase in exposure time for glass/epoxy specimens in all proportion.

Table 5.7: Statistical variation of ILSS with exposure time of Glass/Epoxy composites for varying proportion.

Exposure time (hours)	ILSS for different proportion								
	(55:45)			(60:40)			(65:35)		
	Mean	S.D	C.V	Mean	S.D	C.V	Mean	S.D	C.V
5	31.7	3.56	11.23	33	3.67	11.12	33.3	3.26	9.78
10	31	2.42	7.80	26.6	2.23	8.38	33	2.78	8.42
15	30.3	1.56	5.14	24.8	1.79	7.21	32.6	2.25	6.90
20	30.2	1.69	5.59	24.4	1.23	5.04	32.4	2.56	7.90
25	16.3	0.78	4.78	16.3	1.36	8.34	26.1	2.19	8.39
Average	27.9	2.0	6.90	25.02	2.05	8.01	31.48	2.60	8.27

Table 5.8: Statistical variation of ILSS with exposure time of Glass/Polyester composites for varying proportion.

Exposure time (hours)	ILSS for different proportion								
	(55:45)			(60:40)			(65:35)		
	Mean	S.D	C.V	Mean	S.D	C.V	Mean	S.D	C.V
5	23.7	1.67	7.04	20.7	1.78	8.59	25.4	2.60	8.50
10	21.7	1.36	6.26	20.4	1.64	8.08	25	2.16	8.68
15	18.6	0.86	4.62	17	0.92	5.41	20.4	2.17	4.36
20	16.6	1.30	8.37	15.4	1.46	9.48	15.7	0.83	8.72
25	10.4	0.86	8.26	13.2	1.13	8.56	10.1	1.37	9.4
Average	18.2	1.22	6.91	17.34	1.38	8.02	19.32	0.95	7.93

However, the mean value of ILSS drops suddenly toward the end of exposure time. The low value of standard deviation and C. V. shows the good quality of sample specimen preparation. Similarly, the glass/polyster specimens at 65: 35 proportions show highest mean value of ILSS among the three mix proportions. The standard deviation and coefficient of variation of ILSS decrease with increase in exposure time glass/polyester specimens in all proportion with marginal increase towards the end of exposure time like the glass/epoxy specimens.

The variations of ILSS with increase in exposure time of glass/epoxy and glass/polyster specimens are shown in fig 5.7 and fig 5.8 respectively for all three mixes. As shown in fig 5.7, it is observed that there is a significant continuous reduction of ILSS with the increase in exposure time 20 hours onwards for three proprtions. This may be due to more amount of absorved moisture. However, all the glass/polyster specimens in fig. 5.8 shows considerable reduction of ILSS with increase of exposure time from the beginning to end.

It was reported that the moisture absorption kinetic increases with more conditioning time in glass:epoxy and glass:polyester composites for different proportion at the same constant speed of 200mm/ min. The failure mechanism is due to environmental exposure results in reduced interfacial stress transmissibility due to matrix plasticization,chemical degradation. Matrix plasticization reduces matrix modulus.
Chemical degradation is the result of hydrolysis of interfacial bonds. Mechanical degradation is the result in a function of matrix sweling strain.

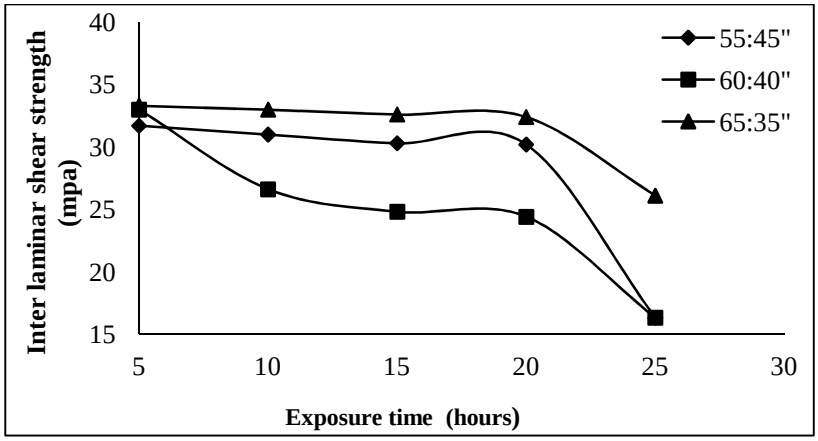

Figure 5.7: Variation of ILSS with different exposure time of glass/epoxy composites for varying proportion

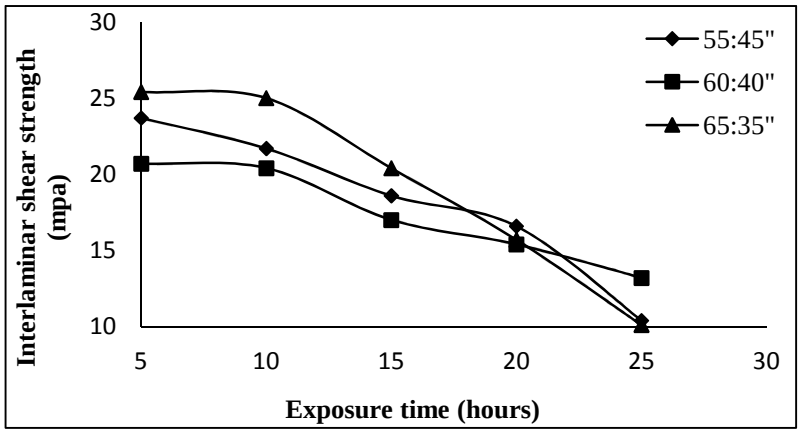

Figure 5.8: Variation of ILSS with different exposure time of glass/Polyester composites for varying proportion. Tensile testing of Composite under hygrothermal loading

The effect of hygrothermal conditions on the elastic modulus of material is studied by tensile testing of specimens at constant loading speed of 200mm/min. The variations of Young's modulii of materials in two orthogonal directions of woven fiber lamina is shown in fig. 5.9. As a result, the tensile strength, ultimate compressive strength that normally decreased with increase of temperature and moisture.

As shown in fig 5.9, both the modulii decrease with increase in temperature. In a similar manner, study is also done to see the effects of hygrothermal conditions on the shear modulus of specimens. The variations of shear modulus with temperature is shown in fig. 5.10. As shown, the shear modulus also decrease with increase of temperature.

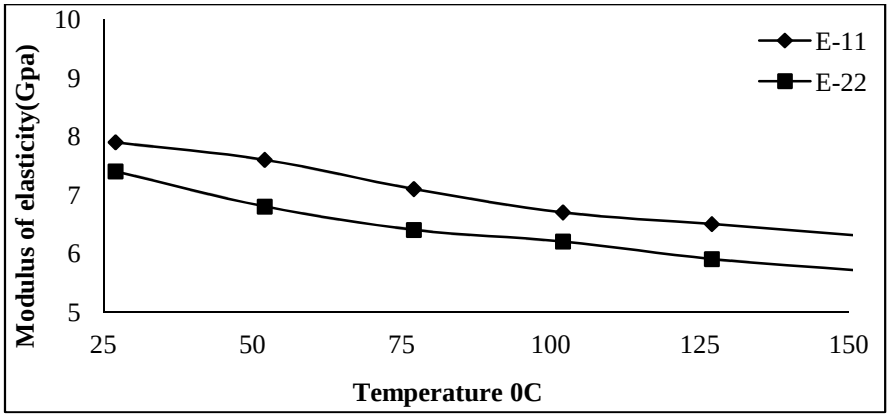

Figure 5.9: Variation of Shear Modulus of elasticity with different temperature of Glass/epoxy composites for 55:45 proportions

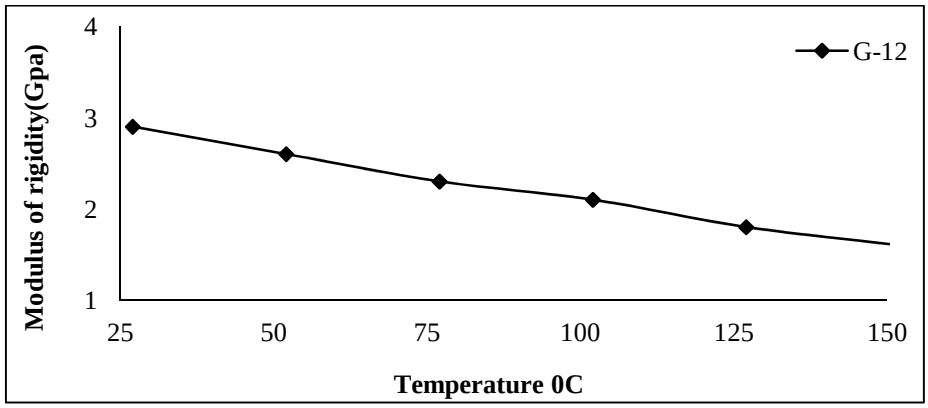

Figure 5.10: Variation of Modulus of rigidity with different temperature of glass /epoxy composites for 55:45 proportions.

The study is then extended to examine the effect of moisture on modulus of elasticity at the same loading speed of 200mm/min. As shown in figure 5.11, the modulus of elasicity decreases with increase of moisture concentrations. Similarly the variations of shear modulus with increase in moisture concentrations is shown in figure 5.12.

As observed, the shear modulus reduces with increase of moisture concentrations. As shown in figure 5.9-5.12, that the modulus of elasticity and modulus of rigidity decreased substantially with increase in temperature and moisture concentration environment. Since temperature and moisture affects all component of composite, principally the matrix and the fibre matrix interface also the fibre. Due to increase in temperature and moisture, the longitudinal and transverse tensile strength varying linearly. Also in the same linear variation appears in case of modulus of rigity in hygrothermal environment. The different degradation rate for young's modulus of elasticity appers due to the difference in fibre-matrix adhesion of the coating on

fibres. It is noticed that along longitudinal fibre direction the modulus of elasticity reduced more than transverse matrix direction because of transverse microcrack.

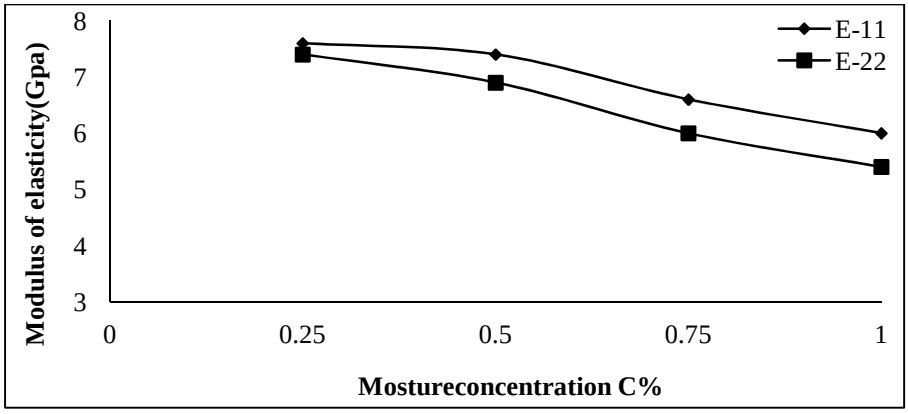

Figure 5.11: Variation of Modulus of rigidity with moisture concentration of glass/epoxy composites for 55:45 proportions.

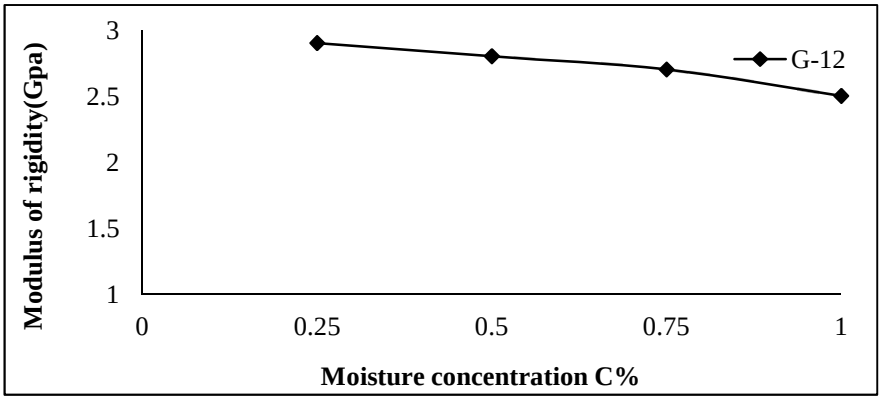

Figure 5.12: Variation of Modulus of rigidity with moisture concentration of glass/epoxy composites for 55:45 proportions.

The lamina materials properties at elevated moisture concentrations and temperatures as per ASTM D3039/D3039M-[2008] are used in the present analysis are shown in Tables 5.9 and 5.10 respectively.

Table 5.9: Elastic moduli of glass fiber / epoxy lamina at different temperatures α_1=0.3 X $10^{-6}/^{O}$K, α_2 =28.1 X $10^{-6}/^{O}$K, β_1=0, β_2=0.44

Elastic moduli	Temperature in (K) 300K	325	350	375	400	425
E_1	7.9	7.6	7.1	6.7	6.5	6.3
E_2	7.4	6.8	6.4	6.2	5.9	5.7
G_{12}	2.9	2.6	2.3	2.1	1.8	1.6
ν_{12}	0.4	0.43	0.41	0.35	0.36	0.35

Table 5.10: Elastic moduli of glass fiber/epoxy lamina at different moisture concentrations α_1=-0.3 X $10^{-6}/^{O}$K, α_2 =28.1 X $10^{-6}/^{O}$K, β_1=0, β_2=0.44

Elastic moduli	0.0	0.25	0.5	0.75	1.0
E_1	7.9	7.6	7.5	7.3	7.2
E_2	7.4	7.4	7.3	7.1	7.0
G_{12}	2.9	2.9	2.8	2.7	2.6
ν_{12}	0.4	0.4	0.4	0.39	0.39

5.2: Flat panels

The studies in this section are grouped into three parts as follows:

- Experimental and numerical study on vibration of woven fiber laminated composite plates in Hygrothermal environment.
- Experimental and numerical study on buckling effects of woven fiber laminated composite plates in Hygrothermal environment.
- Dynamic stability of woven fiber laminated composite plates in Hygrothermal environment subjected to periodic loadings.

5.2.1: Vibration of woven fiber laminated composite flat panels in Hygrothermal environment

The example considered here consists of a woven fiber laminated composite plate 0.235mx0.235mx0.006m subjected to hygrothermal loadings with four sides simply supported and clamped boundary conditions as shown in figure 4.12 and 4.13 respectively.

5.2.1.1: Convergence Study

The convergence study is first done for non-dimensional frequencies of free vibration of 4 layer symmetric cross-ply and symmetric angle-ply laminated composite plates at a temperature of 325K and 0.1% moisture concentration for different mesh divisions as shown in Table 5.9 and 5.10 respectively. As observed, a mesh of 10 ×10 shows good convergence of the numerical solution for the free vibration of composite plates in hygrothermal environment and this mesh is employed throughout for free vibration analysis of woven fiber composite plates in hygrothermal environment.

Table 5.11: Convergence of non-dimensional frequencies of vibration for SSSS four layered laminated composite plates for two lamination sequences at 325K temperature

a/b =1, a/t= 100, At T=300K, E_1=130Gpa, E_2=9.5Gpa, G_{12}=6Gpa, G_{13}=G_{12}, G_{23}=0.5G_{12}, ν_{12}=0.3, α_1=-0.3 X $10^{-6}/^{O}$K, α_2 =28.1 X $10^{-6}/^{O}$K

Non dimensional frequency, $\lambda = \omega_n a^2 \sqrt{\rho / E_2} t^2$

Mess Division	Non- dimensional frequencies at 325K Temperature	
	0/90/90/0	45/-45/-45/45
4x4	8.079	11.380
6x6	8.039	10.785
8x8	8.036	10.680
10x10	8.036	10.680

Table 5.12: Convergence of non-dimensional frequencies of vibration for SSSS four layered laminated composite plates for two lamination sequences at 0.1% moisture concentration

a/b =1, a/t= 100, At T=300K, E_1=130Gpa, E_2=9.5Gpa, G_{12}=6Gpa, G_{13}=G_{12}, G_{23}=0.5G_{12}, ν_{12}=0.3 β1=0, β_2=0.44

Non dimensional frequency, $\lambda = \omega_n a^2 \sqrt{\rho / E_2} t^2$

Mess Division	Non- dimensional frequencies at 0.1% Moisture concentration	
	0/90/90/0	45/-45/-45/45
4x4	9.422	12.383
6x6	9.387	11.858
8x8	9.384	11.765
10x10	9.384	11.765

5.2.1.2: Comparison with previous studies

The present formulation is validated for free vibration analysis of composite plates subjected to temperature and moisture as shown in Table 5.11 & Table 5.12. The square plate has four layers of Graphite / Epoxy composite. The four lowest non-dimensional frequency parameters of the composite plate under hygrothermal loadings obtained by the present finite element are compared with numerical solution published by Sairam and Sinha [1992] and with those of Shen, Zheng and Huang [2004] using a micro-to-macro mechanical analytical model. The present finite element results show good agreement with the previous results in the literature.

Table 5.13: Comparison of non-dimensional free vibration frequencies for SSSS (0/90/90/0) plates at 325K Temperature.

a/b=1, a/t=100, At T = 300*K*, E_1= 130Gpa , E_2= 9.5Gpa, G_{12}= 6Gpa, $G_{13}=G_{12}$, $G_{23}=0.5G_{12}$, $\nu_{12}=0.3$, $\alpha_1=-0.3 \times 10^{-6}/^{O}K$, $\alpha_2 =28.1 \times 10^{-6}/^{O}K$

Non dimensional frequency, $\lambda = \omega_n a^2 \sqrt{\rho / E_2} t^2$

	Non- dimensional frequencies at 325K Temperature		
Mode number	Shen, Zheng and Huang [2004]	Sairam & Sinha [1992]	Present FEM
1	7.702	8.088	8.079
2	17.658	19.196	19.100
3	38.312	39.324	39.335
4	44.038	45.431	45.350

Table 5.14: Comparison of non-dimensional free vibration frequencies for SSSS (0/90/90/0) Plates at 0.1% moisture concentration.

a/b=1, a/t=100, At T = 300*K*, E_1= 130Gpa , E_2= 9.5Gpa, G_{12}= 6Gpa, $G_{13}=G_{12}$, $G_{23}=0.5G_{12}$, $\nu_{12}=0.3$, $\beta_1=0$, $\beta_2=0.44$

Non dimensional frequency, $\lambda = \omega_n a^2\sqrt{\rho / E_2}t^2$

Non- dimensional frequencies at 0.1% Moisture concentration			
Mode number	Shen, Zheng and Huang [2004]	Sairam & Sinha [1992]	Present FEM
1	9.413	9.429	9.422
2	19.867	20.679	20.597
3	39.277	40.068	40.084
4	45.518	46.752	46.708

5.2.1.3: New results for free vibration

New results are presented for modal analysis of woven fiber laminated composite plates in hygrothermal environment. The FEM results based on the present formulation are calculated for vibration frequencies in Hz with respect to rise in temperature and moisture concentration is given below with the following parameter.

- four different modes of frequencies
- Ply orientation
- Number of layers
- Aspect ratios
- Side to thickness ratios

The frequencies of vibration of woven fiber composite plates subjected to hygrothermal environment are observed by using the experimental setup. The variation of frequencies of vibration in Hz of laminated plates (both experimental and numerical) for lowest four modes subjected to temperature is shown in fig 5.13. The frequencies of vibration of composite plates decrease with increase of temperature due to reduction of stiffness. The variation of frequencies in Hz of woven fiber laminated plates, for lowest four modes subjected to moisture concentration is shown in fig 5.14. The frequencies of vibration decrease with increase of percentage of moisture.

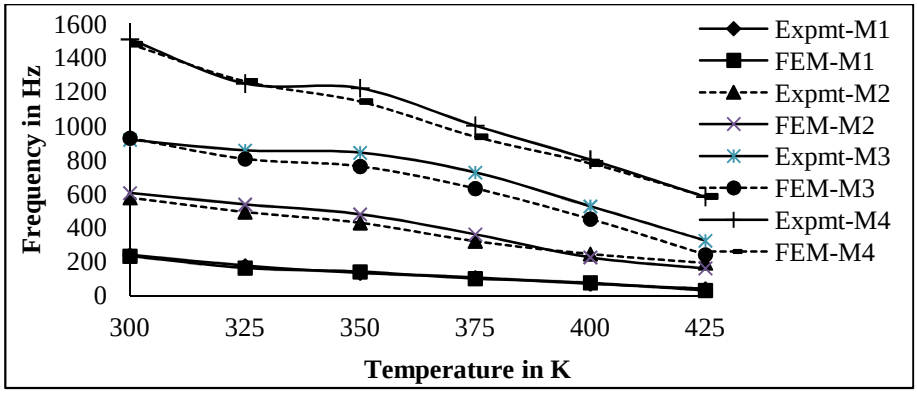

Figure 5.13: Variation of frequency in Hz with temperature for simply supported of 16 layers $[0/0]_{4S}$ woven fiber composite plates

As increase in temperature beyond 400K and 1% moisture concentration for all four lowest mode vibration frequencies are reduced. The experimentally and numerically determined vibration frequencies of woven fiber composite plates with uniform rise in temperature and moisture with respect to their mode shapes (lowest four modes) are shown in figure 5.13 and 5.14 respectively.

The experimentally determined vibration frequencies of symmetric sixteen layers cross-ply laminates with four edges simply supported, is 4%, 8%, 10%, 12% and 3%, 4%, 6%, 7% higher than its numerical counterparts with respect to lowest four modes respectively in hygrothermal environment. The agreement between experimentally and numerically determined resonant frequencies becomes less with higher modes. The reason for variation of frequencies is due to interlaminar or transverse shear deformation and rotary inertia become important even for thin laminate like present one as the wavelength becomes smaller with the rise of the resonant frequency.

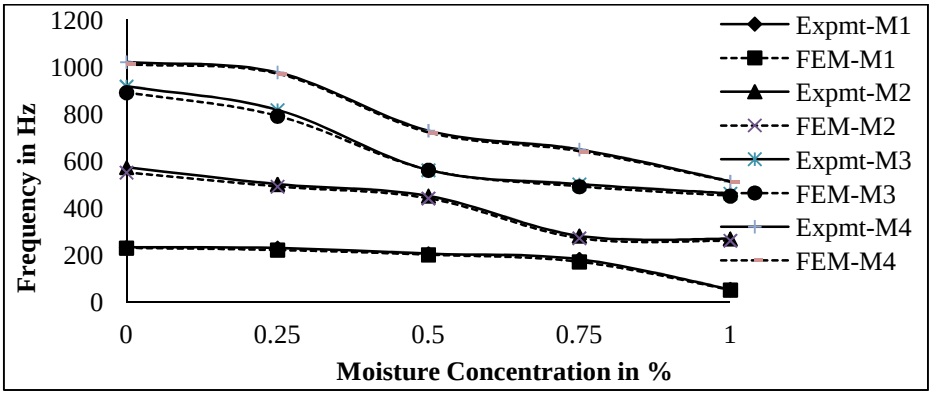

Figure 5.14: Variation of frequency in Hz with moisture concentration for simply supported of 16 layers $[0/0]_{4S}$ woven fiber composite plates

Similar observation is also observed in the study of Vibration of composite plates without hygrothermal loading by Chaudhury *et al.* (2005). The study is then further extended to free vibration of woven fiber composite plates for different lamination sequence. Sixteen layered symmetric and anti symmetric laminates with angle of fiber orientations varying from 0^0 to 90^0 are analyzed. As shown in figure 5.15 and 5.16, the frequencies of vibration in Hz decrease with increase in temperature and moisture concentration for laminates with symmetric and anti-symmetric lay-up. It is observed that the fundamental frequency of vibration for anti-symmetric laminates is more than that for symmetric laminates. This indicates that the free vibration behavior is not much affected by ply orientation for this lay-up. The study is further extended to investigate the effects of other parameters numerically using FEM.

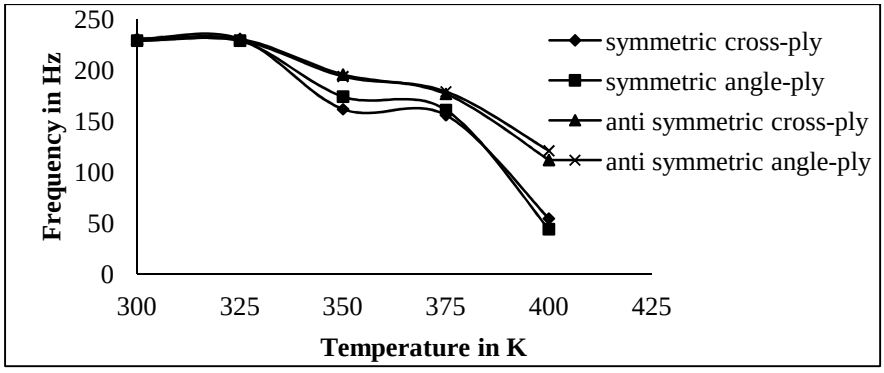

Figure 5.15: Variation of frequency in Hz with temperature for simply supported of 16 layers $[0/90]_{4S}$, $[45/-45]_{4S}$ and $[0/90]_8$, $[45/-45]_8$ woven fiber composite plates

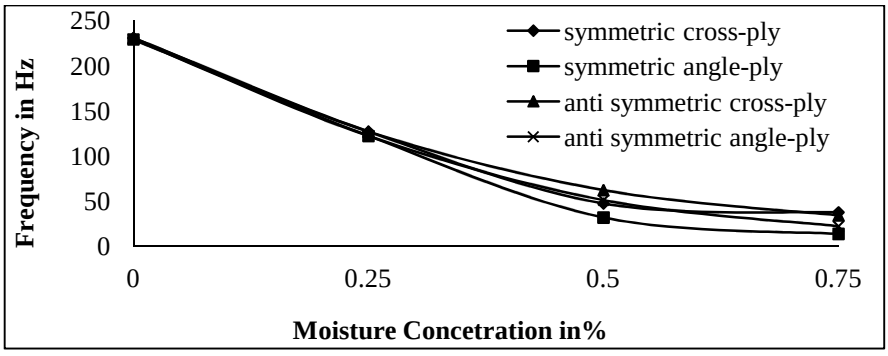

Figure 5.16: Variation of frequency in Hz with moisture concentration for simply supported of 16 layers $[0/90]_{4S}$, $[45/-45]_{4S}$ and $[0/90]_8$, $[45/-45]_8$ woven fiber composite plates

The variation of frequencies in Hz of woven fiber composite plates subjected to rise in temperature and moisture concentration with different number of layers is shown in figure 5.17 and 5.18. The frequencies of vibration decrease with increase in

temperature and moisture for different number of layers. For laminates with symmetric lay-up, the frequencies of vibration increases gradually with increase in the number of layers. The severe hygrothermal environment shall reduce the stiffness of the composite plates.

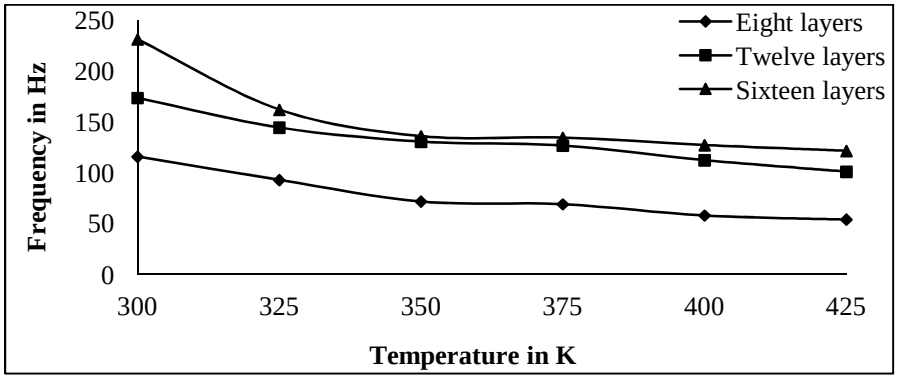

Figure 5.17: Variation of frequency in Hz with temperature for simply supported of 16 layers $[0/0]_{4S}$, 12 layers $[0/0]_{3S}$, 8 layers $[0/0]_{2S}$ woven fiber composite plates

In the present investigation, results are presented for laminates subjected to uniform distribution of temperature and moisture concentration. Sixteen layered Glass fiber/epoxy laminates with simply supported boundary condition have been analyzed experimentally and all computations are made with FEM in MATLAB code.

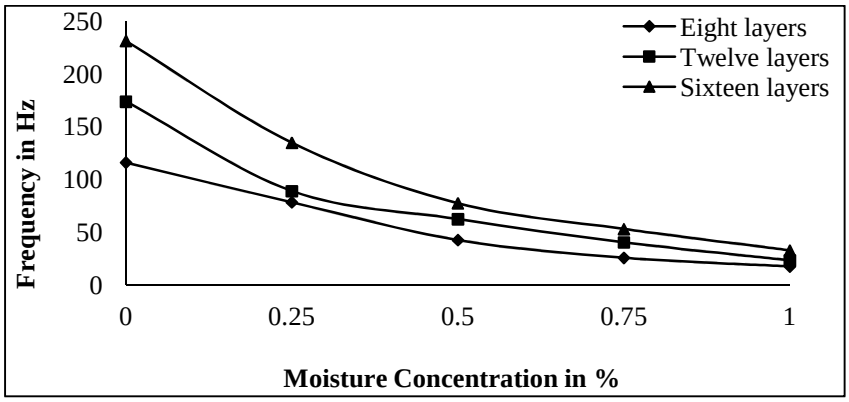

Figure 5.18: Variation of frequency in Hz with moisture concentration for simply supported of 16 layers $[0/0]_{4S}$, 12 layers $[0/0]_{3S}$, 8 layers $[0/0]_{2S}$ woven fiber composite plates

The vibration frequencies in Hz are reported. The aspect ratios considered are 0.5, 1.0 and 2 as shown in figure 5.19 and 5.20. As increase in aspect ratios the frequencies of vibration decreases with increase in temperature and moisture concentration due to reduction of stiffness of the plate. It is observed that for aspect ratio 1 and 2 beyond temperature 400K and moisture concentration 0.75%, frequency of vibration is

decreased and approaches to zero with increase in temperature and moisture concentration due to Hygrothermal buckling starts beyond that point.

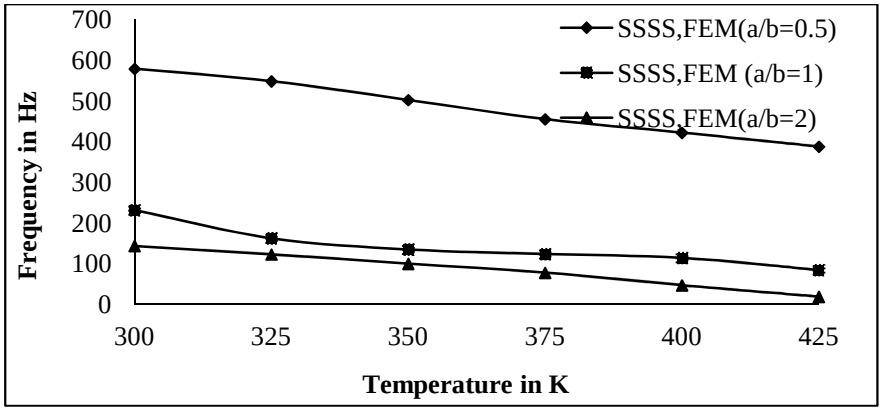

Figure 5.19: Variation of frequency in Hz with temperature for simply supported of 16 layers $[0/0]_{4S}$ woven fiber composite plates

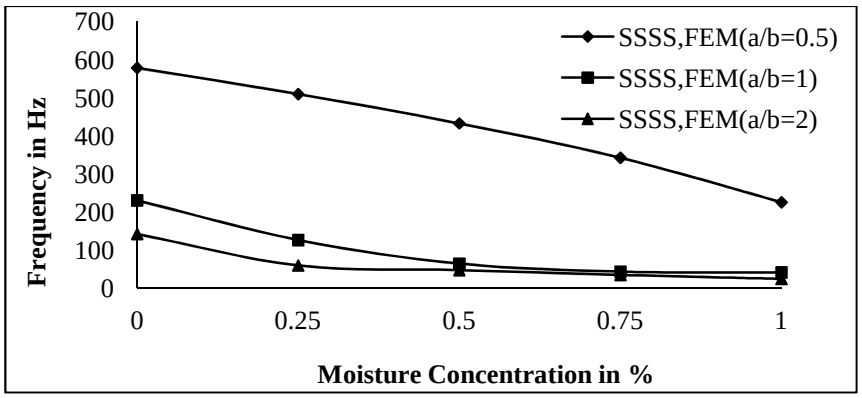

Figure 5.20: Variation of frequency in Hz with moisture concentration for simply supported of $[0/0]_{4S}$ woven fiber 16 layers composite plates

The side to thickness ratios is considered as 25, 40 and 50, as shown in figure 5.21 with increase in temperature and 5.22 with increase in moisture environment. Changes in hygrothermal environment are function of thickness only. It is observed that high temperature and moisture concentration will soften the composite plate. The thicker plate has the stronger stiffness and naturally it has higher vibration frequency as seen in the figure 5.21 and 5.22 in hygrothermal environment. The reason behind the variation of vibration frequencies has rendered the plate more susceptible to localized shear deformation.

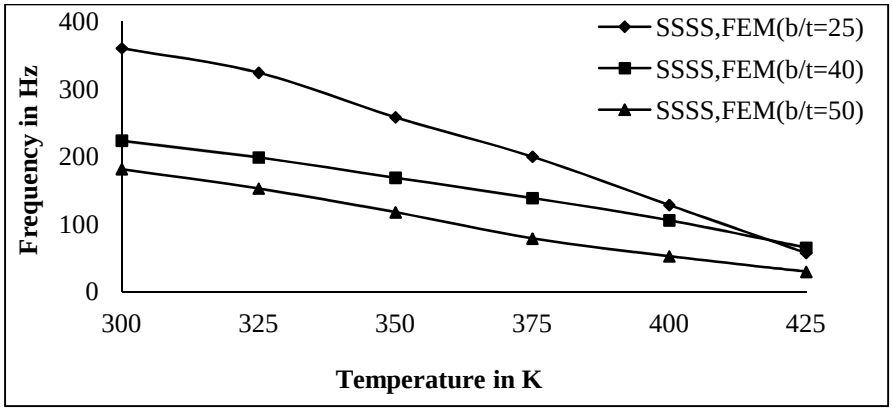

Figure 5.21: Variation of frequency in Hz with temperature for simply supported of 16 layers $[0/0]_{4S}$ woven fiber composite plates

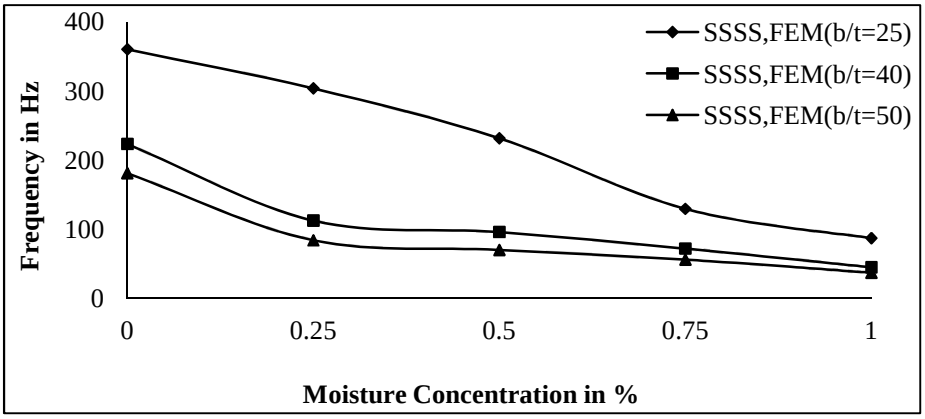

Figure 5.22: Variation of frequency in Hz with moisture concentration for simply supported of 16 layers $[0/0]_{4S}$ woven fiber composite plates

The experimental results for sixteen layered Glass fiber/epoxy with simply supported boundary condition having side to thickness ratios are 40 and 50 are compared with four edges clamped plates, as shown in figure 5.23 with increase in temperature and figure 5.24 with increase in moisture environment. The first mode experimental vibration frequency decrease with increase in side to thickness ratios for simply supported and clamped boundary conditions. The experimental vibration frequency is however higher than its numerical counterparts are due to elastic rigidities.

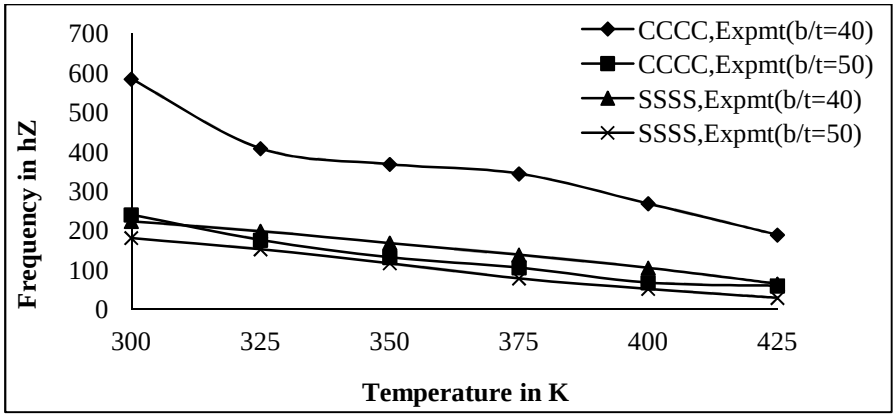

Figure 5.23: Variation of frequency in Hz with temperature for clamped of16 layers $[0/0]_{4S}$ woven fiber composite plates

The clamped plate is subjected to a more sever hygrothermal changes than simply supported plates due to rigid boundaries. The hygrothermal environment shall reduce the stiffness of the composite plates in both clamped and simply supported boundary conditions. The zero frequency point means that the hygrothermal buckling will occur at that point. The vibration frequencies for four sides clamped boundary condition has higher vibration frequencies than simply supported one due to better elastic rigidities and clamping effects at the edges.

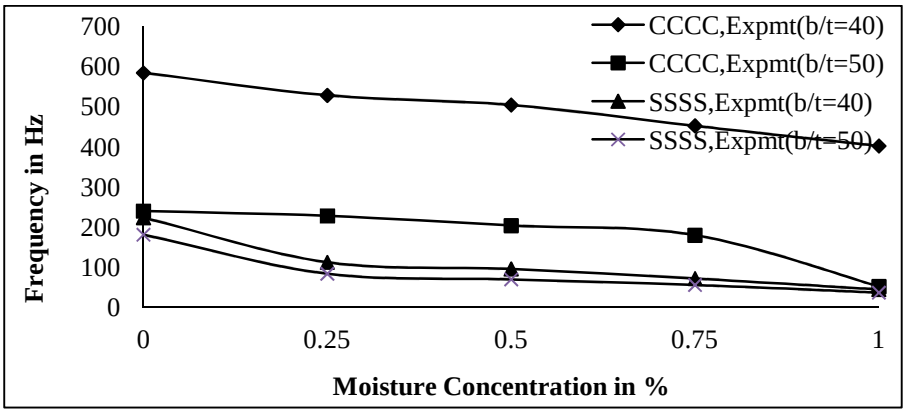

Figure 5.24: Variation of frequency in Hz with moisture concentration for clamped of 16 layers $[0/0]_{4S}$ woven fiber composite plates

5.2.2: Buckling effects of woven fiber laminated composite plates in hygrothermal environment

The example considered here consists of a woven fiber laminated composite plate 0.235mx0.235mx0.006m under hygrothermal loadings with four sides simply supported, two sides clamped and two sides free boundary conditions and subjected to a uniaxial in- plane load as shown in figure 4.15

5.2.2.1: Convergence study

The convergence study is carried out for non-dimensional critical load at a temperature of 325K and 0.1% moisture concentration for different mesh divisions is shown in Table 5.13 and 5.14 respectively. As observed, a mesh of 10 ×10 shows good convergence of the numerical solution for the free vibration and buckling analysis of woven fiber composite plates in hygrothermal environment and this mesh is employed throughout for free vibration and buckling analysis of woven fiber composite plates in hygrothermal environment.

Table 5.15: Convergence of non-dimensional critical load for SSSS four layered laminated composite plates at 325K temperature.

a/b =1, a/t= 100, At T=300K, E_1=130Gpa, E_2=9.5Gpa, G_{12}=6Gpa, $G_{13}=G_{12}$, $G_{23}=0.5G_{12}$, ν_{12}=0.3, α_1=-0.3 X $10^{-6}/^{O}$K, α_2 =28.1 X $10^{-6}/^{O}$K

Critical load, $\lambda = N_{xcr} / (N_{xcr})_{C=0\%}$ or T =300K

Mess Division	Non- dimensional critical load at 325K Temperature	
	0/90/90/0	45/-45/-45/45
4x4	0.4481	0.6120
6x6	0.4459	0.5818
8x8	0.4457	0.5764
10x10	0.4457	0.5745

Table 5.16: Convergence of non-dimensional critical load for SSSS four layered laminated composite plates at 0.1% moisture concentration.

a/b=1, a/t=100, At T=300K, E_1=130Gpa, E_2=9.5Gpa, G_{12}=6Gpa, $G_{13}=G_{12}$, $G_{23}=0.5G_{12}$, $\nu_{12}=0.3$ $\beta_1=0$, $\beta_2=0.44$

Critical load, $\lambda = N_{xcr} / (N_{xcr})_{C=0\%}$ or T =300K

Mess Division	Non- dimensional critical load at 0.1% Moisture concentration	
	0/90/90/0	45/-45/-45/45
4x4	0.6095	0.7255
6x6	0.6079	0.7041
8x8	0.6078	0.7003
10x10	0.6078	0.7003

5.2.2.2: Comparison with previous studies

The present formulation is then validated for buckling analysis of composite plates for temperature and moisture as shown in Table 5.15. The square plate has four layers of Graphite / Epoxy composite. The non-dimensional critical load due to hygrothermal loadings obtained by the present finite element is compared with analytical solution published by Sairam and Sinha [1992] and Patel, Ganapathi and Makhecha [2002]. The present finite element results show good agreement with the previous analytical results published in the literature for buckling of laminated composite plates.

Table 5.17: Comparison of non-dimensional critical load for SSSS (0/90/90/0) layered laminated composite plates at 325K temperature and 0.1% moisture concentration

a/b =1, a/t= 100, At T=300K, E_1=130Gpa, E_2=9.5Gpa, G_{12}=6Gpa, $G_{13}=G_{12}$, $G_{23}=0.5G_{12}$, ν_{12}=0.3 α_1=-0.3 X $10^{-6}/^{O}$K, α_2 =28.1 X $10^{-6}/^{O}$K, β_1=0, β_2=0.44

Non-dimensional Critical load, $\lambda = N_{xcr} / (N_{xcr})_{C=0\%}$ or T =300K

References	Non-dimensional critical load λ	
	At 325K	At 0.1%
Sairam & Sinha [1992]	0.4488	0.6099
Patel,Ganapathi & Makhecha [2002]	0.4466	0.6084
Present FEM	0.4481	0.6095

5.2.2.3. New results for buckling

Numerical results are presented for the static stability behavior of woven fiber composite plates in hygrothermal environment for different parameter. The geometrical and material properties of the laminated composite plates are: a=b=0.235m, h=0.006m (unless otherwise stated). The material properties obtained from tensile testing of glass/epoxy composite plates at different temperatures and moisture as per ASTM D3039/D3039M- [2008] are shown in Table 5.9 and Table 5.10.

- Ply orientation
- Number of layers
- Aspect ratios
- Side to thickness ratios

The results for buckling loads in KN of both the numerical analysis and experimental values with increase in temperature from 300K to 425K in every 25K rise in temperature and 0 to 1% in every 0.25% rise in moisture concentration of sixteen layered woven roving glass fiber/epoxy composites plates are presented for clamped-free-clamped-free boundary condition (CFCF). The variation of buckling loads with increase in temperature and moisture concentrations of the plate is shown in figure

5.25 and 5.26. This shows that there is a good agreement between experimental and numerical results within prescribed FEM formulation.

It is observed that due to the increase in temperature and moisture concentration, there is a decrease in critical buckling loads due to reduction of stiffness and strength. The effect of temperature generally causes a softening of the fibers and the effect of moisture causes plasticization due to absorbed moisture.

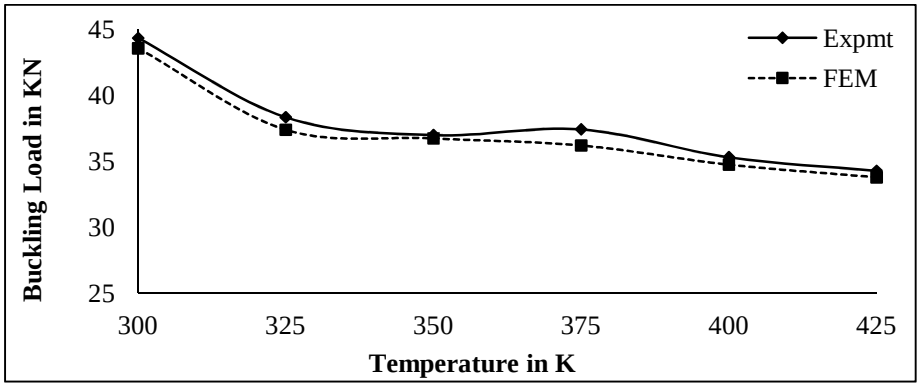

Figure 5.25: Variation of buckling load in KN with temperature of 16 layers $[0/90]_{4S}$ woven fiber composite plates (C-F-C-F)

The critical buckling load decreased severely with increase in temperature upto 425K and moisture concentration beyond 1%, in which hygrothermal buckling appears. In thermal buckling, the composite plate does not remain perfectly flat and suddenly develops a large deformation due to critical temperature stress. The plates will begin to deform as soon as thermal stresses are developed. The deformation will then increase rapidly due to increase in temperature as shown in figure 5.25. The reduction in buckling loads is more pronounced at lower temperature and higher moisture is due to the lowered glass transition temperature at increased moisture concentration. The buckling load is reduced by approximately 27% when the plate is subjected to 1% moisture concentration and temperature increase to 400K.

The effects of reduction in the buckling loads are more prominent for increase in temperature as compared to moisture concentration. It is clearly observed that the detrimental effect of the increased moisture concentration and temperature on the stability of the plate. It is also seen that the hygroscopic condition on the stability of the plate becomes more significant in presence of the thermal loading.

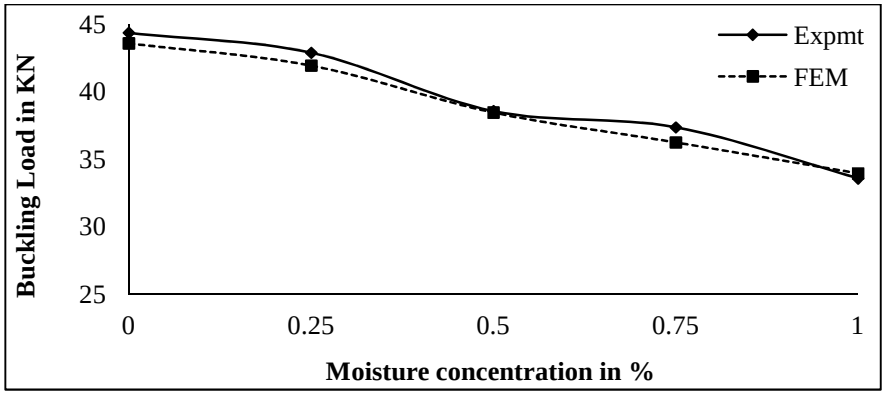

Figure 5.26: Variation of buckling load in KN with moisture concentration of 6 layers $[0/90]_{4S}$ woven fiber composite plates (C-F-C-F)

The variation of buckling load in KN for sixteen layer of composite plates with simply supported boundary conditions are presented for a/b=1 and b/t=40, subjected to uniform distribution of temperature in every increase in temperature of 25K from 300K to 425K and moisture concentration of every increase in 0.25% moisture from 0 to1% with different lamination sequence is analyzed by using FEM formulations in figure 5.27 and 5.28 respectively. It is shown that the buckling loads for anti-symmetric laminates are more than symmetric laminates with increase in uniform temperature and moisture concentration environment. With increase in temperature and moisture concentration the reduction in buckling loads is linear. Due to this reason, the woven fiber laminated plates is marginally affected in thermal and moisture environment. This reduction in buckling loads is due to the effect of decrease in shear modulus.

The reduction of buckling loads with increase in temperature from 300K to 425K, for anti- symmetric laminates are more than 18% and symmetric laminates are about to 15%. Similarly the reductions of buckling loads for increase in moisture concentration from 0 to 1%, for anti-symmetric laminates are nearly 11% and symmetric laminates are approximately 9%.

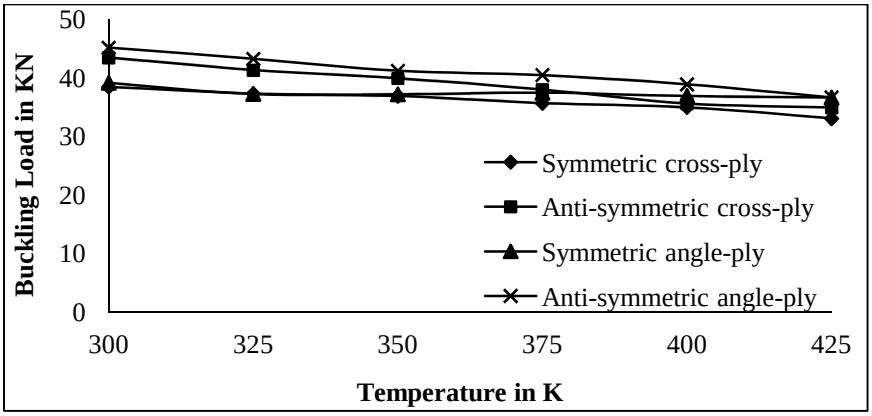

Figure 5.27: Variation of buckling load in KN with temperature of 16 layers $[0/90]_{4S}$, $[45/-45]_{4S}$ and $[0/90]_8$, $[45/-45]_8$ woven fiber composite plates (S-S-S-S)

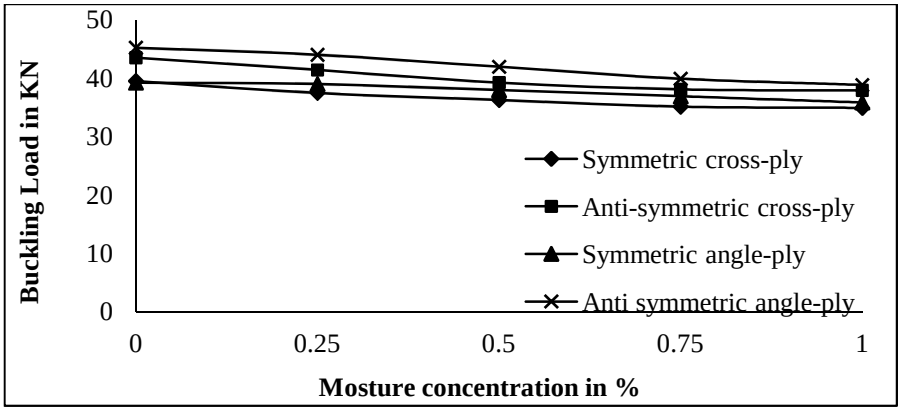

Figure 5.28: Variation of buckling load in KN with moisture concentration of 16 layers $[0/90]_{4S}$, $[45/-45]_{4S}$ and $[0/90]_8$, $[45/-45]_8$ woven fiber composite plates (S-S-S-S)

The variation of buckling loads in KN are observed for a/b=1 for four, eight and twelve layered simply supported cross-ply symmetric laminated plates subjected to uniform distribution of temperature from 300K to 425K in every rise of 25K temperature and moisture concentration from 0 to 1% in every rise of 0.25% moisture are reported by using present FEM formulation in figure 5.29 and 5.30 respectively. It is observed that the buckling loads increase with increase in number of layers up to eight layers beyond that, increase in number of layers the buckling loads remain constant at uniform increase in temperature and moisture concentration. It is also noted that with increase in temperature hardening type non linear behavior of the buckling loads for all layers of laminates. The buckling loads decrease with increase in temperature and moisture concentration environment.

The reductions in buckling loads with increase in temperature from 300K to 425K are 22% and for increase in moisture concentration from 0 to 1% are approximately 9%. This shows that the laminates are severely affected in higher thermal environment.

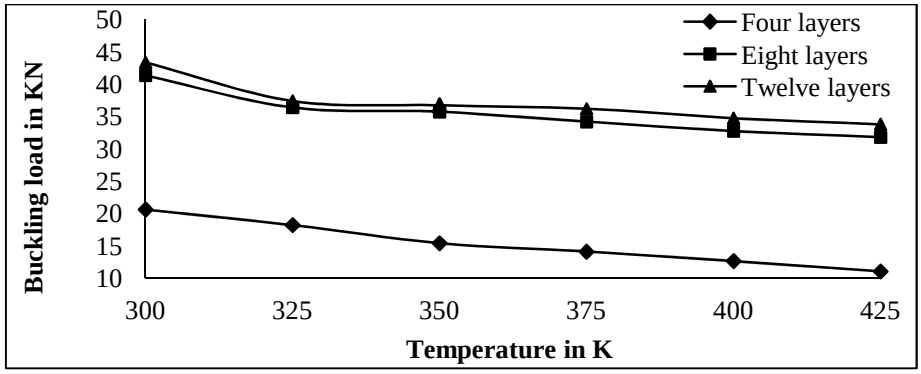

Figure 5.29: Variation of buckling load in KN with temperature of 4 layers $[0/90]_{1S}$, 8 layers $[0/90]_{2S}$, 12 layers $[0/90]_{3S}$ woven fiber composite plates (S-S-S-S)

The variation of buckling loads in KN for different aspect ratios such as a/b=0.5, a/b=1 and a/b=2 for b/t=40, sixteen layered simply supported boundary conditions for symmetric cross-ply laminated plates are subjected to uniform increase of temperature from 300K to 425K in every 25K rise in temperature and moisture concentrations from 0 to 1% in every rise of 0.25% moisture concentration by using FEM results are as shown in figure 5.31 and 5.32 respectively. It is also observed that the buckling loads increase with increase in aspect ratios of woven fiber laminated composite plates in hygrothermal environment. Hygrothermal buckling also starts at room temperature about 300K which is known as stress–free level. Similarly hygroscopic buckling will start at 0.25% of moisture concentration which is also known as stress-free level. As the hygrothermal stress resultants are integrated quantities, their effect increases with the absorption of more moisture until equilibrium is reached.

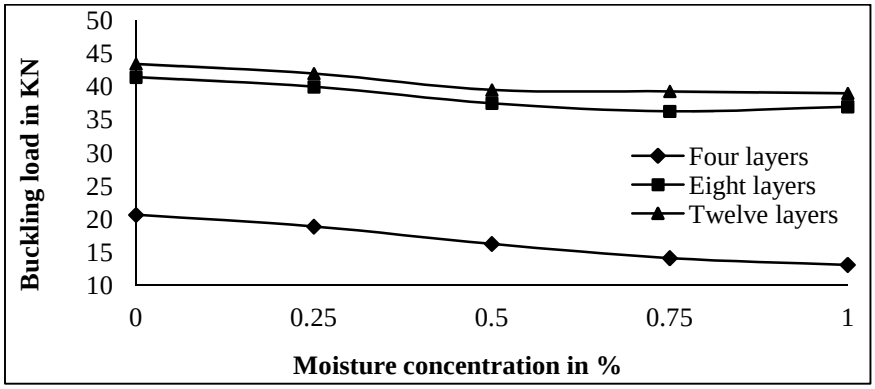

Figure 5.30: Variation of buckling load in KN with moisture concentration of 4 layers $[0/90]_{1S}$, 8 layers $[0/90]_{2S}$, 12 layers $[0/90]_{3S}$ woven fiber composite plates (S-S-S-S)

The reduction in buckling loads for increase in temperature from 300K to 425K are 12.61% for aspect ratio 0.5 and 22.42% for aspect ratios 1 and 9.23% for aspect ratio 2. Similarly the reduction in buckling loads for increase in moisture concentration from 0 to 1% are 6% for aspect ratio 0.5 and 12% for aspect ratios 1 and 1% for aspect ratio 2. The woven fiber laminated composite plates having aspect ratio more than 1 are stable and affected substantially in hygrothermal environment.

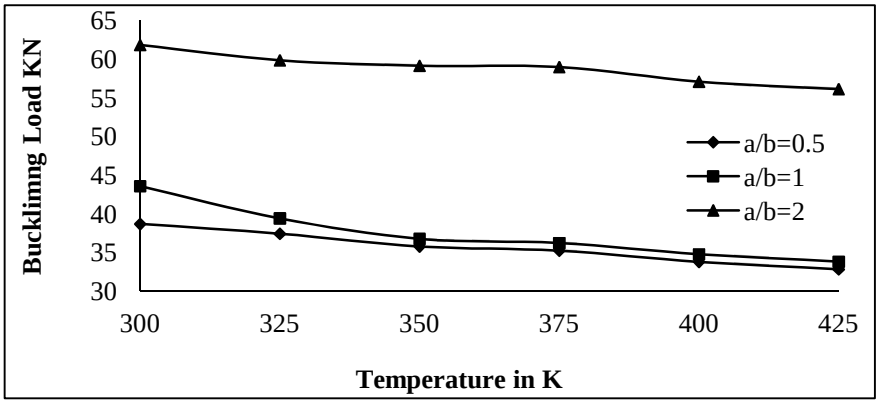

Figure 5.31: Variation of buckling load in KN with temperature of 16 layers $[0/90]_{4S}$ woven fiber composite plates (S-S-S-S)

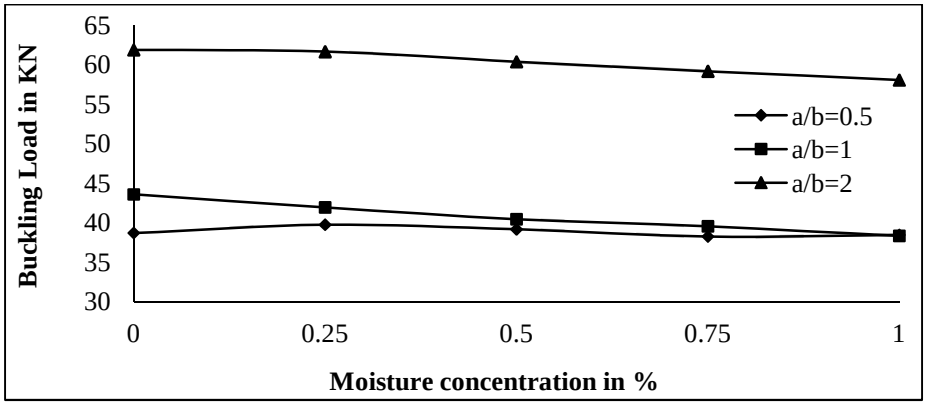

Figure 5.32: Variation of buckling load in KN with moisture concentration of 16 layers $[0/90]_{4S}$ woven fiber composite plates (S-S-S-S)

The experimental results of buckling loads for different aspect ratios a/b=0.5, a/b=1 and a/b=2 for b/t=40, sixteen layered cross-ply symmetric woven fiber laminated composite plates for clamped-free-clamped-free boundary conditions are subjected to uniform distribution of temperature from 300Kto 425K in every rise in temperature of 25K and moisture concentration 0 to 1% in every rise of 0.25% moisture are presented in figure 5.33 and 5.34 respectively. From the results it is clear that the buckling loads are increase with increase in aspect ratios in hygrothermal

environment. The reduction of buckling loads with increase in temperature and moisture concentration is linear. The buckling loads for CFCF boundary conditions are more than four sides simply supported boundary conditions due to rigid boundaries in hygrothermal environment.

The reduction in buckling loads from increase in temperature from 300K to 425K, the experimental results for CFCF boundary conditions with aspect ratio for a/b=0.5 is 8.81%, a/b=1 is 11.04 and a/b=2 is 11.04% respectively. Similarly The reduction in buckling loads from increase in moisture from 0 to 1%, the experimental results for CFCF boundary conditions with aspect ratios for a/b=0.5 is 15.28%. a/b=1 is 19.7% and a/b=2 is 22.92% respectively. The reduction in buckling loads for higher aspect ratio is more than lower one in severe hygrothermal environment.

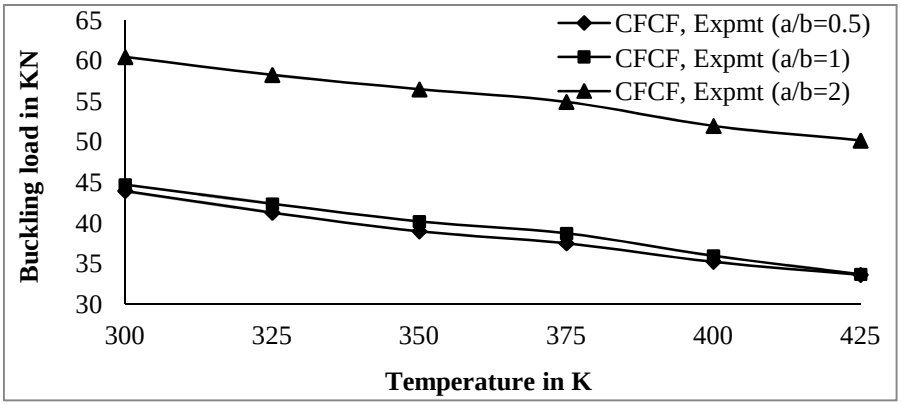

Figure 5.33: Variation of buckling load in KN with temperature of 16 layers $[0/90]_{4S}$ woven fiber composite plates (C-F-C-F) boundary Condition

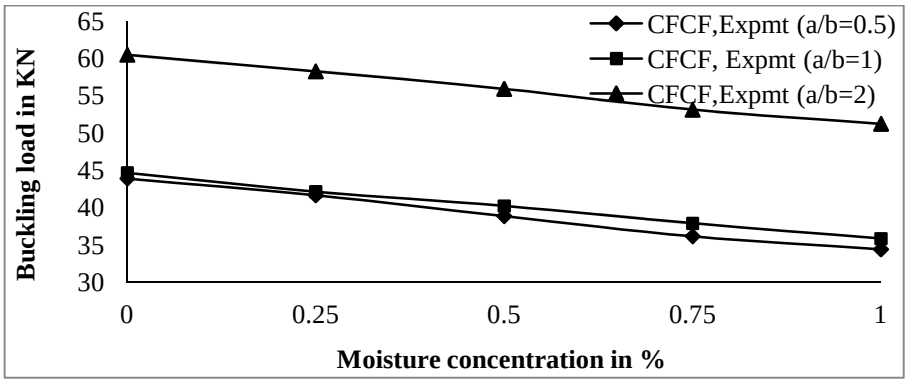

Figure 5.34: Variation of buckling load in KN with moisture concentration 16 layers $[0/90]_{4S}$ of woven fiber composite plates (C-F-C-F) boundary condition

The variation of buckling loads for different side to thickness ratios b/t=25, b/t=40 and b/t=100 for a/b=1, sixteen layered cross-ply symmetric woven fiber laminated

plates for simply supported boundary conditions are subjected to uniform distribution of temperature from 300Kto 425K in every rise in temperature of 25K and moisture concentration 0 to 1% in every rise of 0.25% moisture are observed using FEM results in figure 5.35 and 5.36. From the results it is clear that the buckling loads are more for plates with lower side-to-thickness ratios than higher side-to-thickness ratios. The reduction in buckling loads is linear with increase in temperature and moisture concentration. This present method of analysis has been found efficient in order to evaluate the buckling load of moderately thick composite laminated plate subjected to hygrothermal loading. It is seen that the buckling load decreases with increase in moisture concentration for different aspect and side-to-thickness ratios due to degradation in material properties at higher temperature and moisture concentration.

It is also evident from the figure 35 that the moderately thick laminated composite plates are more stable than thin laminated plates with increase in temperature and moisture concentration environment. The random changes in thickness have more impact on hygrothermal buckling loads scattering as compared to individual random changes in material properties. The sensitivity of hygrothermal buckling loads is due to variation in geometric and material properties which is dependent on thickness only. The reduction in buckling loads with increase in temperature from 300K to 425K are 21.85% for b/t=25, 15.36% for b/t=50 and 24.82% for b/t=100. Similarly the reduction in buckling loads with increase in moisture concentration from 0 to 1% are 17.15% for b/t=25, 4.6% for b/t=50 and 4.32% for b/t=100. It is also observed that the moderately thick woven fiber laminated composite plates are more susceptible to hygrothermal environment and losses its stiffness and strength early as compared to thin composite plates.

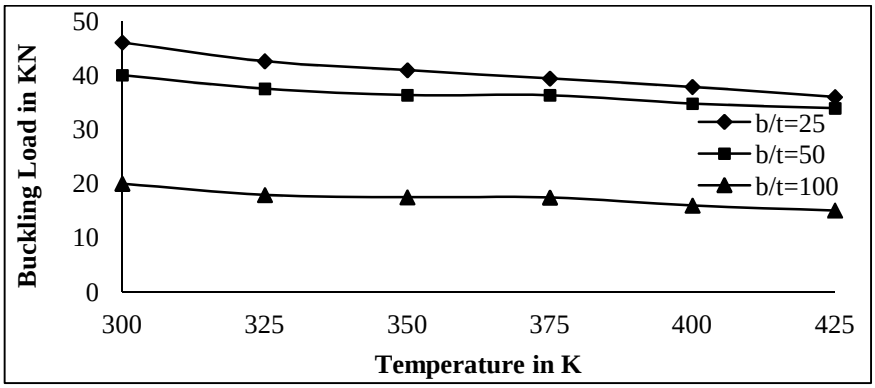

Figure 5.35: Variation of buckling load in KN with temperature of 16 layers $[0/90]_{4S}$ woven fiber composite plates (S-S-S-S)

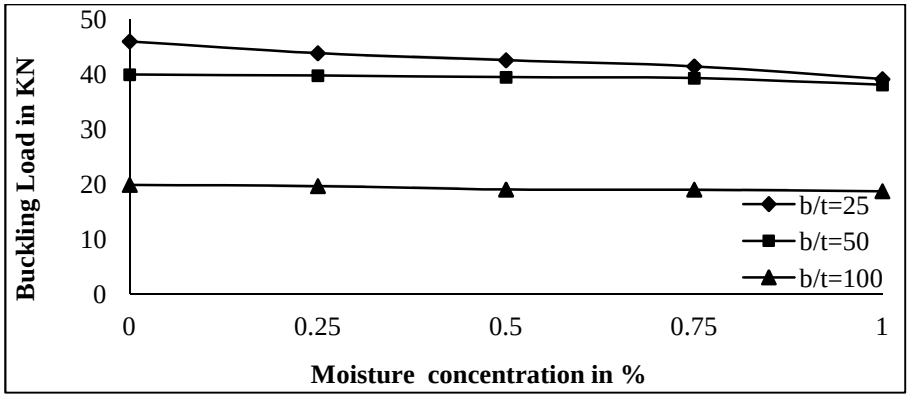

Figure 5.36: Variation of buckling load in KN with moisture concentration of 16 layers $[0/90]_{4S}$ woven fiber composite plates (S-S-S-S)

The experimental results of buckling loads for different side to thickness ratios b/t=40 and b/t=50 for a/b=1, sixteen layered cross-ply symmetric woven fiber laminated composite plates for clamped-free-clamped-free boundary conditions are subjected to uniform distribution of temperature from 300Kto 425K in every rise in temperature of 25K and moisture concentration 0 to 1% in every rise of 0.25% moisture are presented in figure 5.37 and 5.38 respectively.

From the results, it is clear that the buckling loads are decreases with increase in side-to-thickness ratio in hygrothermal environment. The reduction of buckling loads with increase in temperature and moisture concentration is non linear, due to changes in plate thickness. The critical buckling loads for CFCF boundary conditions are more than four sides simply supported boundary conditions due to rigid boundaries in hygrothermal environment.

The reduction in buckling loads from increase in temperature from 300K to 425K, the experimental results for CFCF boundary conditions with side-to-thickness ratio for b/t=40 is 20.54% and b/t=50 is 22.68% respectively. Similarly The reduction in buckling loads from increase in moisture from 0 to 1%, the experimental results for CFCF boundary conditions with side-to-thickness ratio for b/t=40 is 23.87% and b/t=50 is 24.33% respectively. The reduction in buckling loads for higher side-to-thickness ratio is more than lower values in hygrothermal environment due to lower thickness of the plates.

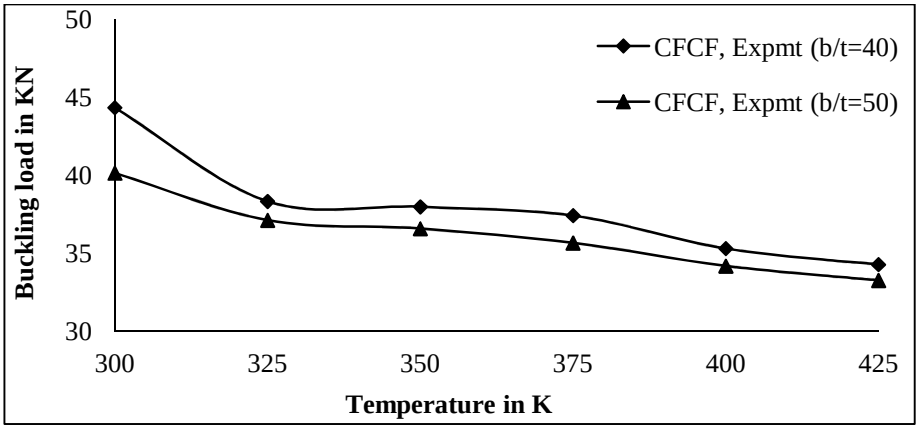

Figure 5.37: Variation of buckling load in KN with temperature of 16 layers $[0/90]_{4S}$ woven fiber composite plates (C-F-C-F) boundary condition.

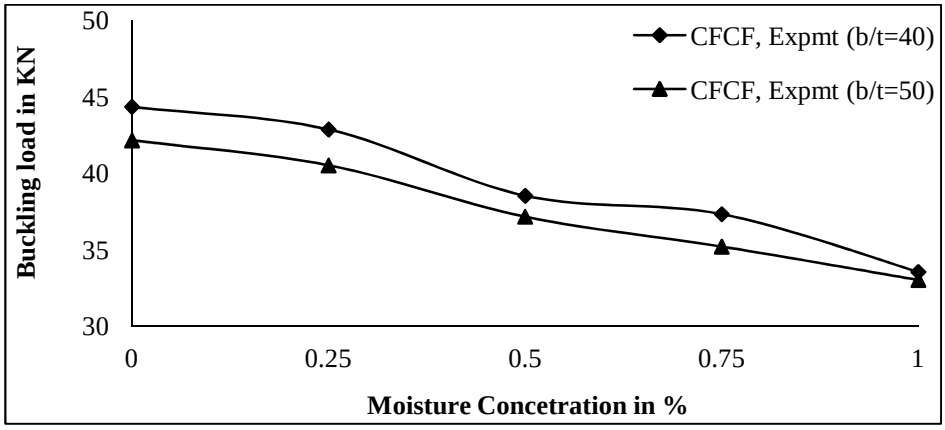

Figure 5.38: Variation of buckling load in KN with moisture concentration of 16 layers $[0/90]_{4S}$ woven fiber composite plates (C-F-C-F) boundary condition

5.2.3: Dynamic instability of woven fiber laminated composite plates in hygrothermal environment

The numerical results of the study of behavior of woven fiber composite plates subjected to hygrothermal conditions under in-plane periodic loads are presented using the formulations as follows.

5.2.4: Non-dimensionalization of parameters

Non-dimensional frequency $\lambda = \omega_n a^2 \sqrt{\rho / E_2} t^2$

Non-dimensional Critical load, $\lambda = N_{xcr} / (N_{xcr})$

Non-dimensional excitation frequency $\Omega = \overline{\Omega} a^2 \sqrt{(\rho / E_{22} h^2)}$

(unless otherwise stated) is used throughout the dynamic instability studies, where

$\overline{\Omega}$ is the excitation frequency in radians/second.

5.2.4.1: Convergence study

The convergence study is done for simply supported square 4 layer symmetric cross-ply and symmetric angle-ply laminated composite plates for elevated temperature and moisture conditions for different mess divisions. Dynamic stability analysis of laminated composite plates subjected to hygrothermal conditions under in-plane periodic loads are presented in Table 5.18 and Table 5.19. As observed, a mesh of 10 ×10 shows good convergence of the numerical solution of dynamic stability of woven fiber composite plates and this mesh is employed throughout the dynamic stability analysis of woven fiber composite plates in hygrothermal environment.

Table 5.18: Convergence of non-dimensional excitation frequency for SSSS four layered laminated composite plates for different ply orientations at 325K temperature

a/b =1, a/t= 100, At T=300K, E_1=130Gpa, E_2=9.5Gpa, G_{12}=6Gpa, $G_{13}=G_{12}$, $G_{23}=0.5G_{12}$, ν_{12}=0.3, α_1=-0.3 X $10^{-6}/^{O}$K, α_2 =28.1 X $10^{-6}/^{O}$K , α = static load factor = 0.2, β = dynamic load factor = 0.2

Non-dimensional excitation frequency $\Omega = \overline{\Omega} a^2 \sqrt{(\rho / E_{22} h^2)}$

Mess Division	Non-dimensional excitation frequency at 325K Temperature	
	0/90/90/0	45/-45/-45/45
4x4	15.23	22.10
6x6	15.16	20.86
8x8	15.16	20.64
10x10	15.16	20.56

Table 5.19: Convergence of non-dimensional excitation frequency for SSSS four layered laminated composite plates for different ply orientations at 0.1% moisture concentration.

a/b =1, a/t= 100, At T=300K,E_1=130Gpa, E_2=9.5Gpa, G_{12}=6Gpa, $G_{13}=G_{12}$, $G_{23}=0.5G_{12}$, ν_{12}=0.3 β_1=0, β_2=0.44,α = static load factor = 0.2, β = dynamic load factor = 0.2 Non-dimensional excitation frequency $\Omega = \overline{\Omega} a^2 \sqrt{(\rho / E_{22} h^2)}$

Mess Division	Non-dimensional excitation frequency at 0.1% Moisture concentration	
	0/90/90/0	45/-45/-45/45
4x4	18.05	24.17
6x6	17.99	23.07
8x8	17.99	22.88
10x10	17.99	22.82

5.2.4.2: Comparison with previous studies

To validate the formulation, the frequencies of excitation frequency during parametric resonance of laminated composite plates are computed and compared with previously

published results from literature without hygrothermal environment as shown in Table 5.20. The boundary frequencies of square plate have four layers of symmetric cross-ply laminates. The boundary frequencies without hygrothermal environment obtained by the present finite element are compared with analytical solution obtained by Wang and Dawe [2002]. The present finite element results show good agreement with the previous analytical results published in the literature for boundary frequencies.

Table 5.20: Comparison of dimensional excitation frequency for SSSS four layered laminated composite plates for symmetric cross-ply laminates

a/b =1, a/t= 100, At T=300K, $G_{12}/ E_2= G_{13}/ E_2 =0.6$, $G_{23}/ E_2= 0.5$, $\nu_{12}= 0.25$

Non-dimensional excitation frequency $\Omega = \overline{\Omega} a^2 \sqrt{(\rho / E_{22} h^2)}$

α = static load factor	β = dynamic load factor	ω^U Upper bound frequency	ω^L Lower bound frequency	Present FEM	
				ω^U	ω^L
0	0	144.57	144.57	143.67	143.67
0	0.3	155.03	133.29	153.12	131.23
0	0.6	164.83	120.95	162.32	118.12
0	0.9	174.08	107.21	171.56	105.87
0	1.2	182.87	91.43	180.45	89.92
0	1.5	191.25	72.28	189.34	70.59
0	0	144.57	144.57	143.67	143.67
0.2	0.06	131.71	126.86	129.77	124.85
0.4	0.12	117.45	106.24	115.28	104.33
0.6	0.18	101.20	80.49	99.47	78.27
0.8	0.24	81.78	40.89	78.94	38.92

5.2.4.3: New results for dynamic stability

After validating the present formulation, the same is employed to study the effect of different parameters on the dynamic instability effects of woven fiber composite plates in hygrothermal environment The parameters are:

- Number of layers
- Aspect ratios
- Side to thickness ratios
- Static load factor
- Increase in hygrothermal conditions
- Ply orientation
- Lamination sequence
- Degree of orthotropy

The non-dimensional excitation frequency $\Omega = \overline{\Omega} a^2 \sqrt{(\rho / E_{22} h^2)}$ is used throughout the dynamic instability studies, where $\overline{\Omega}$ is the excitation frequency in radian/second. The principal instability regions of woven fiber laminated composite flat panel subjected to in-plane periodic loads is plotted with non-dimensional frequency Ω/ω (ratio of excitation frequency to the free vibration frequency) versus the dynamic in-plane load β. Here, a static load factor α=0.2 is taken for parametric study of laminated composite plates in hygrothermal environment unless otherwise stated.

The structural instability may lead to large deflection or large amplitude vibrations of structural elements leading to local or global failures. So the analysis is focused on the determination of the primary instability region of laminated composite plates under hygrothermal loads. The width of primary instability region frequencies is the separation of the boundaries of the primary instability region for the given plate. This can be used as an instability measure to study the influence of the other parameters. This is the most dangerous zone and has the greatest practical importance. As can be seen, the primary instability region that occurs in the vicinity of 2ω (α = β =0) and the upper and lower excitation frequencies of the plates decrease with the increase of the static load parameter. It is also observed that the primary instability region for each plate increase with increasing static and dynamic load parameter, and the width of the unstable zone is becoming more significant at the higher load parameter. The spectrum of the values of parameters causing unstable motion is called the dynamic instability region or DIR or parametric resonance. The industry driven woven fiber composite plates subjected to hygrothermal environment are considered here to study the effect of different parameters on the excitation frequency and width of instability regions of composite plates. The geometrical and material properties of the laminated

composite plates are: a=b=0.235m, h=0.006m. The material properties obtained from tensile testing of glass/epoxy composite plates at different temperatures and moisture as per ASTM D3039/D3039M- [2008] are shown in Table 5.9 and Table 5.10.

The effect of increase in number of layers with thickness of the laminated composite plates on the non-dimensional excitation frequency is illustrated in figure 5.39 at temperature 325K. The 8, 12 and 16 layer laminated plates are having thickness of 6mm, 9mm and 12mm respectively. As observed, the onset of instability occurs later with narrow instability regions with increase in number of layers due to higher stiffness. As expected, woven fiber laminated plates is more stable with increase in number of layers under periodic loads due to bending stretching coupling. The variation of excitation frequency with increase of dynamic load is studied for composite plates with 0.25% moisture concentration for different increase in number of layers as shown in figure 5.40. As observed, the onset of instability occurs earlier and the width of instability regions becomes smaller with decrease in number of layers.

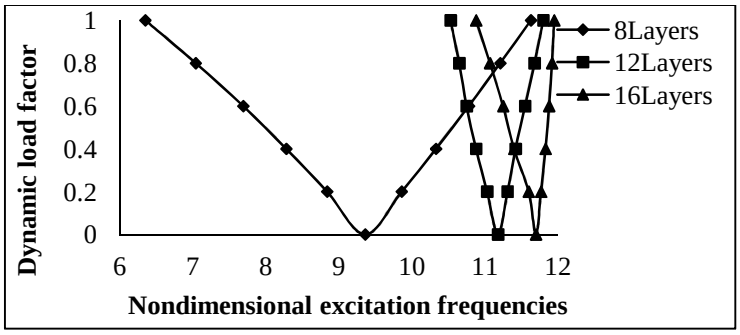

Figure 5.39: Variation of instability regions with temperature at 325K for simply supported of a/b=1, α= 0.2, woven fiber composite plates

The laminated composite plate affected severely and loses its strength and stiffness in hygrothermal environment. All further parametric studies are done with an eight layers laminate combinations. The effects of number of layers shift the instability region to larger excitation frequencies.

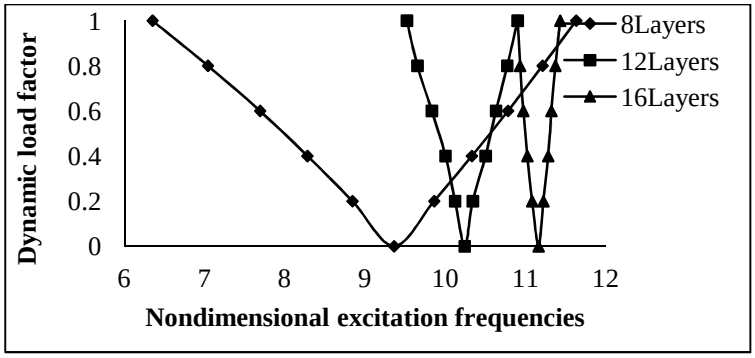

Figure 5.40: Variation of instability regions with moisture concentration at 0.25% for simply supported of a/b=1, α= 0.2, woven fiber composite plates

The effect of increase in aspect ratio for a/b=0.5, 1 and 2 on the non-dimensional excitation frequencies is analyzed for composite plates as shown in figure 5.41 at temperature 325K. The onset of instability occurs earlier for composite plates with increase in aspect ratios. With increase in aspect ratios, the excitation frequencies are decreased, due to reduction of stiffness of the plates in hygrothermal environment.

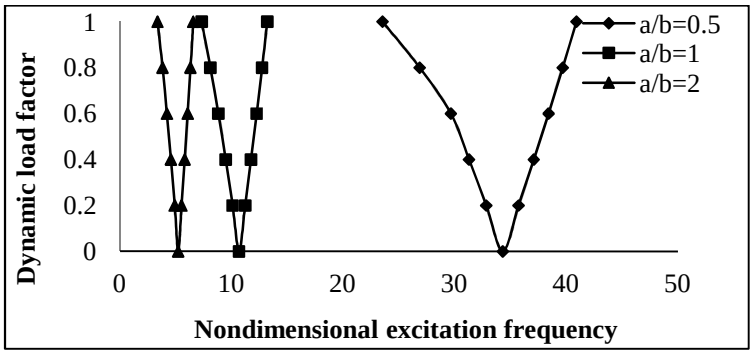

Figure 5.41: Variation of instability regions with temperature at 325K for simply supported of a/b=1, α= 0.2, woven fiber composite plates

The effect of increase in aspect ratios on the non-dimensional excitation frequencies is studied for composite plates as shown in figure 5.42 at moisture concentration 0.25%. The onset instability occurs later for square plates than rectangular plates with wider instability region. The excitation frequencies are decreased with increase in aspect ratios even for composite plates under moisture conditions.

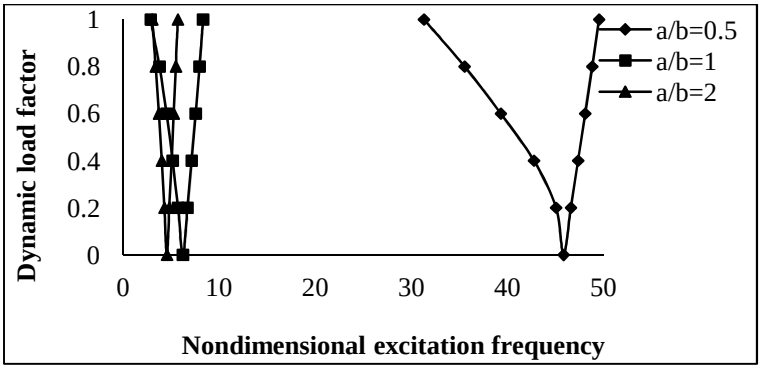

Figure 5.42: Variation of instability regions with moisture concentration at 0.25% for simply supported of a/b=1, α= 0.2, woven fiber composite plates

The effect of increase in side to thickness ratio for b/t=25 and 50 on the non-dimensional excitation frequencies is investigated for composite plates as shown in figure 5.43 at temperature 325K. It is observed from the figure that the onset of instability occurs earlier for increase in side to thickness ratio. The excitation frequencies are decreased with increase in side to thickness ratio. The thick plates are more dynamically stable than thin plates in temperature environment.

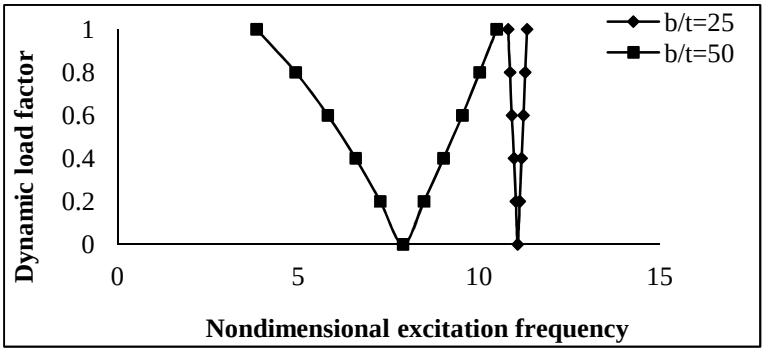

Figure 5.43: Variation of instability regions with temperature at 325K for simply supported of a/b=1, α= 0.2, woven fiber composite plates

The effect of increase in side to thickness ratio for b/t=25 and 50 on the non-dimensional excitation frequencies is investigated for composite plates as shown in figure 5.44 at a moisture 0.25%. It is observed from the figure that the onset of instability occurs earlier for increase in side to thickness ratio. The excitation frequencies are decreased with increase in side to thickness ratio. The thick plates having narrow instability region shows more stiffness and strength than thin plates in hygrothermal environment. The width of instability regions increases due to increase in dynamic loads.

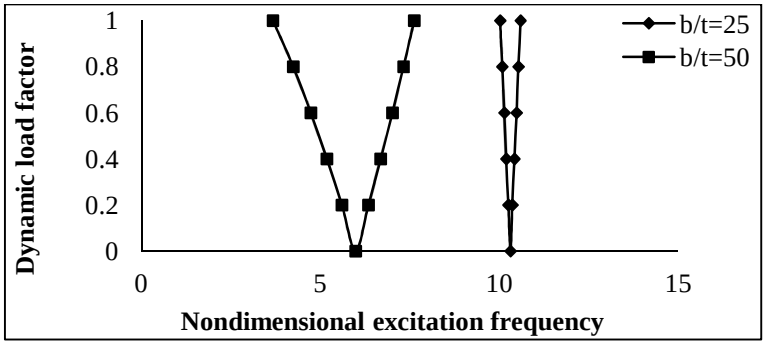

Figure 5.44: Variation of instability regions with moisture concentration at 0.25% for simply supported of a/b=1, α= 0.2, woven fiber composite plates

The effect of increase in static load factor of eight layered anti-symmetric woven fiber laminated composite plates on non-dimensional excitation frequency is analyzed in figure 5.45 at temperature 325K. It is observed that with the increase of static load factor from 0.4 to1, the onset of dynamic instability occurs earlier and the width of dynamic instability region also increases. The reduction of excitation frequencies with increase in static load factors from 0.4 to1 is more than 10% due to reduction of stiffness and strength. All further studies are done with a static load factor α=0.2.

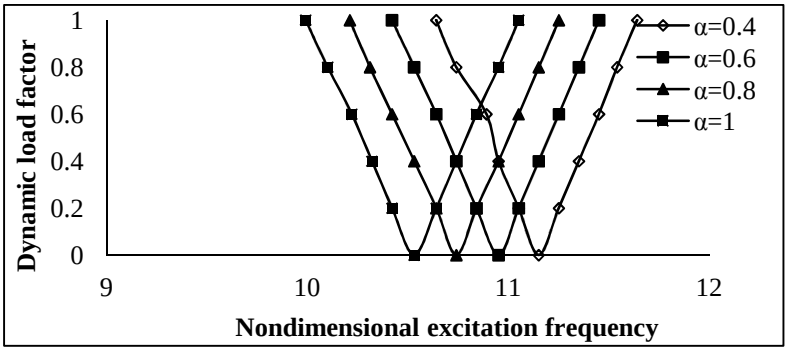

Figure 5.45: Variation of instability regions with temperature at 325K for simply supported of $[45/-45]_4$, woven fiber composite plates

The variations of dynamic instability regions with increase in static in-plane loads of woven fiber composite plates at moisture concentrations 0.25% is observed as shown in figure 5.46. The onset of instability occurs earlier with increase of compressive static in-plane load, the instability region tend to shift to lower frequencies and wider. The reduction of excitation frequencies with increase in static in-plane loads from 0.4 to 1 is more than 5%. The variations of dynamic instability of composite plates with increase in temperature from 325K to 400K is shown in figure 5.47 with a static load factor 0.2, it is observed that the onset of instability occurs earlier with increase in

temperature. The width of instability region decreased with increase in temperature from 325K to 400K. The reduction of excitation frequencies with increase in temperature from 325K to 400K is about 50%. Similarly with increase in moisture concentration from0.25% to 1% is shown in figure 5.48 with static load factor 0.2, it is observed that the onset of instability occurs earlier with increase in moisture concentration. The width of instability region decreased with increase in moisture concentration from 0.25% to 1%. The reduction of excitation frequencies with increase in moisture concentration from 0.25% to 1% is more than 50%.

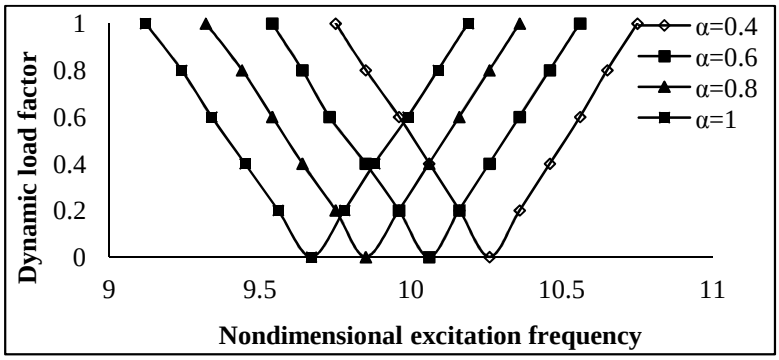

Figure 5.46: Variation of instability regions with moisture concentration at 0.25% for simply supported of $[45/-45]_4$, woven fiber composite plates

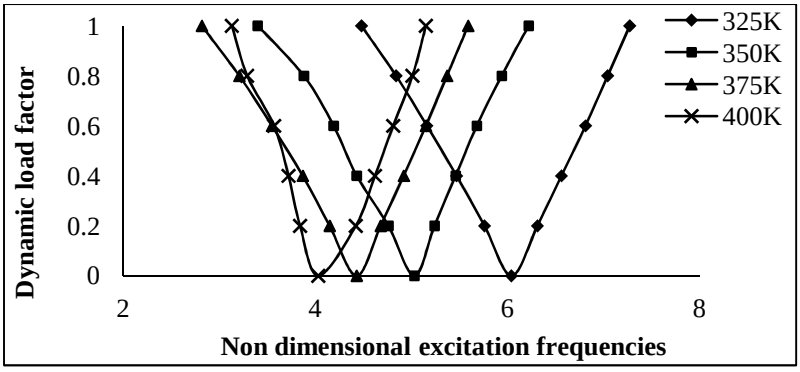

Figure 5.47: Variation of instability regions with different temperature for simply supported of $[45/-45]_4$, woven fiber composite plates

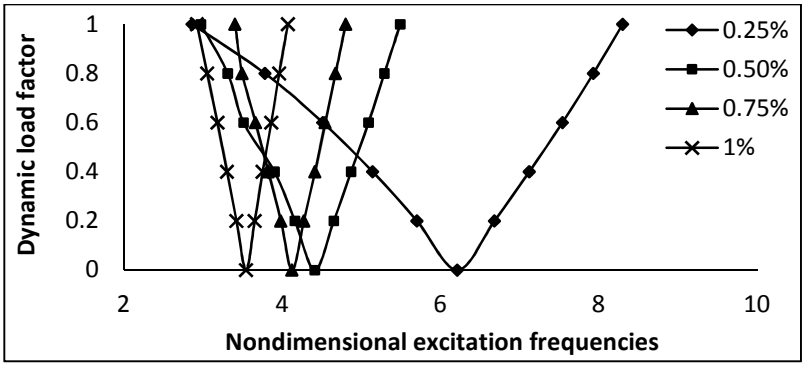

Figure 5.48: Variation of instability regions with different moisture concentration for simply supported of $[45/-45]_4$, woven fiber composite plates

The study is further extended to study the effect of different laminated parameter on composite plates under high temperature environment, here considered at temperature 325K. As shown in figure 5.49, it is observed that the onset of instability occurs for symmetric laminates earlier than anti-symmetric laminates. The non-dimensional excitation frequencies decreased 50% for laminates with symmetric lay-up than anti-symmetric lay-up in temperature environment.

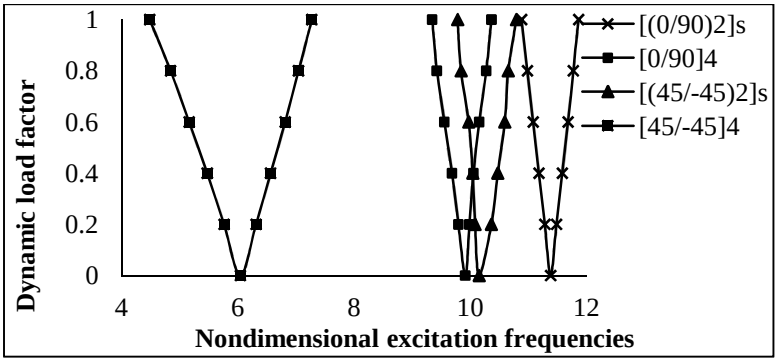

Figure 5.49: Variation of instability regions with temperature at 325K for simply supported α= 0.2, woven fiber composite plates

A study is also under taken to study the effect of different lamination sequence on instability of composite plates under moisture environment. Similar symmetric and anti-symmetric laminates having different lamination sequence with moisture concentration 0.25% are considered in figure 5.50. The onset of instability occurs earlier for symmetric laminates with wider instability regions, where as the narrow instability regions for anti-symmetric laminates. Plates with 45^o ply orientations seem to be stiffer due to shifting of higher frequencies and narrow instability region. The non-dimensional excitation frequencies decreased 50% for laminates with symmetric lay-up than anti-symmetric lay-up in moisture environment.

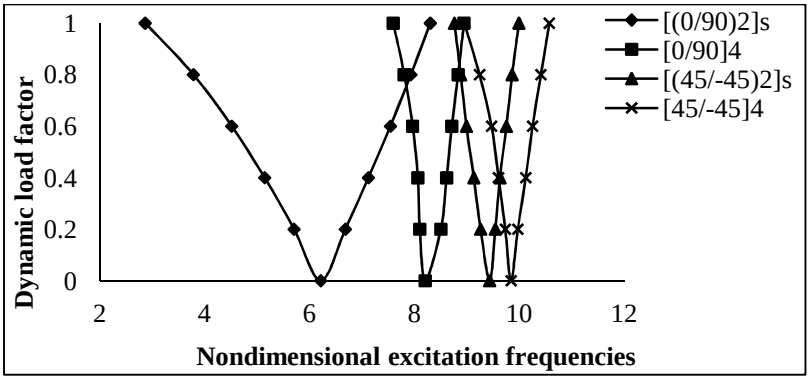

Figure 5.50: Variation of instability regions with moisture concentration at 0.25% for simply supported α= 0.2, woven fiber composite plates

The width of instability region increases with increase in both static and dynamic load parameters. Further studies are done with anti-symmetric angle-ply laminated plates. The effect of ply orientation 0^o to 90^o on the non-dimensional excitation frequencies is considered here for anti-symmetric angle-ply laminated plates at temperature 325K as shown in figure 5.51. The onset of instability occurs earlier with decrease of lamination angle. The excitation frequencies beyond lamination angle 45^o decreased marginally. The excitation frequencies are decreased with increase in lamination angle due to reduction of stiffness and strength of laminated plates. The reduction of excitation frequencies with increase in lamination angle from 0^o to 45^o is about 25%. The onset of instability and the width of instability region and its strength is highly depends on lamination angle. The greater the lamination angle the smaller is the width of instability region. The rectangular laminated plates show that the lamination angle of 45^o is symmetrical. For this the lamination angle of 45^o seems to be the preferential ply orientation for the lamination sequence which is due to the dominance effect of bending-stretching coupling of laminates.

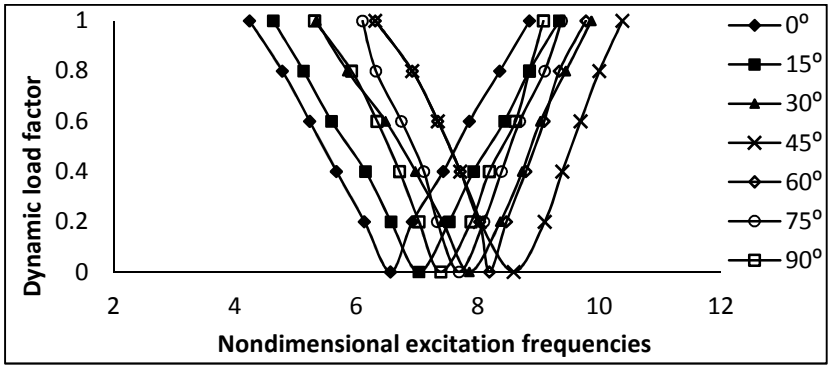

Figure 5.51: Variation of instability regions with temperature at 325K for simply supported of $[45/-45]_4$, α= 0.2, woven fiber composite plates

The effects of increase in lamination angle 0^o to 90^o on the non-dimensional excitation frequencies is reported for composite plates at moisture concentration 0.25% is shown in figure 5.52. It is observed from the figure that the onset of instability occurs for lower values of lamination angle. The reduction of excitation frequencies with increase in lamination angle 0^o to 45^o is about 50%. Which shows that the anti-symmetric angle-ply laminated plates is severely affected and reduced its maximum strength and stiffness with increase in lamination angle in moisture environment.

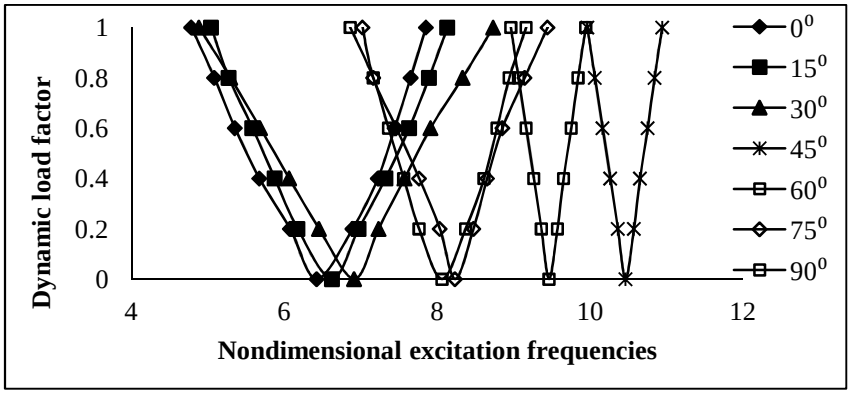

Figure 5.52: Variation of instability regions with moisture concentration at 0.25% for simply supported α= 0.2, woven fiber composite plates

The effect of degree of orthotropy is examined for the eight layered anti-symmetric angle-ply laminated plates on the non-dimensional excitation frequency as shown in figure 5.53 at temperature 325K. It is seen that with increase in the values of E_1/E_2 =10, 20 and 40, the onset of instability occurs earlier with decrease in degree of orthotropy. The width of instability zones increases with increase of degree of orthotropy in temperature environment.

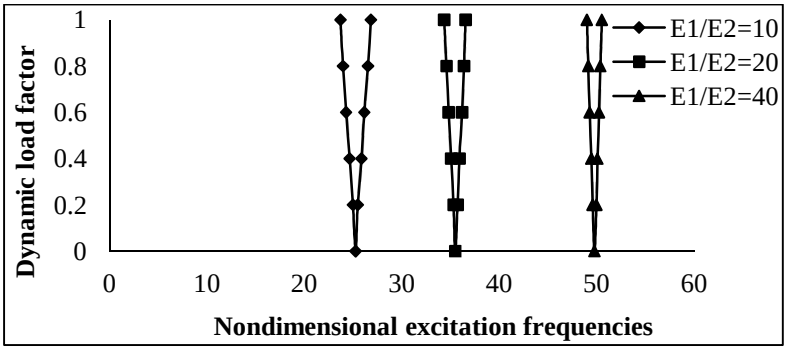

Figure 5.53: Variation of instability regions with temperature at 325K for simply supported of $[45/-45]_4$, α= 0.2, woven fiber composite plates

With the increase of degree orthotropy i.e. the increase in E_1/E_2 the instability occurs at higher frequencies. The reduction of excitation frequency with decrease in E_1/E_2 =40 to 10 about 50%. This shows that there is worst variation of stiffness and strength with increase in degree of orthotropy characteristics.

The variations of dynamic instability regions with increase in the values of degree of orthotropy E_1/E_2 =10, 20 and 40 are presented as shown in figure 5.54 at a moisture 0.25%. The onset of instability occurs earlier with decrease in degree of orthotropy. The width of instability region is narrow with increase in degree of orthotropy of laminated plates, which shows more stiffness and strength in hygrothermal environment.

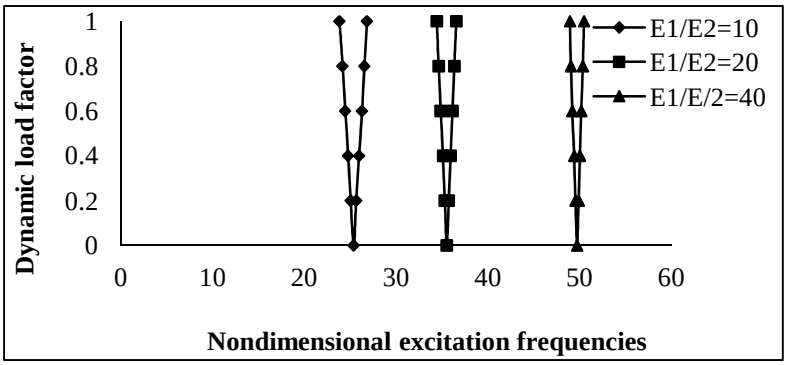

Figure 5.54: Variation of instability regions with moisture concentration at 0.25% for simply supported of $[45/-45]_4$, α= 0.2, woven fiber composite plates

The reduction of excitation frequency is about to 50% with decrease in degree of orthotropy E_1/E_2 =40 to 10. The larger the ratio of E_1/E_2, for the high-modulus-fiber material plates, the laminated plates is most stable and better stiffness in adverse hygrothermal environment.

The effect of increase in dynamic load factor of eight layered anti-symmetric woven fiber laminated composite plates on non-dimensional excitation frequency is analyzed in figure 5.55 at temperature 325K. It is observed that with the increase of dynamic load factor from 0.4 to 1, the onset of dynamic instability occurs earlier and the width of dynamic instability region also increases. The reduction of excitation frequencies with increase in dynamic load factors from 0.4 to 1 is more than 10% due to reduction of stiffness and strength.

The variations of dynamic instability regions with increase in dynamic load factors of woven fiber composite plates at moisture concentrations 0.25% is observed as shown

in figure 5.56. The onset of instability occurs earlier with increase of dynamic load, the instability region tend to shift to lower frequencies and narrower. The reduction of excitation frequencies with increase in dynamic loads from 0.4 to 1 is more than 10%. This implies that the presence of the compressive static in-plane load reduces the stiffness of the laminates, and thus shifts the resonance frequencies downwards in hygrothermal environment.

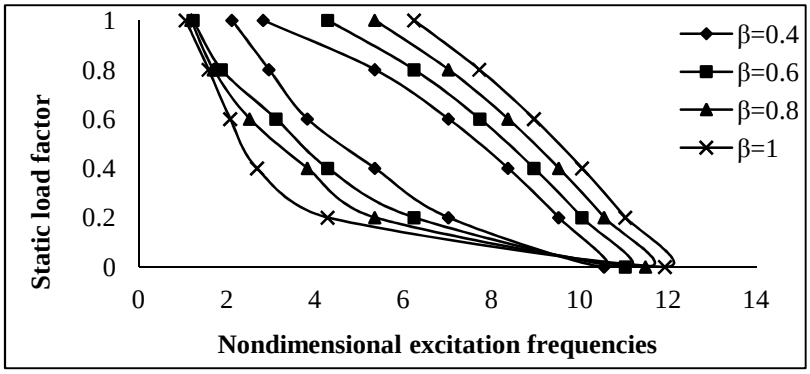

Figure 5.55: Variation of instability regions with temperature at 325K for simply supported of a/b=1, α= 0.2, woven fiber composite plates

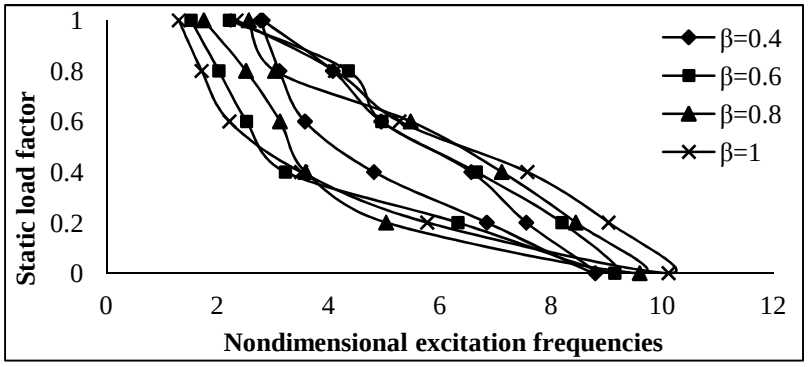

Figure 5.56: Variation of instability regions with moisture concentration at 0.25% for simply supported of a/b=1, α= 0.2, woven fiber composite plates

It is observed from the above figure that the laminated plates become more dynamically unstable with increase in dynamic load factor as compared to increase in static load factor in hygrothermal environment.

The variations of dynamic instability of composite plates with increase in temperature from 300K to 375K is shown in figure 5.57 with a dynamic load factor 0.2, it is observed that the onset of instability occurs earlier with increase in temperature. The width of instability region decreased with increase in temperature from 300K to

375K. The reduction of excitation frequencies with increase in temperature from 325K to 375K is about 20%.

Similarly with increase in moisture concentration from 0.25% to 1% is shown in figure 5.58 with dynamic load factor 0.2, it is observed that the onset of instability occurs earlier with increase in moisture concentration. The width of instability region decreased with increase in moisture concentration from 0.25% to 1%. The reduction of excitation frequencies with increase in moisture concentration from 0.25% to 1% is about 50%.

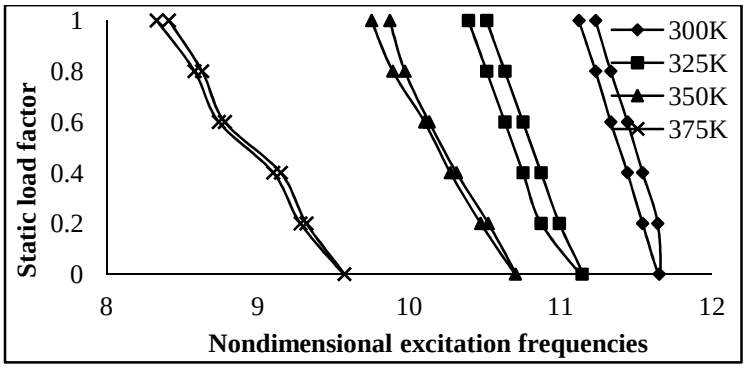

Figure 5.57: Variation of instability regions with different temperature for simply supported of $[45/-45]_4$, woven fiber composite plates

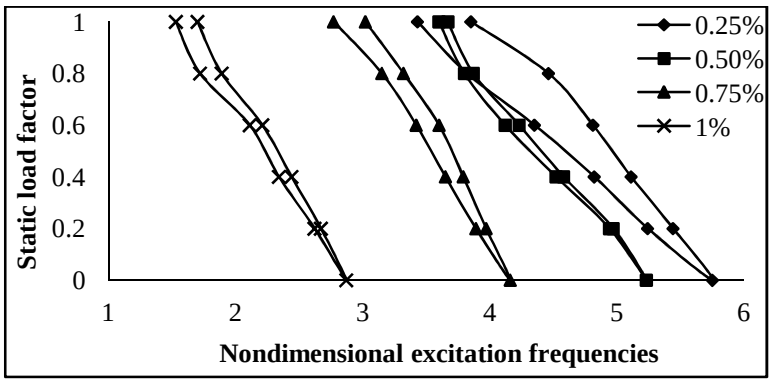

Figure 5.58: Variation of instability regions with different moisture concentration for simply supported of $[45/-45]_4$, woven fiber composite plates

It is seen from the figure when static load factor remains constant $\alpha = 0.2$, the excitation frequency is less as compared to figure 5.57 and 5.58 but the plates is stable in former than later with increase in temperature and moisture concentration environment.

5.3: Curved panels

The study is further extended to Dynamic stability of woven fiber laminated composite curved panels in hygrothermal environment subjected to periodic loadings.

5.3.1: Convergence study

The convergence study is done for simply supported square 4 layer symmetric cross-ply and symmetric angle-ply laminated composite plates and shells for elevated temperature and moisture conditions for different mess divisions. Dynamic stability analysis of laminated composite panels subjected to hygrothermal conditions are presented in Table 5.18 and Table 5.19. As observed, a mesh of 10 ×10 shows good convergence of the numerical solution of dynamic stability of woven fiber composite panels and this mesh is employed throughout the dynamic stability analysis of woven fiber composite plates and shells in hygrothermal environment.

5.3.2: Comparison with previous studies

To validate the formulation, the frequencies of vibration the buckling load and excitation frequency during parametric resonance of laminated composite plates are computed and compared with previously published results from literature.

5.3.2.1: Vibration of composite shells in hygrothermal environment

The present formulation is validated for free vibration analysis of composites for shells with ambient temperature are compared with analytical solution published by Reddy (1984), Chandrasekhar (1989) as shown in Table 5.20. The non-dimensional frequency parameters for shell with hygrothermal condition is as shown in Table 5.21 is compared with results published by Parhi *et al*. (2001) and Naidu & Sinha (2006).

The present finite element results show good agreement with the previous numerical results published in the literature for free vibration of laminated composite shells subjected to hygrothermal conditions.

Table 5.21: Comparison of non-dimensional free vibration frequencies for SSSS (0/90/90/0) spherical shell at ambient temperature

a/b=1, a/t=100, At T = 300*K*, E_1= 125Gpa , E_2= 5 Gpa, G_{12}= 2.5Gpa, $G_{13}=G_{12}$, $G_{23}=1G_{12}$, $\nu_{12}=0.25$

Non dimensional frequency, $\lambda = \omega_n a^2\sqrt{\rho/E_2}t^2$

R/b	Reddy (1984)	Chandrasekhara (1989)	Present
1	126.33	126.7	126.460
2	68.294	68.294	68.364
3	47.415	47.553	47.459
4	37.082	37.184	37.110
5	31.079	31.159	31.097
10	20.38	20.417	20.376

Table 5.22: Comparison of natural frequencies for SSSS (0/90/90/0) shell at 1% moisture concentration

a/b=1, a/t=100, At T = 300*K*, E_1= 172.5Gpa, E_2= 6.9Gpa (C=0), G_{12}= 3.45Gpa, E_2= 6.17Gpa (C=1%), $G_{13}=G_{12}$, $G_{23}=1.38G_{12}$, $\nu_{12}=0.25$, $\beta_1=0$, $\beta_2=0.44$, $\rho=1600$

Fundamental natural frequency, $\lambda = \omega_n a^2\sqrt{\rho/E_2 t^2}$ 1/2*pi

Stacking sequence	References	C=0	C=1%
R/a=5 $(0/90)_2$	Naidu & Sinha(2006)	201.82	201.68
	Parhi *et al*. (2001)	202.02	201.64
	Present	201.93	201.61
R/a=10 $(0/90)_2$	Naidu & Sinha(2006)	129.13	127.54
	Parhi *et al*. (2001)	129.20	128.32
	Present	129.08	128.62

5.3.2.2: Buckling of composite shells in hygrothermal environment

The present formulation is then validated for buckling analysis of laminated composite shells for normal temperatures and moistures. The non-dimensional critical loads due to ambient temperature and moisture obtained by the present finite element as shown in Table 5.22 is compared with analytical solution published by Scuiva & Carrera (1990). The square plate has four layers of Graphite/Epoxy composite. The present finite element results show good agreement with the previous numerical results published in the literature for buckling of composite plates subjected in hygrothermal environment.

Table 5.23: Comparison of Non-dimensional buckling loads of a square simply supported symmetric cross-ply cylindrical laminated curved panels with (0/0/90/0)

a/b=1,R/a=20.0, $\lambda=Nxa^2/E_2\ h^3$, $E_{11}=40E_{22}$, $G_{23}=0.6E_2$, $G_{12}=G_{13}=0.5E_{22}$, $\nu_{12}=\nu_{13}=0.25$

Theory	a/h=50	a/h=100
FSDT(Scuiva & Carrera) (1990)	35.42	35.843
Present	35.235	36.803

5.3.2.3: New results for dynamic stability

After validating the present formulation, the same is employed to study the dynamic stability effects of woven fiber composite shells in hygrothermal environment. Numerical results are presented on the dynamic stability of cross-ply and angle-ply laminated shell to study the effects of various parameters on instability regions. The geometrical properties of the laminated shell are as follows a=500mm, b=500mm, t=5mm, E_1=130Gpa, E_2=9.5Gpa, G_{12}=6Gpa, G_{23}/G_{12}=0.5, υ12=0.3, $G_{13}=G_{12}$, α_1=-0.3*10^-6 /K, α_2=28.1*10^-6 /K

The non-dimensional excitation frequency $\Omega=\bar{\Omega}a^2\sqrt{(\rho/E_{22}h^2)}$ is used throughout the dynamic instability studies, where $\bar{\Omega}$ is the excitation frequency in radian/sec. The principal instability regions of laminated composite curved panel subjected to in-plane periodic loads is plotted with non-dimensional frequency Ω/ω (ratio of excitation frequency to the free vibration frequency) versus the dynamic in-plane load β. The analysis is focused on the determination of the primary instability regions of laminated composite shells under hygrothermal loads.

The effect of static component of load for α= 0.0, 0.2, 0.4, 0.6 and 0.8 on the instability region of laminated composite panel subjected to elevated temperature 325K is shown in fig.5.59. Due to increase of static component, the instability regions tend to shift to lower frequencies and become wider. With increase in static load factor from 0 to 0.8, the excitation frequency is reducing by 2.3%. All further studies are made with a static load factor of 0.2 (unless otherwise mentioned).

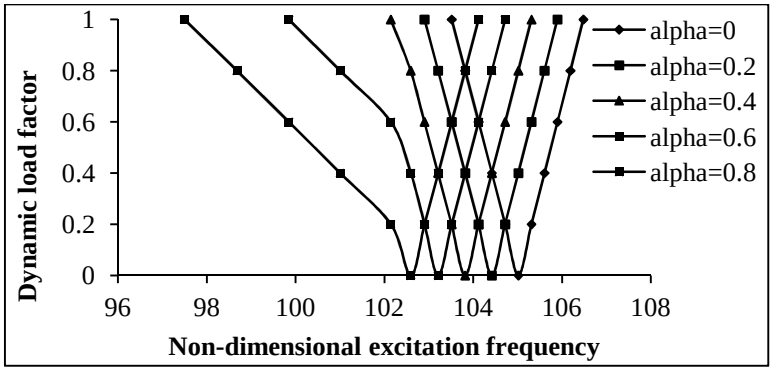

Figure 5.59: Variations of instability region with static load factor of composite shell subjected to temperature (Temp=325K, a/b=1, Ry/b=Rx/b=5, b/t=100)

The variation of excitation frequency with dynamic load factor of composite laminated simply-supported symmetric cross-ply square shells subjected to uniform distribution of temperature from 300K and 325K is shown in fig.5.60. It is observed that the onset of instability occurs earlier with wider DIR for symmetric cross-ply laminated composite panels subjected to elevated temperature compared to composite panel with normal temperature. With increase in temperature from 300K to 325K, the excitation frequency is reducing by 31.6%. The width of instability region for laminated panel with elevated temperature is increased by 46.67% from the plate with normal temperature for a dynamic load factor of 0.6.

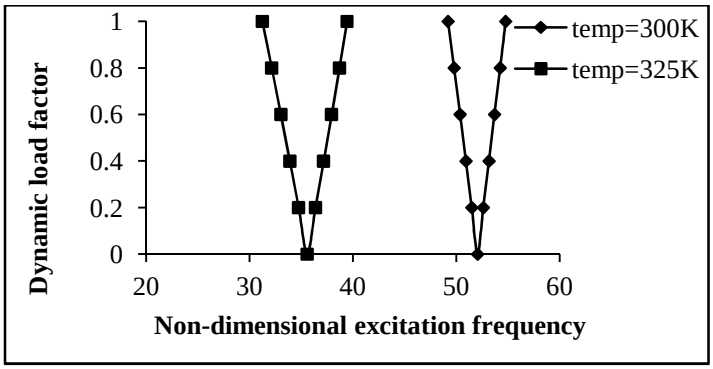

Figure 5.60: Variations of instability region with temperature of composite symmetric cross-ply (0/90/90/0) curved panel (a/b=1, b/t=100, Ry/b=5)

The variation of excitation frequency with dynamic load factor of composite laminated simply-supported anti-symmetric angle-ply square shells subjected to uniform distribution of temperature from 300K, 325K, 350K, 375K & 400K is shown in fig.5.61. As shown, the onset of instability occurs earlier with wider DIR for anti-symmetric angle-ply laminated composite shells subjected to elevated temperature

compared to composite shells with normal temperature. With increase in temperature from 300K to 350K, the excitation frequency is reducing by 65.2%.

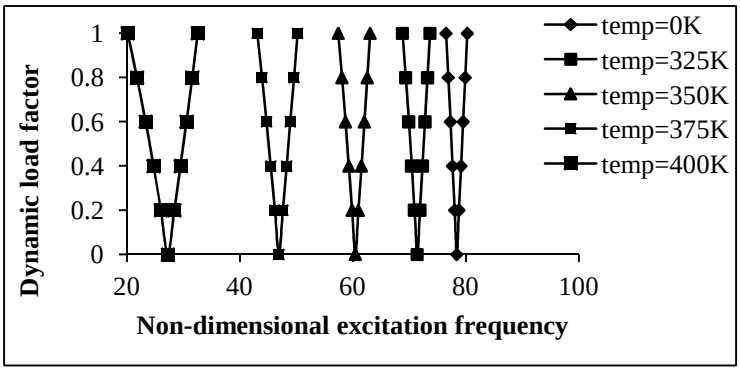

Figure 5.61: Variations of instability region with temperature of composite anti-symmetric angle-ply (45/-45/45/-45) curved panel (a/b=1, b/t=100, Ry/b=5)

The variation of excitation frequency with dynamic load factor of composite laminated simply-supported symmetric cross-ply curved panel subjected to uniform distribution of moisture concentration from 0% & 0.1% is shown in fig.5.62. It is revealed that the onset of instability occurs earlier with wider DIR for symmetric cross-ply laminated composite shells subjected to elevated moisture condition compared to composite shells with normal moisture. When moisture concentration is increased from 0% to 0.1% then excitation frequency reduces for about 21%. The width of instability region for laminated shell with elevated temperature is increased by 46.67% from the shell with normal temperature for a dynamic load factor of 0.6.

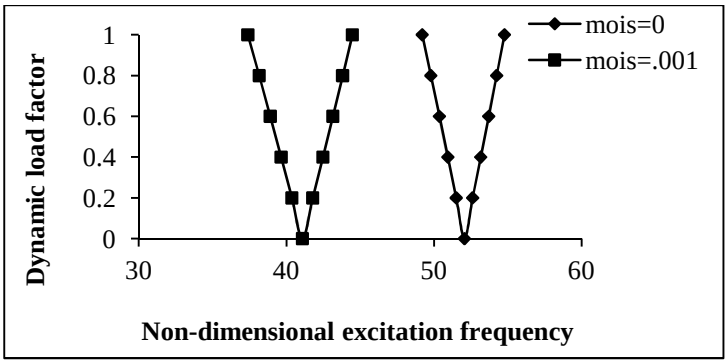

Figure 5.62: Variations of instability region with moisture of composite symmetric cross-ply (0/90/90/0) shell (Ry/b=5, a/b=1, b/t=100)

The variation of excitation frequency with dynamic load factor of composite laminated simply-supported anti-symmetric angle-ply shell subjected to uniform distribution of moisture concentration from 0%, 0.1%, 0.25% & 0.5% is shown in fig. 5.63. It is revealed that the onset of instability occurs earlier with wider DIR for anti-

symmetric angle-ply laminated composite shells subjected to elevated moisture condition compared to composite shells with normal moisture concentration. When moisture concentration is increased from 0% to 0.25% then excitation frequency reduces for about 49.3%.

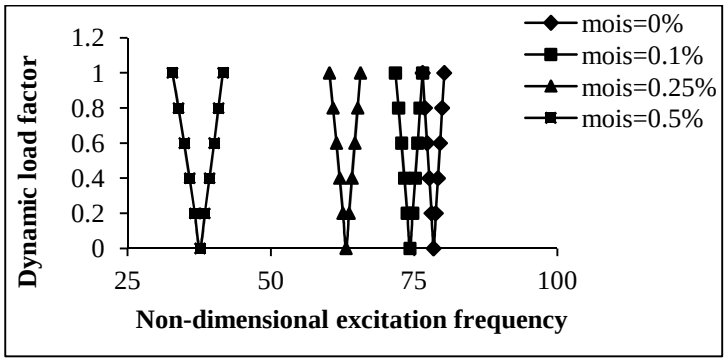

Figure 5.63: Variations of instability region with moisture of composite anti-symmetric angle-ply (45/-45/45/-45) shell (Ry/b=5, a/b=1, b/t=100)

Studies have also been made in Fig.5.64 for comparison of instability regions for different shell geometries. The effect of curvature on instability region of different curved panels for a/b=1, flat panel ($a/R_x = b/R_y = 0$), Cylindrical ($a/R_x = 0$, $b/R_y = 0.2$) & Spherical ($a/R_x = b/R_y = 0.2$) is investigated.

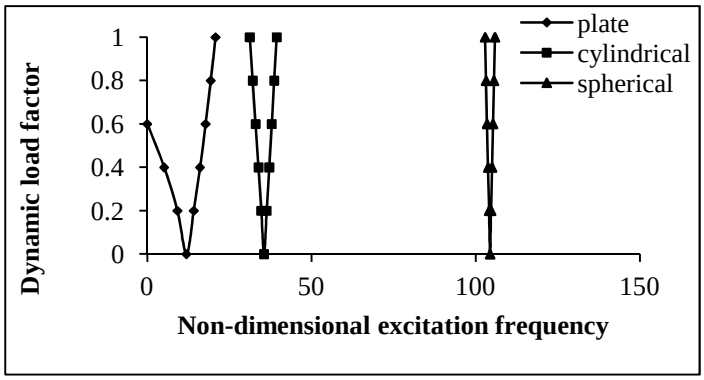

Figure 5.64: Variations of curvature of composite symmetric cross-ply (0/90/90/0) curved panel with elevated temperature (Temp=325K, a/b=1, b/t=100)

It is observed that the excitation frequency increases with introduction of curvatures from flat panel to doubly curved panel in elevated temperature. The onset of dynamic instability region occurs earlier with wider dynamic instability region (DIR) coming from spherical laminated composite shell panel to laminated composite flat panel subjected to uniform distribution of temperature.

The variation of instability region with dynamic load factor of composite laminated simply supported symmetric cross-ply and anti-symmetric angle-ply shells with excitation frequency subjected to uniform distribution of elevated temperature with different aspect ratio (a/b =1, 2 & 3) are shown in figures 5.65 and 5.66.

From the fig5.65 and 5.66, it is observed that the onset of instability occurs earlier with decrease of the aspect ratio with decreasing width of instability region & the onset of instability occurs latter for rectangular anti-symmetric angle-ply laminated composite shells than square shells subjected to elevated temperature but with wider instability regions. The width of instability regions increased marginally for rectangular plates than square plates with uniform rise in temperature and moisture concentration. The increase in aspect ratio shifts the frequency of instability region to higher values and reduces the dynamic stability strength. As a result the plates having higher values of aspect ratios are dynamically unstable in elevated temperature and lose its stiffness.

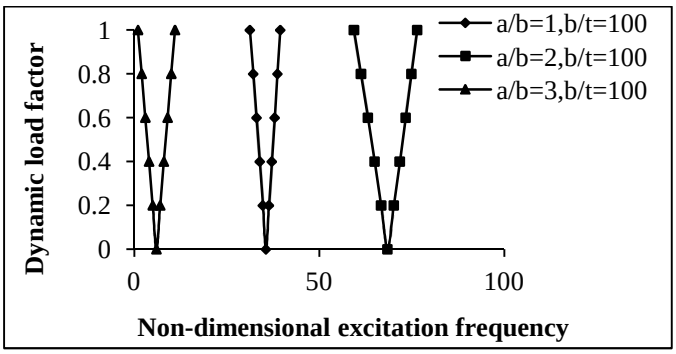

Figure 5.65: Effect of aspect ratio on instability region of (0/90/90/0) laminate for elevated temperature (Ry/b=5, Temp=325K, b/t=100)

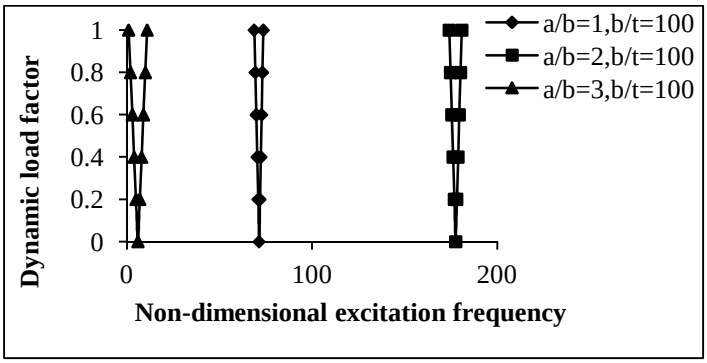

Figure 5.66: Effect of aspect ratio on instability region of (45/-45/45/-45) laminate for elevated temperature (Ry/b=5, Temp=325K, b/t=100)

The variation of instability region with dynamic load factor of composite laminated simply supported symmetric cross-ply and anti-symmetric angle-ply shells with excitation frequency subjected to uniform distribution of elevated moisture with different aspect ratio (a/b =1, 2 & 3) is shown in figures 5.67 for symmetric cross-ply and 5.68 for anti-symmetric angle ply laminates.

From the figure 5.67 and 5.68, it is observed that the onset of instability occurs earlier with decrease of the aspect ratio with decreasing width of instability region & the onset of instability occurs latter for rectangular anti-symmetric angle-ply laminated composite shells than square shells subjected to elevated moisture but with wider instability regions. The width of instability regions increased marginally for rectangular shells than square shells with uniform rise in moisture concentration. The increase in aspect ratio shifts the frequency of instability region to higher values and reduces the dynamic stability strength. As a result the shells having higher values of aspect ratios are dynamically unstable in elevated moisture condition and lose its stiffness.

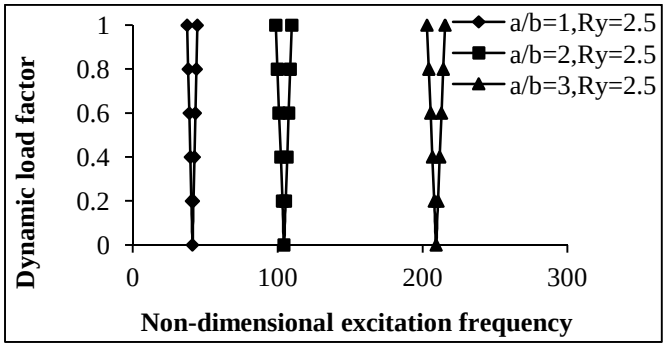

Figure 5.67: Effect of aspect ratio on instability region of (0/90/90/0) laminate for elevated moisture (Ry/b=5, Mois=0.001, b/t=100)

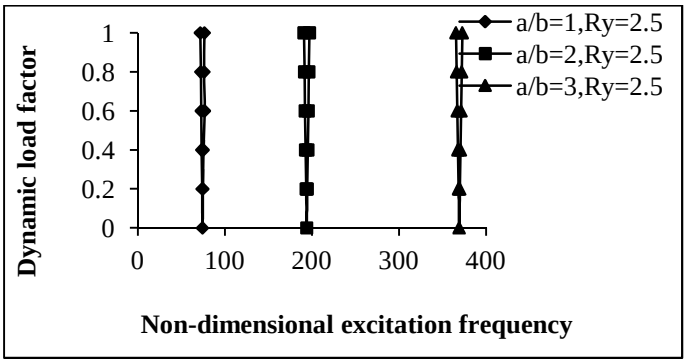

Figure 5.68: Effect of aspect ratio on instability region of (45/-45/45/-45) laminate for elevated moisture (Ry/b=5, Mois=0.001, b/t=100)

The variation of excitation frequency with dynamic load factor of composite laminated simply supported symmetric cross-ply and for anti-symmetric angle-ply shells subjected to uniform distribution of temperature are shown in figures 5.69 and 5.70 The effect of degree of orthotropy is studied for E_1/E_2 = 10, 20, 40 keeping other material properties constant.

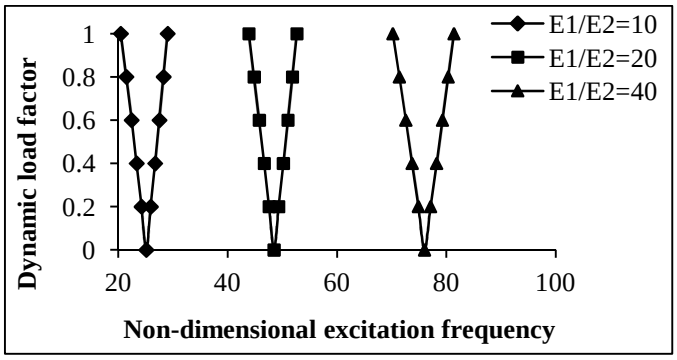

Figure 5.69: Effect of degree of orthotropy on instability region of (0/90/90/0) laminate for elevated temperature (Ry/b=5, Temp=325K, b/t=100, a/b=1)

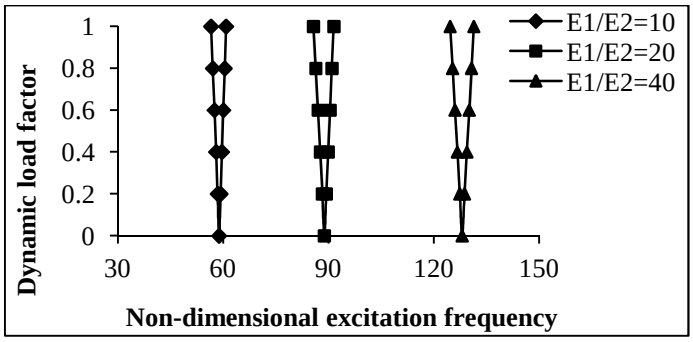

Figure 5.70: Effect of degree of orthotropy on instability region of (45/-45/45/-45) laminate for elevated temperature (Ry/b=5, Temp=325K, b/t=100, a/b=1)

It is observed that the onset of instability occurs latter with increase of degree of orthotropy for symmetric cross-ply and anti-symmetric angle-ply laminated composite shells subjected to elevated temperature but with wider instability regions. The excitation frequency is reduced but the instability region is wider in cross-ply symmetric laminate rather than anti-symmetric angle-ply laminate.

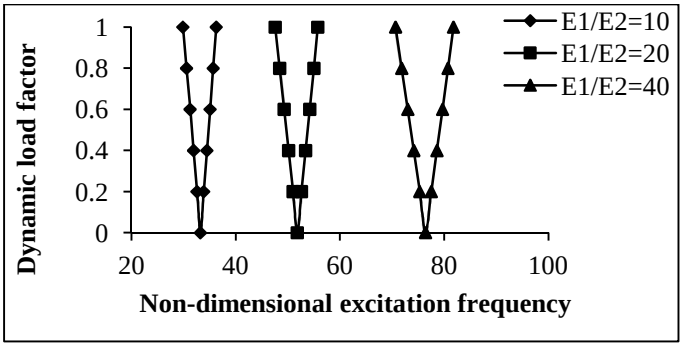

Figure 5.71: Effect of degree of orthotropy on instability region of (0/90/90/0) laminate for elevated moisture (Ry/b=5, Mois=0.001, b/t=100, a/b=1)

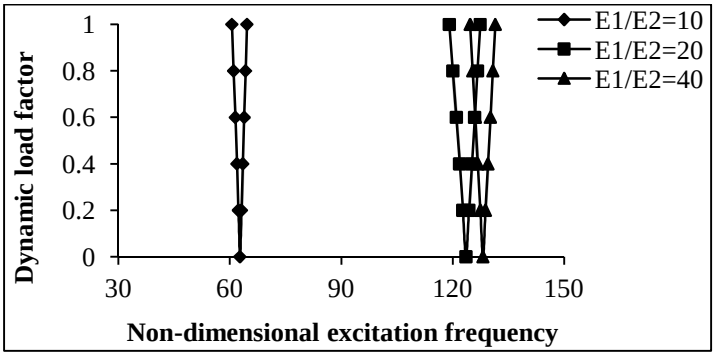

Figure 5.72: Effect of degree of orthotropy on instability region of (45/-45/45/-45) laminate for elevated moisture (Ry/b=5, Mois=0.001, b/t=100, a/b=1)

The variation of excitation frequency with dynamic load factor of composite laminated simply supported symmetric cross-ply and for anti-symmetric angle-ply shells subjected to uniform distribution of moisture are shown in figures 5.71 and 5.72. The effect of degree of orthotropy is studied for E_1/E_2 = 40, 20, 10 keeping other material properties constant. It is observed that the onset of instability occurs latter with increase of degree of orthotropy for symmetric cross-ply and anti-symmetric angle-ply laminated composite shells subjected to uniform distribution of moisture but with wider instability regions. The excitation frequency is reduced but the instability region is wider in cross-ply symmetric laminate rather than anti-symmetric angle-ply laminate.

The variation of excitation frequency with dynamic load factor of composite laminated simply supported symmetric cross-ply and for anti-symmetric angle-ply shells subjected to uniform distribution of temperature are shown in figures 5.73 and 5.74. The effect of radius to thickness ratio is studied for $R_x/h = R_y/h$ = 625, 500, 375 keeping other geometries and material properties constant. It is observed from the fig. that the onset of dynamic instability region occurs later with increase of R_y/h ratio but

with wider instability region. The excitation frequency is reduced but the instability region is narrower in cross-ply symmetric laminate rather than anti-symmetric angle-ply laminate in elevated temperature.

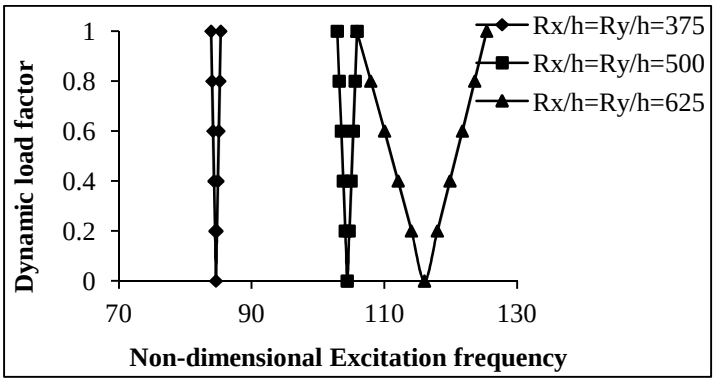

Figure 5.73: Effect of thickness on instability region of (0/90/90/0) laminate for elevated temperature (a/b=1, Temp=325K, $R_x/b= R_y/b = 5$)

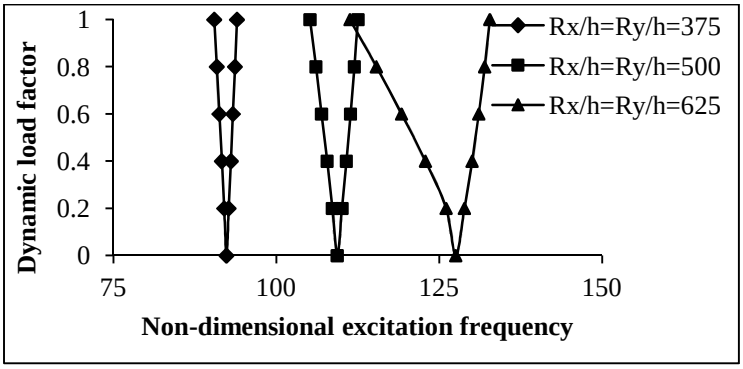

Figure 5.74: Effect of thickness on instability region of (45/-45/45/-45) laminate for elevated temperature (a/b=1, b/t=100, Temp=325K, $R_x/b= R_y/b = 5$)

The variation of excitation frequency with dynamic load factor of composite laminated simply supported symmetric cross-ply and for anti-symmetric angle-ply shells subjected to uniform distribution of moisture are shown in figures 5.75 and 5.76. It is observed from the fig. that the onset of dynamic instability region occurs earlier with decrease of R_y/h ratio but with narrower instability region. The excitation frequency is reduced but the instability region is narrower in cross-ply symmetric laminate rather than anti-symmetric angle-ply laminate in elevated moisture.

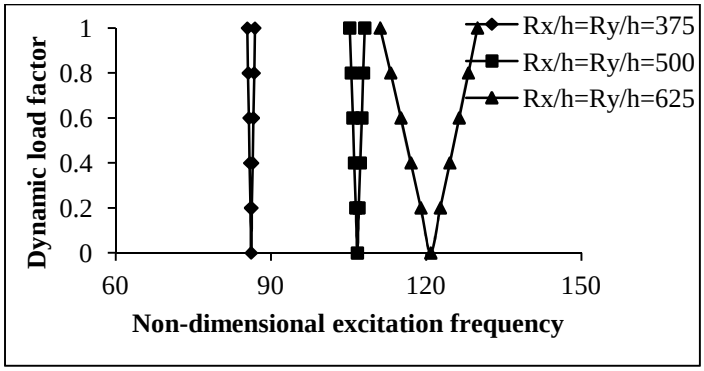

Figure 5.75: Effect of thickness on instability region of (0/90/90/0) laminate for elevated moisture (a/b=1, b/t=100, Mois=0.001, $R_x/b= R_y/b = 5$)

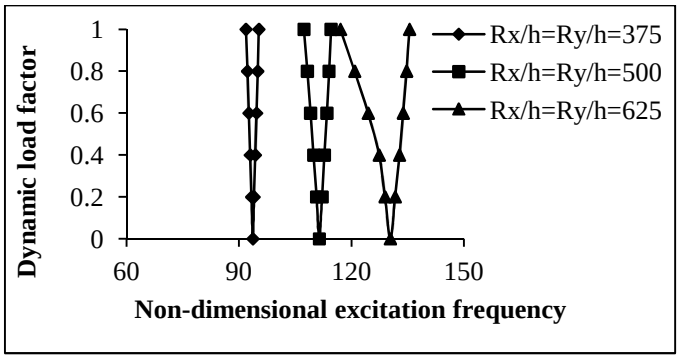

Figure 5.76: Effect of thickness on instability region of (45/-45/45/-45) laminate for elevated moisture (a/b=1, b/t=100, Mois=0.001, $R_x/b= R_y/b = 5$) effect of shallowness ratio

The variation of excitation frequency with dynamic load factor of composite laminated simply supported symmetric cross-ply and for anti-symmetric angle-ply shells subjected to uniform distribution of temperature are shown in figures 5.77 and 5.78. The effect of shallowness ratio on instability regions is studied for $R_x/a = R_y/b =$ 3, 5, 10 keeping other geometries and material properties constant. As seen from the fig., the instability excitation frequency is higher for decrease of shallowness by decreasing R_x and R_y. The onset of instability occurs earlier with increase of shallowness ratio but with wide instability region. The excitation frequency is reduced but the instability region is wider cross-ply symmetric laminate rather than anti-symmetric angle-ply laminate in elevated temperature.

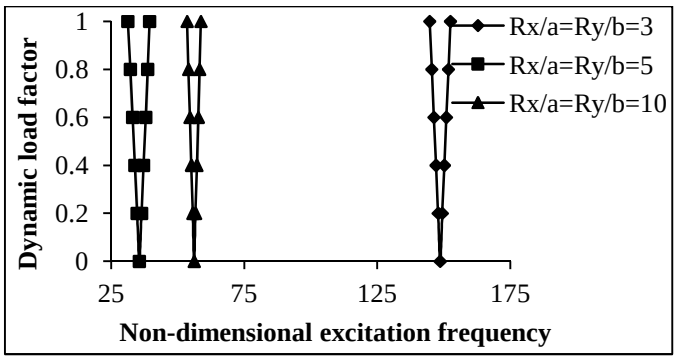

Figure 5.77: Effect of R_y/b on instability region of (0/90/90/0) laminate for elevated temperature (a/b=1, b/t=100, Temp=325K, R_y=R_x = 1.5, 2.5, 5)

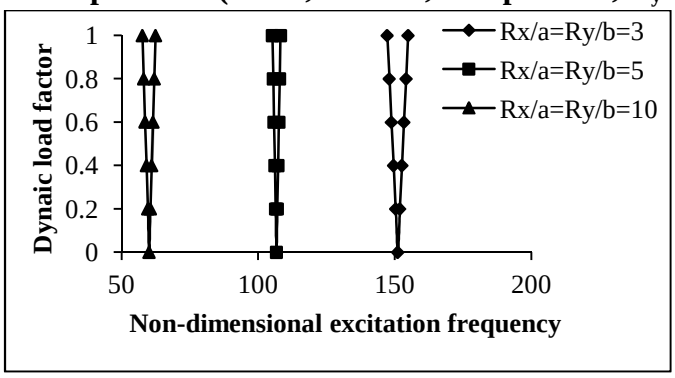

Figure 5.78: Effect of R_y/b on instability region of (0/90/90/0) laminate for elevated moisture (a/b=1, b/t=100, Mois=0.001, R_y=R_x = 1.5, 2.5, 5)

The variation of excitation frequency with dynamic load factor of composite laminated simply supported symmetric cross-ply and for anti-symmetric angle-ply shells subjected to uniform distribution of moisture are shown in figures 5.79 and 5.80. The effect of shallowness ratio on instability regions is studied for $R_x/a = R_y/b$ = 3, 5, 10 keeping other geometries and material properties constant.

As seen from the fig., the excitation frequency is higher for decrease of shallowness by decreasing R_x and R_y. The onset of instability occurs earlier with increase of shallowness ratio but with wide instability region. The excitation frequency is reduced but the instability region is wider in cross-ply symmetric laminate rather than anti-symmetric angle-ply laminate in elevated moisture.

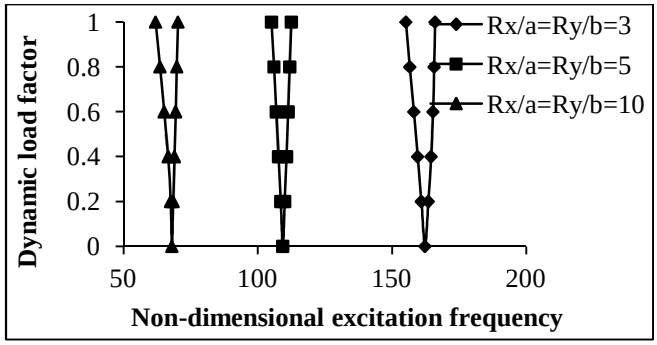

Figure 5.79: Effect of R_y/b on instability region of (45/-45/45/-45) laminate for elevated temperature (a/b=1, b/t=100, Temp=325K, Ry=R_x = 1.5, 2.5, 5)

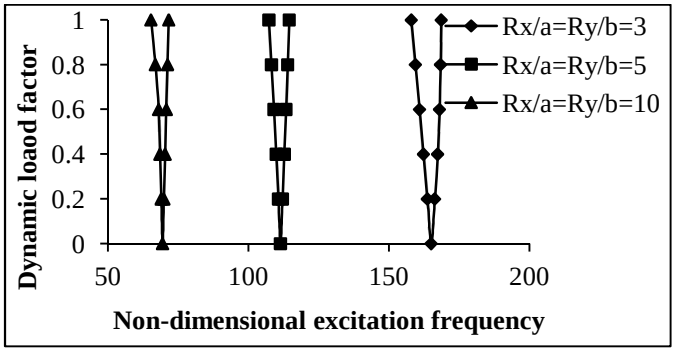

Figure 5.80: Effect of R_y/b on instability region of (45/-45/45/-45) laminate for elevated moisture (a/b=1, b/t=100, Mois=0.001, R_y=R_x= 1.5, 2.5, 5)

The variation of instability region with dynamic load factor of composite laminated simply supported anti-symmetric angle-ply shells with excitation frequency subjected to uniform distribution of temperature with different ply orientation is shown in figure 5.81. It is observed that the onset of instability occurs earlier for anti-symmetric angle-ply laminated composite shells with 0 degree of ply orientation than the shells with higher degree of ply orientation subjected to elevated moisture condition but with narrow DIR. The value of ply orientation for which the instability region is narrower is 45 and for the wider DIR the ply orientation value is 0. The instability region is less wide for increase in lamination angle but the excitation frequencies are decreased with decrease in uniform temperature distribution. The ply orientation for 0^0 seems to be the preferential ply orientation for the lamination sequence which is due to dominance effect of bending-stretching coupling.

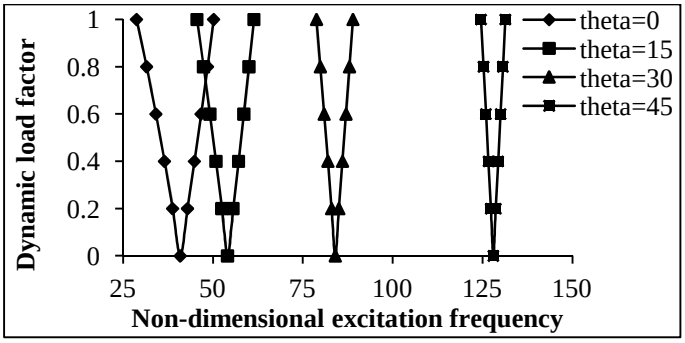

Figure 5.81: Effect of different ply orientation on instability region of anti-symmetric angle-ply laminate for elevated temperature (a/b=1, b/t=100, Temp=325K, R_y/b=5)

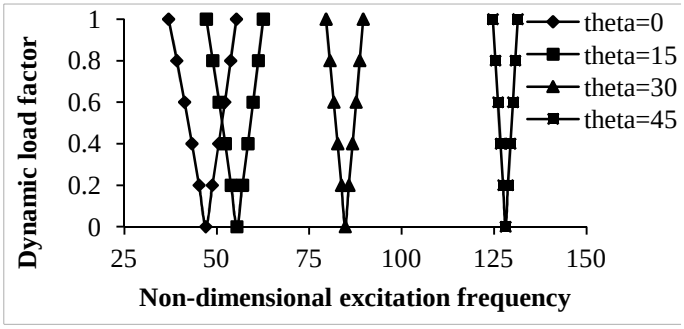

Figure 5.82: Effect of different ply orientation on instability region of anti-symmetric angle-ply laminate for elevated moisture (a/b=1, b/t =100, Mois=0.1%, R_y/b= 5)

The variation of instability region with dynamic load factor of composite laminated simply supported anti-symmetric angle-ply shells with excitation frequency subjected to uniform distribution of moisture with different ply orientation is shown in figure 5.82. It is observed that the onset of instability occurs earlier for anti-symmetric angle-ply laminated composite shells with 0 degree of ply orientation than the shells with higher degree of ply orientation subjected to elevated moisture condition but with narrow DIR. The value of ply orientation for which the instability region is narrower is 45 and for the wider DIR the ply orientation value is 0. The instability region is less wide for increase in lamination angle but the excitation frequencies are decreased with decrease in uniform moisture concentration.

CHAPTER 6

CONCLUSIONS

The present work deals with the experimental and numerical study on static, vibration and buckling of woven fiber laminated composite plates in hygrothermal environment. The parametric instability characteristics of composite flat and curved panels are carried out using numerical approach by finite element approach. The formulation is based on the first order shear deformation theory, taking into account transverse shear and rotary inertia effects. The development of regions of instability arises from Floquet's theory developed by Bolotin and the boundaries of the primary instability regions with period 2T, where $T = 2\pi/\Omega$ which are of practical importance have been determined to study the effect of various parameters of the laminated composite plates and shells on the dynamic instability regions.

The effects of various geometrical parameters like aspect ratio, side to thickness ratio, static load factor, degree of orthotropy and lamination details on the vibration and stability characteristics of woven fiber laminated composite plates and shells in hygrothermal environment has been analysed.

A general formulation is presented for the vibration, buckling and dynamic stability of laminated composite curved panels in hygrothermal environment subjected to in-plane harmonic loads. The conclusions are presented separately for each cases.

6.1: Static behavior of composites in hygrothermal environment

Experimental investigations on static strength of composite specimens under hygrothermal loading are carried out. The conclusions are summarized as:

- In the same weight fraction of fiber matrix of glass: epoxy composites gives higher inter laminar shear strength in all loading speed than glass: polyester specimens.
- The variations of inter laminar shear strength of woven fiber laminated composites is significant for low loading speed and is not so prominent for high speed.
- Matrix resins such as polyester and epoxy are known to be highly rate sensitive.
- Woven roving E-Glass fibers are found to be rate sensitive
- The S.D and C.V for all specimens are low showing good quality control of preparation of test specimens.
- The variations of ILSS with respect to temperature are higher for all percentage constituent in glass fiber: epoxy than glass fiber: polyester specimens.
- The variations of ILSS with respect to moisture concentration are higher for glass fiber: polyester than glass fiber: epoxy for all percentage constituents.
- The interfacial adhesion for glass/ epoxy and glass/ polyester composites are more affected by hygrothermal ageing at higher conditioning temperature and for more exposure time.
- The glass: epoxy composites are most affected with $E_{22,}$ and least affected in G_{12} in hygrothermal environment.

6.2: Vibration of composite flat panels in hygrothermal environment

The present study deals with the parametric study on free vibration behavior of woven fiber composite plates subjected to uniform temperature and moisture experimentally and comparing them using finite element method. From the discussion, the following observation can be made:

- There is a good agreement between natural frequencies of laminated composite plates under hygrothermal environment.
- The natural frequencies of vibration of fiber composite plates decrease with increase of temperature due to reduction of stiffness for all laminates.
- The frequencies of vibration of laminated plates also decrease substantially with increase of moisture concentration for all laminates.
- The frequencies of vibration for anti-symmetric laminates are higher than symmetric laminates. However, the frequency decreases with increase of hygrothermal conditions.
- The frequencies of vibration of composite plates under hygrothermal loads are more with increase in number of layers. However, the frequency decreases with increase of hygrothermal conditions.
- The fundamental frequencies of vibration decrease with increase in aspect ratios of plates in hygrothermal environment.
- The frequencies of vibration increase with increase in thickness of composite plates in hygrothermal environment.

6.3: Buckling effects of composite flat panels in hygrothermal environment

The present study deals with the parametric study on buckling behavior of woven fiber laminated composite plates subjected to uniform temperature and moisture experimentally and comparing them using finite element method. From the discussion, the following observation can be made:

- There is a good agreement between the experimental and numerical results for buckling of laminated composite plates at different temperature and moisture concentration.
- A general formulation on buckling of industry driven woven fiber composite plates which accounts for hygrothermal effects due to moisture diffusion, temperature and mechanical loads in addition to transverse shear, deformation and bending-stretching coupling is presented.
- The buckling loads decreases with increase in temperature and moisture concentration due to reduction of stiffness and strength of laminated plates.
- The buckling loads of laminated composite plates with hygrothermal loads increase with increase in number of layers.
- The reduction of buckling loads for anti-symmetric laminates is more than symmetric laminates with increase in temperature and moisture concentration environment.
- The buckling loads are decreased with increase in side-to-thickness ratios in hygrothermal environment.
- The thick and moderately thick laminated composite plates are more stable than thin plates in hygrothermal environment.
- The buckling loads may reduce significantly depending upon the temperature, moisture concentration, lamination sequence, side-to-thickness ratios and aspect ratios.
- The clamped-free-clamped-free boundary condition shows better buckling loads compared to four sides simply supported edges in hygrothermal conditions.
- The buckling loads are more for clamp-free-clamp-free boundary conditions as compared to four sides simply supported edges in extreme hygrothermal environment.

6.4: Dynamic instability of composite flat panels in hygrothermal environment

The parametric instability study of woven fiber laminated composite plates in hygrothermal environment subjected to periodic in- plane loads is examined. A general formulation for dynamic instability of laminated composite plates subjected to hygrothermal under in-plane periodic load is presented for the first time. From the detailed study, the following observation can be made:

- The excitation frequencies of laminated fiber composite plates decrease with increase of temperature and moisture concentration due to reduction of stiffness for all laminates. The greater is the lamination angle the smaller is the instability region of composite plates in hygrothermal environment.
- With increase in aspect ratios the excitation frequencies are decreased, due to reduction of effective stiffness of the plates in hygrothermal environment.
- Woven fiber laminated plates is more stable with increase in number of layers in hygrothermal environment
- The thick plates having narrow instability region shows more stiffness and strength than thin plates in hygrothermal environment.
- The width of instability zones decreases with increase of degree of orthotropy in hygrothermal environment.
- The high-modulus-fiber material plate is most stable in hygrothermal environment.
- The width of the instability regions increases with increase in both static and dynamic load parameters.
- Instability occurs earlier with an increase of the static compressive in-plane load, the instability regions tend to shift to lower frequencies, showing a destabilizing effect on the dynamic stability behavior of the plates in hygrothermal environment.

6.5: Dynamic instability of composite curved panels in hygrothermal environment

A general formulation for vibration, buckling and parametric resonance characteristics of laminated composite curved panels subjected to hygrothermal loads is presented.

- The excitation frequencies of laminated composite curved panels decrease with increase of temperature due to reduction of stiffness for all laminates.
- The excitation frequencies of laminated composite curved panels also decrease substantially with increase of moisture concentration for all laminates.
- Due to static component of load, the onset of instability shifts to lower frequencies with wide instability regions of the laminated composite curved panels.
- The instability region is observed to be influenced by the lamination angle.
- Increasing the thickness of the panels results in better dynamic stability strength.
- Increasing the aspect ratio, shifts the frequencies of instability region to higher values and reduces the dynamic stability strength.
- The width of dynamic instability region is smaller for square panels than rectangular panels.
- The excitation frequency increases with introduction of curvatures from flat panel to doubly curved panel in hygrothermal environment.

From the present studies, it is concluded that the instability behavior of woven fiber laminated composite plates and shells is greatly influenced by the geometry, lamination parameter and hygrothermal conditions. The figures dealing with variation of the frequencies, buckling loads and dynamic instability regions are recommended as design aids for flat and curved panels in hygrothermal environment. The above recommendations for design of composite panels are valid within the range of geometry and material considered in this study. So the designer has to be cautious while dealing with structures subjected to hygrothermal loading. This can be utilized to the advantage of tailoring during design of laminated composite structures in hygrothermal environment.

6.6: Future scope of research

Possible extensions to the present work are:

- forced vibration of laminated plates in hygrothermal environment.
- dynamic stability of stiffened plates and shells subjected to hygrothermal condition.
- dynamic stability of delaminated plates and shells in hygrothermal environment.
- dynamic stability of plates and shells involving arbitrary shaped openings in hygrothermal environment.
- The effects of damping on instability regions of plates and shells can be studied.
- non-conservative forces like follower loading in hygrothermal environment.
- large deflection and large amplitude vibration analyses of dynamic stability of plates and shells subjected to hygrothermal condition.
- Material nonlinearity may be taken into account in the formulation
- can be plates and shells of varying thickness.
- Besides all these, there is a large scope experimental investigation on dynamic stability of plates and shells in hygrothermal environment.

REFERENCES

ASTM Standard: D5687/D5687M-07. (2007): Standard Guide for Preparation of Flat Composite Panels With Processing Guidelines For Specimen Preparation.

ASTM Standard: D5229/D5229M-04. (2004): Stanndard Test Method For Moisture Absorption Properties And Equilibrium Conditioning of Polymer Matrix Composite Materials.

ASTM Standard: D2344/D2344M-06. (2006): Standard Test Method for Short-Beam Strength of Polymer Matrix Composite materials and Their Laminates.

ASTM Standard: D3039/D3039M-08. (2008): Standard Test Method for Tensile Properties of Polymer Matrix Composite Materials.

Adams, R.D and **Singh, M.M.** (1995): The effect of immersion in sea water on the dynamic properties of fiber- reinforced flexibilised epoxy composites, *Journal of Composite Structures*, Vol.**31**, pp. 119-127.

Anderson, T.J and **Nayfeh, A.H.** (1996): Natural frequencies and mode shapes of laminated composite plates: Experiment and FEA, *Journal of Vibration and Control,* Vol.**2** (4), pp. 381-414.

Argento, A and **Scott, R.A.** (1993): Dyamic instability of laminated anisotropiccircularcylindrical shells part II numerical results, *Journal of Sound and Vibration,* Vol.**162** (2), pp. 323-332.

Argento, A. (1993): Dynamic stability of of a composite circular cylindrical shell subjected to combined axial and torsional loading. Journal of composite materials, Vol.**27**(18).

Atas C and **Sayman O.** (2008): An overall view on impact response of woven fabric composite plates, *Journal of Composite Structures*, Vol.**82**, pp. 336-345.

Aditya, P.K. and **Sinha, P.K**. (1992): Diffusion coefficient of polymeric composites subjected to periodic hygrothermal exposure, *Journal of Reinforced Plastics and composites*, Vol.**9**(1): 1035-1047.

Babu, C.S. and **Kant, T.** (2000): Refined higher order finite element models for thermal buckling of laminated Composite and sandwich plates. *Journal of Thermal Stresses,* Vol.**23**, pp.111-130.

Baley, Christophe., Grohens, Yves.Busnel, Frederic. and **Devies, Peter**. (2004: Application of interlaminar shear test to marine composites, *Journal of Applied Composite Materials,* **11,** pp. 77-98.

Balamurugan, V. Ganapathi, **M**. and **Varadan, T.K.** (1996): Nonlinear dynamic instability of laminated composite plates using finite element method, *Computers and Structures,* Vol.**60** (1), pp.125-130.

Berger, S., Moshonv, A. and **Kenig, S.** (1989): The effect of thermal and hygrothermal ageing on the failure mechanism of graphite-fabric epoxy composites subjected to flexural loading, *Journal of composite,* Vol.**20** (4), pp. 341-348.

Bert, C.W and **Birman, V**. (1987): Dynamic instability of shear deformable anti- symmetric angle-ply plates, *International Journal Solids Structures*, Vol.**23**, pp. 1053-1067.

Bert, C.W, and **Birman, V.** (1988): Parametric instability of thick, orthotropic, circular cylindrical shells, *Acta Mechanica,* Vol.**71**, pp. 61-76.

Bolotin, V.V. (1964). The Dynamic stability of elastic systems, *Holden-Day*, San Francisco, 19. Nagai, K and Yamaki, N. (1988). Dynamic stability of circular cylindrical shells, *Acta. Mech*. **71** :61-76.

Biswas, S., Datta, P.K. and **Kong, C.K**. (2011): Static and dynamic instability characteristics of curved laminates with internal damage subjected to follower loading, *Journal of Mechanical Engineering Science*, Vol.**225**, pp.1589-1600.

Botelho, E.C., Pardini,L.C. and **Rezende, M.C**. (2006): Hygrothermal effects on the shear properties of carbon fiber/epoxy composites, *Journal of Material Science,* Vol.**41**, pp.7111-7118.

Botelho, E.C., Pardini, L.C and **Rezende, M.C.** (2005): Hygrothemal effects on damping behavior of metal/glass fiber/epoxy hybrid composites, *Journal of Material Science and Engineering A,* Vol.**399**, pp. 190-198.

Chakraborty, S., Mkhopadhyay, M and **Mohanty, A. R.** (2000): Free vibration responses of FRP composite plates, Experimental and Numerical studies. *Journal of Reinforced plastics and Composites,* Vol.19 (7**)**, pp.535-551.

Chakrabarti, A. and **Sheikh, A. H.** (2006): Dynamic instability of laminated sandwich plates subjected to in-plane partial edge loading, *Journal of Ocean Engineering,* Vol.**33**, pp. 2287-2309.

Chan, A.,Chiu, W.K. and **Liu, X.L**.(2007): Determining the elastic interlaminar shear modulus of composite laminates, *Journal of Composite Structures,* Vol.**80**, pp. 396-408.

Chandrasekhar, K. Free vibration of anisotropic laminated doubly curved shells, *Computers and Structures,* Vol. **33** (2), pp.435-440.

Chamis, C.C. (1989): Mechanics of composite materials: past,present,and future, *Journal of composites technology and research,* Vol.**11**(1), pp. 3-14.

Chen, B and **Chou, T-W.** (1999): Free vibration analysis of orthogonal-woven fabric Composites, *Journal of Composites part A,* Vol.**30**, pp. 285-297.

Chao, L-P. and **Shyu, S-L.** (1996): Nonlinear buckling of fiber-reinforced composite plates under hygrothermal effects, Journal of the Chinese Institute of Engineers, Vol.**19 (**6), pp.657-667.

Chatopadhyay, A. and **Radu, A.G**. (2000): Dynamic instability of composite laminates, *Journal of Computers and Structures*, Vol.**77**, pp.453-460.

Chaudhuri, R.A, Balaraman, K and **Kunuakkasseril, V.X.** (2005): A combined theoretical and experimental Investigation on free vibration of thin symmetrically laminated anisotropic plates. *Composite Structures*, Vol.**67:** 85-97.

Chen, L. W. and **Chen, Y.M.** (1989): Vibration of hygrothermal elastic composite Plates, *Journal of Engineering Fracture Mechanics,* Vol.**31** (2), pp. 209-220.

Chen L. W. and **Lee J. H.** (1988): Vibration of thermal elastic orthotropic plates, *Journal of Applied Acoustics*, Vol. **27** (4), pp.287-304.

Chen, W. J. L, P. D. and **Chen, L. W**. (1991): Thermal buckling behavior of composite laminated plates with a circular hole, *Composite Structures*, Vol.**18**, pp. 379-397.

Chen L-W. and **Yang J-Y**. (1990): Dynamic stability of laminated composite plates by the finite element method, Computers and Structures, Vol.**36** (5), pp. 845-851.

Chen, L-W and **Chen, L-Y.** (1987): Thermal buckling of laminated composite plates, *Composite Structures*, Vol.**8**, pp.189-205.

Chun-Sheng, Chen. Wei-Ren, Chen. and **Rean-Der, Chien.** (2009): Stability parametric vibrations of hybrid Composite plates, *European Journal of Mechanics A/Solids*, Vol.**28**, pp. 329-337.

Constantinos, S.L and **Dimitri, A. B.** (1990): Hygrothermal effects on structure-borne Noise transmission of stiffened laminated composite plates, *Journal of Aircraft*, Vol. **27,** pp. 722-730.

Dash, P.K., Sathisbabu, R. and **Ganesan, C**. (2011): Effect of corrosive environment on elasto-buckling strength of GFRC Plate, *Asian Journal of Material Science*, Vol.3 (1), pp. 5-19.

Dey, P. and **Singha, M. K**. (2006): Dynamic stability analysis of composite skew plates subjected to periodic in-plane load, *Journal of Thin-Walled Structures*, Vol.**44**, pp. 937-942.

Dhotarad, M.S and **Ganesan, N.** (1978): Influence on thermal gradient on natural frequency of rectangular plate vibration, *Journal of Nuclear Engineering and Design*, Vol.**52** (1), pp. 71-81.

Eslami H and **Maerz, S.** (1995): Thermally induced vibration of asymmetric cross-ply plate with hygrothermal effects. *American Institute of Aeronautics of Astronautics Journal*, Vol.**33** (10), pp. 1986-1988.

Fakhari, V and **Ohadi, A.** (2011): Nonlinear vibration control of functionally graded plate with piezoelectric layers in thermal environment, *Journal of Vibration and Control*, Vol.**17** (3), pp. 449- 469.

Fazilati, J. and **Ovesy, H.R.** (2010): Dynamic instability analysis of composite laminated thin walled structures using two versions of FSM, *Journal of composite Structures*, Vol.**92**, pp. 2060-2065.

Flaggs, D.L and **Vinson, J.K.** (1978): Hygrothermal effects on the buckling of laminated composite plates, *Journal of fiber Science and Technology*, Vol.**11**, pp. 353- 365.

Fu, Yiming. Li, Sheng. and **Jiang, Yejie**. (2008): Analysis of interlaminar stresses for composite laminated plate with interfacial damage, *Journal of Acta Mechanica Solida Sinia*, Vol.**21**(2), pp. 127-140.

Gandhi, M.V., Usman, M and **Chao, L**. (1988): Nonlinear vibration of laminated composite plates in hygrothermal environments, *Journal of Engineering Material Technology*, Vol.**110** (2), pp. 140-146.

Ganapathi, M. (1998): Dynamic instability of laminates subjected to temperature field, *Journal of Engineering Mechanics*, Vol.**124**, pp.1166-1168.

Ganapathi, M. Patel, B.P. and **Pawargi, D.S**. (2002): Dynamic analysis of laminated cross-ply composite non-circular thick cylindrical shells using higher-order theory, *International Journal of Solid and Structures*, Vol.**39**, pp. 5945-5962.

Ganapati, M. Patel, **B.P. Boisse, P** and **Touratier, M**. (2000): Nonlinear dynamic Stability characteristics of elastic plates subjected to periodic in-plane load, *International Journal Non- linear Mechanics*, Vol.**35**, pp. 467-480.

Ganapati, M., Patel, B.P., Boisse, **P.** and **Touratier. M.** (2000): Nonlinear dynamic stability characteristics of elastic plates subjected to periodic in-plane load, *International journal Non-linear Mechanics*, Vol.**35**, pp. 467-480.

Gigliotti, Marco., Jacquemin, Frederic., Molimard, Jerome. and **Vautrin,Alain**. (2007): Modelling and Experimental characterisation of hygrothermoelastic stress in polymer matrix composites, *Journal of polymer composites*, Vol.**247** (1), pp. 199-210.

Govindarajan, R., Krishna Murty, A.V., Vijaykumar, K. and **Raghuram, P. V**. (1993): Finite element estimation of elastic interlaminar stresses in laminates, *Journal of Composite E ngineering*, Vol.**3** (5): pp. 451-466.

Gupta A.K, Panwar V and **Vats RP**. (2010): Vibrations of non-homogeneous rectangular plate of variable thickness in both directions with thermal gradient effect, *Journal of Applied Mathematics*, Vol.**1**, pp. 456- 463.

Gupta, A.K and **Sharma, P**. (2011): Effect of linear thermal gradient on vibrations of trapezoidal plates whose thickness varies parabolically, *Journal of Vibration and Control,* Vol.**17** (8).

Harding, J. and **Li, Y.L.** (1992): Determination of interlaminar shear strength for glass/epoxy and carbon/epoxy laminates at impact rates of strain, *Journal of Composite Science and Technology,* Vol.**45**, pp.161-171.

Harding, J. and **Dong, L.** (1994): Effect of strain rate on the interlaminar shear strength of carbon-fiber-reinforced laminates, *Journal of Composite Science and Technology*, Vol.**51**, pp. 347-358.

Huang, X. L., Shen, Hui-Shen and **Zheng, Jian-Jun**. (2004): Nonlinear vibration and dynamic response of shear deformable laminated plates in hygrothermal environments, *Journal of composites science and Technology*, Vol.**64**, pp. 1419-1435.

Huang, N.N. and **Tauchert, T.R**. (1991): Large deformations of laminated cylindrical and doubly curved panels under thermal loading, *Computers Structures,* Vol.**41** (2), pp. 303-12.

Ishai, O. and **Arnon, U**. (1977): The effect of hygrothermal on residual strength of glass fiber reinforced plastic laminates, *Journal of testing and evaluation,*Vol.**5**(4),pp. 7.

Jeyaraj, P., Ganesan, N and **Padmanabhan, C**. (2009): Vibration and acoustics response of a composite plate with inherent material damping in a thermal environment, *Journal of Sound and Vibration*, Vol.**320**, pp. 322-338.

Jones, R. M. (2005): Thermal buckling of uniformly heated unidirectional and symmetric cross-ply laminated fiber-reinforced composite uniaxial in-plane restrained simply supported rectangular plates, *Composites Part A*, Vol.**36**, pp.1355-1367.

Karbhari, V.M. (2004): E-Glass composites in aqueous environments, *Journal of composites for construction*, Vol.**8**(2), pp. 148-156.

Kumar, S.K. and **Singh, B .N.** (2008): Thermal buckling analysis of SMA fiber reinforced composite plates using layerwise Model, *Journal Aerospace Engineering*, and Vol.53 (1), pp. 1-7.

Kundu, C.K and **Han, Jae-Hung**. (2009): Nonlinear buckling analysis of hygrothermoelastic composite shell panels using finite element method, *Composite Part B,* Vol.**40,** pp. 313-328.

Kundu, C.K. and **Han. J.H.** (2009): Vibration characteristics and snapping behavior of Hygro-thermo-elastic composite doubly curved shells, *Composite Structures*, Vol.**91,** pp**.** 306-317.

Kwon, Y.W. (1991): Finite element analysis of dynamic instability of layered composite plates using a high-order bending theory, Computers and Structures, Vol.**38** (1), pp. 57-62.

Lal, A. and **Singh, B. N**. (2010): Stochastic free vibration of laminated composite plates in thermal environments, *Journal of Thermoplastic Composite Materials*, Vol.**23**, pp. 57-77.

Lal, A., Singh, B. N. and **Kumar, R**. (2009): Effects of random system properties on the thermal buckling analysis of laminated composite plates. *Computers and Structures*, Vol.**87**, pp.1119-1128.

Lal, A. and **Singh, B. N**. (2010): Effect of uncertain system properties on thermo elastic stability of laminated Composite Plates under nonuniform temperature distribution, *International Journal of Applied Mechanics*, Vol.**2** (2), pp. 399-420.

Lal, A. Singh, B.N and **Kale, S**. (2011): Stochastic post buckling analysis of laminated composite cylindrical shell panel subjected to hygrothermo-mechanical loading, *Computers Structures*, Vol. **93**, pp. 1187-1200.

Lanhe, Wu. and **Hangjur, W**. Daobin. (2007): Dynamic stability analysis of functionally graded material plates by the moving square differential quadrature method, *Journal of Composite Structures*, Vol.**77**, pp. 383-394.

Laughlan, J. (1999): The influence of bend-twist coupling on the shear buckling response of thin laminated composite plates, *Journal of thin-walled strut*, Vol.**34** (2), pp. 97-114.

Lee, S.Y and **Yen, W.J.** (1989): Hygrothermal effects on the stability of cylindrical composite shell panel, *Computers and Structures*, Vol.**33** (2), pp. 551-559.

Leissa, A.W. (1987): A review of laminated composite plate buckling, *journal Applied Mechanics Review*, Vol.**40** (5), pp. 575-591.

Liao, C.L and **Cheng, C.R.** (1994): Dynamic stability of stiffened laminated composite plates and shells subjected to in-plane pulsating forces, *Journal of Sound and Vibration*, Vol.**174** (3), pp. 335-351.

Liao, C-Li. and **Cheng, C-R**. (1994): Dynamic stability of stiffened laminated composite plates and shells subjected to in-plane pulsating forces, *International Journal for Numerical Methods in Engineering,* Vol.**37**, pp.4167-4183.

Librescu, L and **Lin,W.** (1996): Vibration of geometrically imperfect panels subjected to thermal and mechanical loads, *Journal of Spacecraft Rockets*, **33**(2), pp.285-91.

Liew, K.M., He, X.Q., Tan, M.J. and **Lim, H.K.** (2004): Dynamic analysis of laminated composite plates with piezoelectric sensor/actuator patches using the FSDT mesh free method, *International Journal of Mechanical Sciences*, Vol.**46**, pp. 411-431.

Liew, K.M., Lee, Y.Y., Ng, T.Y. and **Zhao, X.** (2007): Dynamic stability analysis of composite cylindrical panels, *International Journal of Mechanical Sciences*, Vol.**49**, pp. 1156-1165.

Liew, K.M, Hu, Y.G. Zhao, X and **Ng, T.Y**. (2006): Dynamic stability analysis of Composite laminated Cylindrical Shells via the mesh-free kp-Ritz method, *Journal of Composite Methods in Applied Mechanics and Engineering*, Vol.**196**, pp.147-160.

Liu, C-F and **Huang, C-H.** (1995): Free vibration of composite laminated plates Subjected to temperature changes, *Journal of Computers and Structures*, Vol.**60**, (1), pp. 95-101.

Lua, J., Gregory, W. and **Sankar, J.** (2006): Multi-scale dynamic failure prediction tool for marine composite structures, *Journal of material science*, Vol. **41**(20), pp. 6673-6692.

Marques, S.P.C. and **Creus, G.J**. (1994).Geometrically nonlinear finite element analysis of viscoelastic composite materials under mechanical and hygrothermal loads, *Computers and Structures*, Vol. **53** (2), pp. 449-56.

Melvin, A.D., Lucia, A.C.and **Solomos, G.P**. (1993): The thermal response to deformation to fracture of a carbon/epoxy composite laminate, *Journal of Composite Science and Technology*, Vol.**46**, pp. 345-351.

Mond, M. and **Cederbaum, G**. (1992): Dynamic instability of anti-symmetric laminated Plates, *Journal of Sound and Vibration*, Vol.**154**, pp. 271-279.

Moorty, J., Reddy, J. N. and **Plaut R.H**. (1990): Parametric instability of laminated composite plates with transverse shear deformation, *International Journal Solids Structures*, Vol.**26**, pp. 801-811.

Mutsunaga, H. (2007): Free vibration and stability of angle-ply laminated composite and Sandwich plates under thermal loading, *Journal Composite Structures*, Vol. **77**(2**)**, pp. 249-262.

Mutsunaga, H. (2007): Free vibration and stability of angle-ply laminated composite and sandwich plates under thermal Loading, *Journal Composite Structures*, Vol.**77** (2), pp. 249-262.

Naik, N.K., Chandra sekhar, Y and **Meduri, S**. (2000): Damage in woven-fabric composites subjected to low- velocity impact. *Journal of Composite Science and Technology*, Vol.**60**, pp. 731-744.

Nagai, K. and **Yamaki, N**. (1988): Dynamic stability of circular cylindrical shells, *Acta Mechanica*, Vol.**71**, pp.61-76.

Naik, N.K., Reddy, K.S., Meduri, S.,Raju, N.B. and **Prasad,P.P**.(2002): Interlaminar fracture characterization for plain weave fabric composites, *Journal of Material Science*, Vol.**37**, pp. 2983-2987.

Naidu, N.V.S and **Sinha, P.K**. (2006): Nonlinear free vibration of laminated Composite Shells in Hygrothermal condition, *Journal of Composite Structures*, Vol.**77**, pp. 475-483.

NG, T.Y., Lam, K.Y and **Reddy, J.N**. (1998): Dynamic stability of cross-ply laminated composite cylindrical shells, *International Journal of Mechanical Sciences*, Vol. **8**, pp. 805-823.

Noor, A. K and **Burton, W. S.** (1992): Three-dimensional solutions for the free Vibrations and buckling of thermally stressed multilayered angle-ply composite Plates, *Journal of Applied Mechanics*, Vol.**59** (4), pp. 868-877.

Patel, B.P. Ganapathi, M. Prasad, K.R. and **Balamurugan, V**. (1999): Dynamic instability of layered anisotropic composite plates on elastic foundations *Engineering Structures*, Vol.**21**, pp. 988-995.

Patel, S. and **Case, S.W**. (2002): Durability of hygrothermally aged epoxy woven composite under combined hygrothermal conditions, *International Journal of Fatigue*, Vol.**24**, pp. 1295-1301.

Patel, B.P, Ganapathi, M and **Makhecha, D.P.** (2002): Hygrothermal effect on the structural behavior of thick composite laminates using higher-order theory, *Journal of Composite structures*, Vol.**56**, pp. 25-34.

Patel, B.P., Ganapathi, M. and **Makhecha, D. P.** (2003): Hygrothermal effects on the structural behavior of thick Composites using higher-order theory, *Composite Structures*, Vol.**56**, pp.25-34.

Parhi, P.K. Bhattacharyya, S.K and **Sinha, P.K**. (2001): Hygrothermal effect on the dynamic behaviour of multiple delaminated composite plates and shells, *Journal of Sound and Vibration*, Vol.**248** (2), pp.195-214.

Pandey, R., Upadhaya, A.K. and **Shukla, K.K**. (2010): Hygro- thermo elastic post buckling response of laminated composite Plates, *Journal of Aerospace* Engineering, Vol.**23**, pp.1-13.

Patel, S.N., Datta, P.K and **Sheikh, A.H**. (2007): Dynamic instability analysis of stiffened shell panels subjected to partial edge loading along the edges, *International Journal of Mechanical Sciences*, Vol. **49**, pp.1309-1324.

Pilli, Sonment., P, Simmons. and **Kevin, L**. (2009): A novel accelerated moisture absorption test and characterisation, *Journal of composites, partA*, Vol.(**40**), pp.1501-1505.

Prabhu, M. R. and **Dhanaraj, R.** (1993): Thermal buckling of laminated composite plates, *Cmputers and Structures*, Vol.**53** (1), pp.1-7.

Panda.S.K. and **Singh, B.N**. (2011): Large amplitude free vibration analysis of thermallypost-buckled composite doubly curved panel using non-linear FEM, *Finite Element in Anaalysis and Design*, Vol.**47,** pp. 378-386.

Rao, V.V.S and **Sinha, P.K.** (2003): Dynamic response of multidirectional composites in hygrothermal environments, *Journal of Composite structures*, Vol.**64**, pp. 329-338.

Ravi Kumar, L., Datta, P.K. and **Prabhakara, D.L**. (2003): Dynamic instability characteristics of laminated composite plates subjected to partial follower edge load with damping, *International Journal of Mechanical Sciences*, Vol.**45**, pp.1429-1448.

Ray, B.C. (2006): Temperature effect durring humid ageing on interfaces of glass and carbon fibres reinforced epoxy composites, *Journal of Collid and Interface science,* Vol.**298**, pp.111-117.

Ribeiro, P. and Jansen, E. (2008): Non-linear vibrations of laminated cylindrical shallow shells under thermomechanical loading, *Journal of Sound and Vibration,*Vol. **315**, pp.626-640.

Saburcu, M. and **Evran, K**. (2006): Dynamic stability of a rotating pre-twisted asymmetric cross-section Timoshenko beam subjected to an axial periodic force. *International Journal of Mechanical Sciences*, Vol.**48**, pp. 579-590.

Sahu, S.K. and **Date, P.K**. (2000): Dynamic instability of laminated composite rectangular plates subjected to non-uniform harmonic in-plane edge loading, *Journal of Aerospace Engineering,* Vol.**214**, pp. 295-312.

Sahu, S.K. and **Asha, A.V.** (2008): Parametric resonance characteristics of angle-ply twisted curved Panels, *International Journal of Structural Stability and Dynamics,* Vol. **8**, pp. 61-76.

Sahu, S.K and **Datta, P.K.** (2001): Parametric resonance characteristics of Laminated composite doubly curved shells subjected to non uniform loading, *Journal of Reinforced Plastics and Composite*, Vol.**20** (18), pp.1556-1576.

Sahu, S.K and **Datta, P.K.** (2003): Dynamic stability behaviour of laminated composite curved panel with cutout, *Journal of Engineering Mechanics (ASCE)*, Vol.**129**, pp.11, 1245.

Sai Ram, K.S and **Sinha, P.K.** (1992): Hygrothermal effects on the free vibration of laminated composite plates, *Journal of Sound and Vibration*, Vol.**158** (1), pp.133-148.

Sai Ram, K. S. and **Sinha, P.K**. (1992): Vibration and buckling of laminated composite plates with a cutout in Hygrothermal Environment, *ASME Institution of Aerospace of Astrological Journal*, Vol.**30**(9), pp. 2353-2355.

Sai Ram, K.S. and **Sinha, P.K.** (1992): Hygrothermal effects on the buckling of laminated composite plates, *Composite Structures,* Vol. **21**, pp. 233-247.

Selzer, R. and **Friedrich, K.** (1997): Mechanical properties and failure behaviouof carbon fibre-reinfoeced polymer composites under the influence of moisture, *Journal of Composites part A,* Vol.**28A**, pp. 595-604.

Sereir, Z. and **Boualem, N**. (2007): Damage of hybrid composites under long term hygrothermal loading and stacking sequence, *Journal of Theoretical and applied fracture mechanics,* Vol.**47**, pp. 145-163.

Shen, C.H. and **Springer, G.S.** (1976): Moisture absorption and desorption of composite materials, *Journal of composite materials*, Vol.**10**, pp. 272-280.

Shibasaki, M. and **Somiya, M.** (1999): Time dependence of degadation phenomena of plain woven FRP in hot, wet environmental exposure, *Jounal of mechanics of time-dependent materials*, Vol.**2**, pp. 351-369.

Shen, Hui-Shen., Zheng, Jian-Jun and **Hung, Xio-Lin**. (2004): The effects of hygrothermal conditions on the dynamic response of shear deformable laminated plates resting on elastic foundations, *Journal of Reinforced plastics and Composites,* 23(10): 1095-1113.

Shen, H-S. (1990): Elasto-plastic analysis for the buckling and postbuckling of rectangular plates under uniaxial compression, *Journal of Applied Mathematics and Mechanics,* Vol.**11** (10), pp. 931-939.

Shen-H-S. (2000): Hygrothermal effects on the postbuckling of shear deformable laminated plates, *Computers Structures,* Vol.**53** (5), pp.193-1204.

Shen, S.H. (2001): The effects of hygrothermal conditions on the post-buckling of shear deformable laminated cylindrical shells, *International Journal of Solids and Structures*, Vol.**38**, pp. 6357-6380.

Shariyat, M. (2007): Thermal buckling analysis of rectangular composite plates with temperature-dependent properties based on a layer wise theory, *Journal of Thin-walled Structures*, Vol.**45**, pp. 439-452.

Singh, B.N. and **Verma, V.K.** (2008): Hygrothermal effects on the buckling of laminated composite plates with random geometric and material properties, *Journal of Reinforced Plastics and Composites*, Vol. **28**: pp. 409-427.

Srinivasan, R.S. and **Chellapandi, P**. (1986): Dynamic stability of rectangular laminated composite plates, *Computers and Structures*. Vol.**24** (2), pp. 233-238.

Spallino, R. and **Thierauf, G.** (2000): Thermal buckling optimization of composite laminates by evolution strategies, *Computers and Structures*, Vol.**78**, pp.691-697.

Striat, L.H., Karasek, M.L. and **Amateau, M.F**. (1992): Effects of sea water immersion on the impact resistance of glass fiber reinforced epoxy composites, *Journal of Composite Materials*, Vol.**26** (14), pp. 2118-2133.

Tauchert, T.R. (1991): Thermally induced flexure, buckling, and vibration of plates, *Journal of Applied Mechanics Review*, Vol.**44** (8), pp. 347-360.

Thangaratnam, K.R., Palaninathan and **Ramachanran, J**. (1989): Thermal buckling of composite laminated plates, *Computer and Structures*, Vol.**32**, pp.1117-1124.

Thompson, S.P. and **Laughlan, J**. (2000): The control of post buckling response in thin composite plates using smart technology, *Journal of thin-walled structures*, Vol.36, pp. 231-263

Tsai, Y.I., Bosze, E.J., Barjastech, E. and **Nutt, S.R.** (2009): Inluence of hygrothermal environment on thermal and mechanical properties of carbon fiber/fiber glass hybrid composites, *Jounal of composite science and technology*, Vol.**69**, pp. 432-437.

Udar, R.S. and **Datta, P.K.** (2007): Dynamic analysis of parametrically excited laminated composite panels under non-uniform edge loading with damping, *Journal of Composite Structures*, Vol.**79**, 356-368.

Vijayraghavan, A. and **Evan-Iwanowski, R.M**. (1967): Parametric instability of circular cylindrical shell TASME, *Journal of Applied Mechanics*, Vol.**31**, pp.985-990.

Wang, S. and **Dawe, D.J**. (2002): Dynamic instability of composite laminated rectangular plates and prismatic plate structures, *Journal of Computer Methods in Applied Mechanics and Engineering*, Vol.**191**, pp.1791-1826.

Whitney, J.M and **Ashton, J .E**. (1971): Effect of environment on the elastic response of layered composite plates, *American Institute of Aeronautics of Astronautics Journal*, Vol.**9** (9), pp. 1708-1713.

Wu, G-Y. and **Shih, Y-S.** (2005): Dynamic stability of rectangular plate with an edge Crack, *Journal of Computers and Structures*, Vol.**84,** pp. 1-10.

Wu, G.Y. and **Shih, Y.S**. (2006): Analysis of dynamic instability for arbitrarily laminated skew plates, *Journal of Sound and Vibration*, Vol.**292**, pp. 315-340.

Xiao, S. and **Chen, B**. (2005): Dynamic and buckling analysis of a thin elastic-plastic square plate in a uniform temperature field, *Acta Mechanica Sinica*, Vol.**21**, pp.181-186.

Yao, J.C. (1965): Non-linear elastic buckling and parametric excitation of a cylinder under axial loads, *Journal of Applied Mechanics*, Vol.29.pp.109-115.

Young-Wann, K. (2005): Temperature dependent vibration analysis of functionally graded rectangular plates, *Journal of Sound and Vibration*, Vol. **284**(3-5), pp.531-549.

Zai, B.A., Park, M.K., Choi, H.S, Mehboob, H and **Ali, R**. (2009): Effect of Moisture absorption on dynamic stiffness of carbon fiber/epoxy composites, *Journal of Mechanical Science and Technology*, Vol. **23**, pp. 2298-3004.

Zenkour, A.M. and **EL-Sheikh, K**. (2001): Buckling and free vibration of elastic plates using simple and mixed shear deformation theories, *Acta Mechanica*, Vol.46, pp.183-197.

Zhou, C. (1991): Theory of nonlinear dynamic stability for composite laminated plates, *Journal of Applied Mathematics and Mechanics*, Vol.**12**, pp. 113-120.

Znasni, R. and **Bachir, A.S**. (2006): Effect of hygrothermomechanical aging on the interlaminar fracture behaviour of woven fiber composite materials, *Journal of thermoplastic composite materials*, Vol.**19** (4), pp. 385-398.